MEASURED ROTORDYNAMIC COEFFICIENTS AND LEAKAGE FOR A TOOTH-ON-ROTOR LABYRINTH SEAL WITH COMPARISONS TO A TOOTH-ON-STATOR LABYRINTH SEAL

A Thesis

by

STEPHEN PATRICK ARTHUR

Submitted to the Office of Graduate and Professional Studies of
Texas A&M University
in partial fulfillment of the requirements for the degree of

MASTER OF SCIENCE

Chair of Committee,	Dara Childs
Committee Members,	Gerald Morrison
	Paul Cizmas
Head of Department,	Andreas Polycarpou

December 2015

Major Subject: Mechanical Engineering

ABSTRACT

Rotordynamic and leakage data are presented for a see-through tooth-on-rotor (TOR) labyrinth seal with comparisons to a see-through tooth-on-stator (TOS) labyrinth seal. Measurements for both seals are also compared to predictions from XLLaby. Both seals have identical diameters and can be considered as relatively long labyrinth seals. The TOR seal has a length-to-diameter ratio of 0.62, whereas the TOS seal is longer and has a length-to-diameter ratio of 0.75. Both seals also differ by number of teeth, tooth height, and tooth cavity length. TOR labyrinth tests were carried out at an inlet pressure of 70 bar-a (1,015 psia), pressure ratios of 0.4, 0.5, and 0.6, rotor speeds up to 20,200 rpm, a radial clearance of 0.1 mm (4 mils), and three preswirl ratios. For comparison, TOS labyrinth tests were run at identical conditions as the TOR tests but for only one positive preswirl ratio.

TOR labyrinth measurements show a pronounced dependence of rotordynamic coefficients on rotor speed, especially when compared to prior documented TOS labyrinth seal tests run at a radial clearance of 0.2 mm (8mils). The TOR labyrinth cross-coupled stiffness is higher in magnitude and increases at a higher rate for increasing speed than that of the TOS labyrinth. However, the TOR labyrinth effective damping was determined to be greater due to higher measurements of direct damping. Measured leakage rates for the TOR labyrinth were approximately 5-10% less than the TOS labyrinth. XLLaby underpredicted the rotordynamic coefficients for both seals. However, as with measurements, it predicted the TOR labyrinth to have higher effective damping than the TOS labyrinth.

DEDICATION

This research work is dedicated to my family.

ACKNOWLEDGEMENTS

First and foremost, I would like to thank Dr. Dara Childs for giving me the opportunity to work at the Turbomachinery Laboratory. The experience that I gained while working under Dr. Childs is invaluable and I sincerely appreciate his support and guidance throughout my tenure as a research assistant.

I would also like to thank Dr. Gerald Morrison and Dr. Paul Cizmas for graciously serving as members on my committee.

Special thanks to Ray Mathews for always being available to help on the test rig and in the machine shop. His guidance helped me (and many others) achieve our goals, especially during unforeseen circumstances.

Sincere thanks to Stephen Phillips for his assistance in the test cell. His insight on the intricacies of the test rig was invaluable in diagnosing and solving problems.

Many thanks to fellow graduate research assistants Dr. Jason Wilkes, Naitik Mehta, Michael Vannarsdall, Rasish Khatri, David Tschoepe, David Coghlan, and Michael Murphey. I would also like to thank the undergraduate assistants, Mauricio Ramirez and Joshua Weed for their help on day-to-day activities on the test rig.

Lastly, I would like to thank my parents for their unwavering support and sacrifice. Their lives have been (and continue to be) an inspirational example for me to follow.

NOMENCLATURE

A	-	Rotor precession amplitude [L]
$\boldsymbol{A}_{ij}$	-	FFT of stator acceleration [L/T^2]
C_{xx}, C_{yy}, C	-	Direct damping [FT/L]
C_{xy}, C_{yx}, c	-	Cross-coupled damping [FT/L]
C_r	-	Seal radial clearance [L]
$\boldsymbol{D}_{ij}$	-	FFT of relative rotor/stator displacement [L]
D_s	-	Seal diameter [L]
$\boldsymbol{f}$	-	Excitation force [F]
$\boldsymbol{F}_{ij}$	-	FFT of excitation force [F]
$\boldsymbol{f}_{seal}$	-	Seal reaction force [F]
$\boldsymbol{H}_{ij}$	-	FFT of complex dynamic stiffness [F/L]
$\boldsymbol{j}$	-	$\sqrt{-1}$
K_{xx}, K_{yy}, K	-	Direct stiffness [F/L]
K_{xy}, K_{yx}, k	-	Cross-coupled stiffness [F/L]
L	-	Seal length [L]
m_s	-	Effective stator mass [M]
$\dot{m}$	-	Seal leakage mass flow rate [M/T]
P_{exit}	-	Seal exit pressure [F/L^2]
P_{inlet}	-	Seal inlet pressure [F/L^2]
Q	-	Volumetric flow rate measured by flow meter [L^3/T]
R	-	Rotor radius [L]
$\ddot{\boldsymbol{R}}_s$	-	Stator absolute acceleration [L/T^2]
$R_z(\theta)$	-	Coordinate rotation matrix [-]
$V_\theta(0)$	-	Air inlet circumferential velocity [L/T]
X,Y	-	Relative displacement between rotor and seal [L]
$\dot{X},\dot{Y}$	-	Relative velocity between rotor and seal [L/T]

ΔP	-	Pressure drop across seal [F/L^2]
ω	-	Rotor spin speed [1/T]
Ω	-	Rotor precession speed [1/T]
PR	-	Pressure ratio [-]
PSR	-	Preswirl Ratio [-]
WFR	-	Whirl frequency ratio [-]

TABLE OF CONTENTS

Page

ABSTRACT ii

DEDICATION iii

ACKNOWLEDGEMENTS iv

NOMENCLATURE v

TABLE OF CONTENTS vii

LIST OF FIGURES ix

LIST OF TABLES xii

1. INTRODUCTION 1

2. TEST RIG DESCRIPTION 8

2.1 Test Section 8
2.2 Stator Assembly 10
2.3 Preswirl Rings 11
2.4 Seal Leakage 12
2.5 Test Seal 13
2.6 Instrumentation 14
2.7 Test Conditions 15

3. EXPERIMENTAL PROCEDURE 17

3.1 Parameter Identification 17
3.2 Baseline Data 21
3.3 Static Uncertainty 23
3.4 Dynamic Repeatability 24

4. DISCUSSION OF RESULTS 25

4.1 Direct Stiffness 25
4.2 Cross-Coupled Stiffness 26
4.3 Cross-Coupled Damping 28

4.4 Effective Damping....29
4.5 Whirl Frequency Ratio (WFR)....30
4.6 Leakage....31

5. TOR AND TOS LABYRINTH SEAL COMPARISONS....33

5.1 TOR vs. TOS - Non-Dimensional Direct Stiffness....35
5.2 TOR vs. TOS - Non-Dimensional Cross-Coupled Stiffness....36
5.3 TOR vs. TOS - Normalized Direct Damping....37
5.4 TOR vs. TOS - Normalized Effective Damping....38
5.5 TOR vs. TOS - Leakage Flow Coefficient....39

6. PREDICTIONS VERSUS MEASUREMENTS....41

6.1 Predictions vs. Measurements - Direct and Cross-Coupled Stiffness....42
6.2 Predictions vs. Measurements - Direct and Effective Damping....42
6.3 Predictions vs. Measurements - Leakage Mass Flow Rate....43

7. SUMMARY AND CONCLUSIONS....44

REFERENCES....45

APPENDIX....47

LIST OF FIGURES

Page

Figure 1. Annular gas seal locations in the final stage of a straight-through centrifugal compressor (adapted from [1]) 1

Figure 2. Illustration of tooth-on-stator (TOS) and tooth-on-rotor (TOR) configurations for a labyrinth seal 2

Figure 3. Dynamic model of a gas labyrinth seal with a centered rotor 3

Figure 4. Direct and cross-coupled seal reaction forces acting on a precessing rotor 4

Figure 5. Lateral section view of the annular gas seal test stand (AGSTS) 8

Figure 6. Top and front views of the annular gas seal test stand (AGSTS) 9

Figure 7. Lateral section view of assembled stator with TOR labyrinth test seals 10

Figure 8. Preswirl ring cross-section for zero, medium, and high preswirl [8] 11

Figure 9. Preswirl ring showing pitot tube and static pressure orifice 11

Figure 10. TOR test seal schematic (dimensions are in inches) 13

Figure 11. Stator assembly with instrumentation 15

Figure 12. Schematic showing test rig frame (X-Y) and horizontal/vertical frame (x_1-y_1) as viewed from the non-drive end 17

Figure 13. Complex dynamic stiffness coefficients for baseline - 500 psi back pressure, 20.2 kRPM 22

Figure 14. Complex dynamic stiffness coefficients for TOR labyrinth test prior to subtracting baseline data - 0.5 PR, 20.2 kRPM, positive high preswirl 22

Figure 15. Complex dynamic stiffness coefficients for TOR labyrinth with subtracted baseline - 0.5 PR, 20.2 kRPM, positive high preswirl 23

Figure 16. TOR direct stiffness versus PSR, ω, and PR - 70 bar supply pressure and 0.1 mm radial clearance....26

Figure 17. TOR cross-coupled stiffness versus PSR, ω, and PR - 70 bar supply pressure and 0.1 mm radial clearanceDirect Damping....27

Figure 18. TOR direct damping versus PSR, ω, and PR - 70 bar supply pressure and 0.1 mm radial clearance....28

Figure 19. TOR cross-coupled damping versus PSR, ω, and PR - 70 bar supply pressure and 0.1 mm radial clearanceEffective Damping....29

Figure 20. TOR effective damping versus PSR, ω, and PR - 70 bar supply pressure and 0.1 mm radial clearance....30

Figure 21. TOR whirl frequency ratio versus PSR, ω, and PR - 70 bar supply pressure and 0.1 mm radial clearance....31

Figure 22. TOR leakage versus PSR, ω, and PR - 70 bar supply pressure and 0.1 mm radial clearance....32

Figure 23. Tooth profile comparison between the TOR and TOS test seals....34

Figure 24. TOR vs. TOS - Non-dimensional direct stiffness versus ω and PR at 70 bar supply pressure and medium preswirl....36

Figure 25. TOR vs. TOS - Non-dimensional cross-coupled stiffness versus ω and PR at 70 bar supply pressure and medium preswirl....37

Figure 26. TOR vs. TOS - Normalized direct damping versus ω and PR at 70 bar supply pressure and medium preswirl....38

Figure 27. TOR vs. TOS - Normalized effective damping versus ω and PR at 70 bar supply pressure and medium preswirl....39

Figure 28. TOR vs. TOS - Leakage flow coefficient versus ω and PR at 70 bar supply pressure and medium preswirl....40

Figure 29. Screenshot of XLLaby inputs used to generate predictions for the TOR test seal....41

Figure 30. Screenshot of XLLaby inputs used to generate predictions for the TOS test seal 41

Figure 31. XLLaby predictions versus measurements of K and k for the TOR and TOS seal - Medium preswirl and PR=0.5 42

Figure 32. XLLaby predictions versus measurements of C and Ceff for the TOR and TOS seal - Medium preswirl and PR=0.5 43

Figure 33. XLLaby predictions versus measurements of leakage mass flow for the TOR and TOS seal - Medium preswirl and PR=0.5 43

LIST OF TABLES

Page

Table 1. Measured inner diameters at the inlet and outlet of each smooth stator seal 14

Table 2. TOR Labyrinth seal testing conditions 16

Table 3. Static uncertainties 24

Table 4. Comparison of critical dimensions between the TOR and TOS test seals 33

Table 5. Raw data for TOR labyrinth seal at 10,200 rpm, 0.4 PR, and zero preswirl 47

Table 6. Raw data for TOR labyrinth seal at 15,350 rpm, 0.4 PR, and zero preswirl 47

Table 7. Raw data for TOR labyrinth seal at 20,200 rpm, 0.4 PR, and zero preswirl 48

Table 8. Raw data for TOR labyrinth seal at 10,200 rpm, 0.5 PR, and zero preswirl 48

Table 9. Raw data for TOR labyrinth seal at 15,350 rpm, 0.5 PR, and zero preswirl 49

Table 10. Raw data for TOR labyrinth seal at 20,200 rpm, 0.5 PR, and zero preswirl 49

Table 11. Raw data for TOR labyrinth seal at 10,200 rpm, 0.6 PR, and zero preswirl 50

Table 12. Raw data for TOR labyrinth seal at 15,350 rpm, 0.6 PR, and zero preswirl 50

Table 13. Raw data for TOR labyrinth seal at 20,200 rpm, 0.6 PR, and zero preswirl....51

Table 14. Raw data for TOR labyrinth seal at 10,200 rpm, 0.4 PR, and medium preswirl....51

Table 15. Raw data for TOR labyrinth seal at 15,350 rpm, 0.4 PR, and medium preswirl....52

Table 16. Raw data for TOR labyrinth seal at 20,200 rpm, 0.4 PR, and medium preswirl....52

Table 17. Raw data for TOR labyrinth seal at 10,200 rpm, 0.5 PR, and medium preswirl....53

Table 18. Raw data for TOR labyrinth seal at 15,350 rpm, 0.5 PR, and medium preswirl....53

Table 19. Raw data for TOR labyrinth seal at 20,200 rpm, 0.5 PR, and medium preswirl....54

Table 20. Raw data for TOR labyrinth seal at 10,200 rpm, 0.6 PR, and medium preswirl....54

Table 21. Raw data for TOR labyrinth seal at 15,350 rpm, 0.6 PR, and medium preswirl....55

Table 22. Raw data for TOR labyrinth seal at 20,200 rpm, 0.6 PR, and medium preswirl....55

Table 23. Raw data for TOR labyrinth seal at 10,200 rpm, 0.4 PR, and high preswirl....56

Table 24. Raw data for TOR labyrinth seal at 15,350 rpm, 0.4 PR, and high preswirl....56

Table 25. Raw data for TOR labyrinth seal at 20,200 rpm, 0.4 PR, and high preswirl 57

Table 26. Raw data for TOR labyrinth seal at 10,200 rpm, 0.5 PR, and high preswirl 57

Table 27. Raw data for TOR labyrinth seal at 15,350 rpm, 0.5 PR, and high preswirl 58

Table 28. Raw data for TOR labyrinth seal at 20,200 rpm, 0.5 PR, and high preswirl 58

Table 29. Raw data for TOR labyrinth seal at 10,200 rpm, 0.6 PR, and high preswirl 59

Table 30. Raw data for TOR labyrinth seal at 15,350 rpm, 0.6 PR, and high preswirl 59

Table 31. Raw data for TOR labyrinth seal at 20,200 rpm, 0.6 PR, and high preswirl 60

1. INTRODUCTION

The leakage of the working fluid in compressors, turbines, and pumps has a major impact on overall efficiency. This leakage occurs due to the necessary clearances between rotating components and the fixed housing. As the working fluid leaks away from the desired flow path, energy is lost that could have otherwise been used to generate power (turbines) or consume power (pumps and compressors). Annular seals are used to impede this leakage flow thereby increasing efficiency. The schematic of Figure 1 shows the typical placement of annular gas seals in the final stage of a straight-through centrifugal compressor. The eye-packing seal acts to control leakage across the

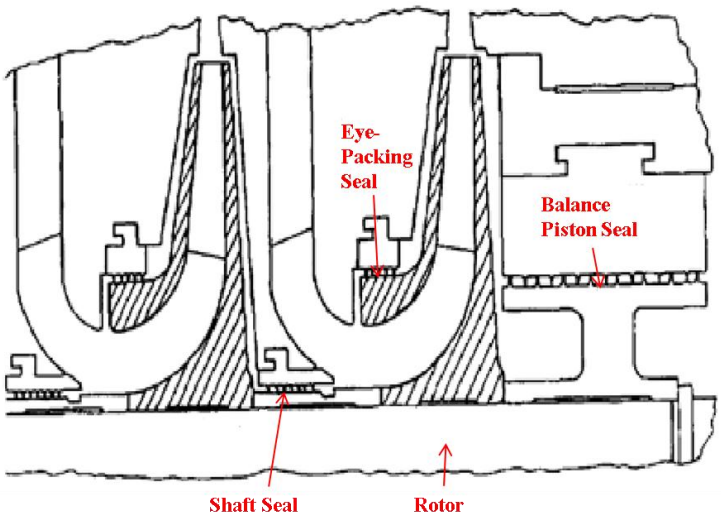

Figure 1. Annular gas seal locations in the final stage of a straight-through centrifugal compressor (adapted from [1])

front of the impeller; whereas, the shaft seal inhibits backflow to the previous stage. In the design of Figure 1, both of these seals use a tooth-on-stator (TOS) labyrinth that has teeth on the stator protruding radially towards the smooth rotor. An opposite configuration (commonly used in turbines) is called a tooth-on-rotor (TOR) labyrinth that uses a smooth stator with teeth on the rotor. In addition, the balance piston seal uses a configuration called an interlocking labyrinth. This design contains teeth on the stator and rotor that interlock axially. The balance piston seal is designed to counteract the

axial thrust generated within compressor stages, by providing an opposing thrust of equal magnitude due to the pressure drop across the seal.

Figure 2 illustrates both TOR and TOS designs; they are non-contacting with a small gap between the stator and rotor. This research is focused solely on the performance comparison of similar TOR and TOS labyrinth seals, although additional seal designs exist including hole-

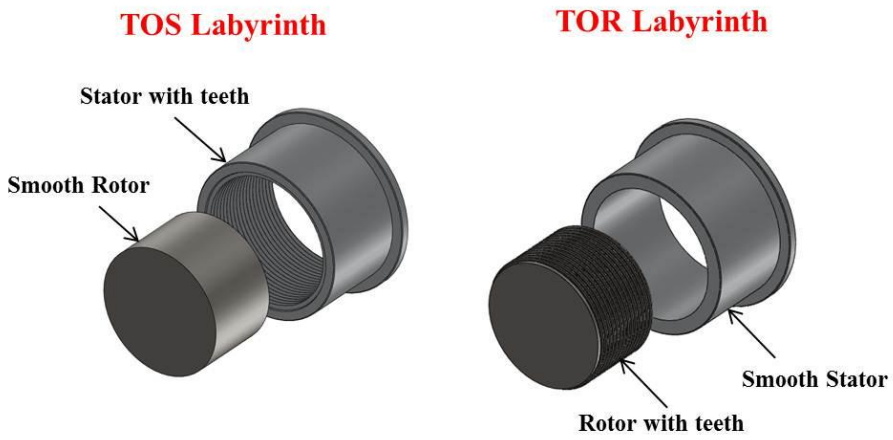

Figure 2. Illustration of tooth-on-stator (TOS) and tooth-on-rotor (TOR) configurations for a labyrinth seal

pattern, honeycomb, and smooth annular seals. The performance of both seals is determined by carrying out tests to obtain leakage flow rates and rotordynamic coefficients at identical operating pressures and rotor speeds. Rotordynamic coefficients characterize a seal's dynamic performance and are important since seals also impact the dynamics of a rotor-bearing system, such as the compressor of Figure 1.

As a rotor moves radially due to vibration, reaction forces develop due to fluid film interaction between the seal and rotor. Figure 3 depicts a rotor that is centered within a gas labyrinth seal. The *X*-*Y* frame represents two orthogonal displacement directions for the rotor.

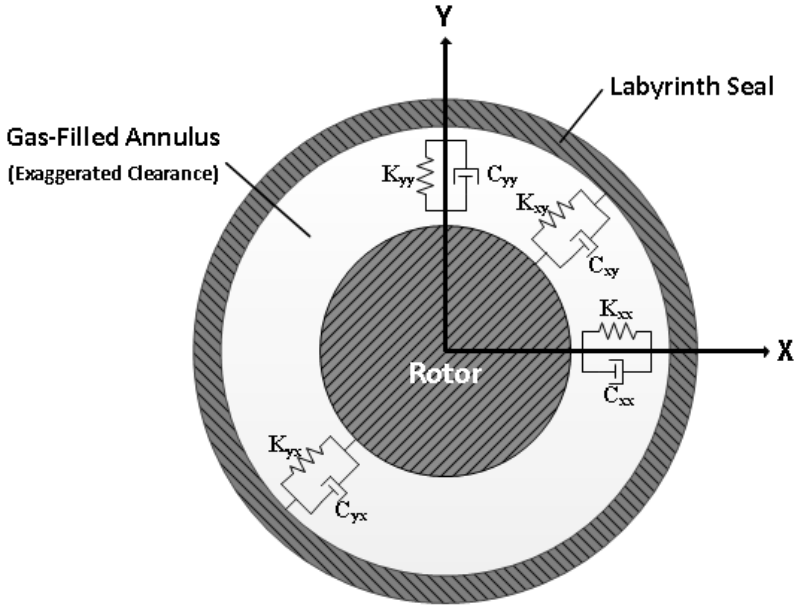

Figure 3. Dynamic model of a gas labyrinth seal with a centered rotor

As the rotor is displaced, the seal imparts a reaction force that can be modeled (for small motion) by linear stiffness and damping coefficients, taken from Childs [2] to be

$$-\begin{Bmatrix} f_{seal_x} \\ f_{seal_y} \end{Bmatrix} = \begin{bmatrix} K_{xx} & K_{xy} \\ K_{yx} & K_{yy} \end{bmatrix} \begin{Bmatrix} X \\ Y \end{Bmatrix} + \begin{bmatrix} C_{xx} & C_{xy} \\ C_{yx} & C_{yy} \end{bmatrix} \begin{Bmatrix} \dot{X} \\ \dot{Y} \end{Bmatrix} \tag{1}$$

where f_{seal_x} and f_{seal_y} are seal reaction forces, K_{xx} and K_{yy} represent *direct* stiffness, K_{xy} and K_{yx} are *cross-coupled* stiffness, C_{xx} and C_{yy} represent *direct* damping, C_{xy} and C_{yx} are *cross-coupled* damping, X and Y are relative displacements between the seal and rotor, and $\dot{X}$ and $\dot{Y}$ represent relative velocities between the seal and rotor. Direct and cross-coupled stiffness and damping are commonly referred to as rotordynamic coefficients. Cross-coupled forces arise due to fluid rotation within the seal. As a result, if the rotor is displaced in the X direction, a reaction force develops along both the X and Y directions. As discussed later, this behavior can lead to rotor instability.

For small motion about a centered position, Equation (1) is simplified by assuming that $K_{xx}=K_{yy}=K$, $K_{xy}=-K_{yx}=k$, $C_{xx}=C_{yy}=C$, and $C_{xy}=-C_{yx}=c$. This leads to

$$-\begin{Bmatrix} f_{seal_x} \\ f_{seal_y} \end{Bmatrix} = \begin{bmatrix} K & k \\ -k & K \end{bmatrix} \begin{Bmatrix} X \\ Y \end{Bmatrix} + \begin{bmatrix} C & c \\ -c & C \end{bmatrix} \begin{Bmatrix} \dot{X} \\ \dot{Y} \end{Bmatrix} \quad (2)$$

To better understand the physical effect of direct and cross-coupled seal reaction forces, Figure 4 illustrates a rotor undergoing vibration by precessing around its centered position at the frequency Ω, and spinning about its own axis at the running speed ω. The amplitude of precession is *A*. Positive direct stiffness *K* acts to center the rotor and resist radial rotor motion. When negative, as has been proven with labyrinth seals, direct stiffness acts to pull the rotor outward towards the seal. Positive cross-coupled stiffness *k* provides a reaction force in the same direction as the rotor precession, and therefore promotes instability. Positive direct damping *C* acts as a drag force in the opposite direction of rotor precession and therefore acts to stabilize rotor vibration. For gas labyrinth seals, cross-coupled damping *c* is of little importance and does not have a large effect on dynamics.

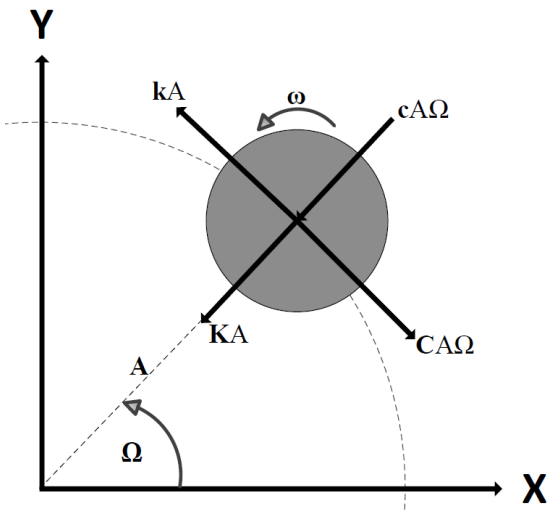

Figure 4. Direct and cross-coupled seal reaction forces acting on a precessing rotor

As mentioned before, cross-coupled stiffness is destabilizing and arises due to fluid rotation within the seal. Rotation of the fluid prior to entering the seal is referred to as preswirl. Shaft-induced swirl also occurs within the seal as the rotor spins. A common parameter used to characterize fluid rotation is called the preswirl ratio (*PSR*), defined as

$$PSR = \frac{V_\theta(0)}{R\omega} \tag{3}$$

where $V_\theta(0)$ is the fluid inlet circumferential velocity, R is the rotor's radius, and ω is the rotor's spin velocity. Hence, *PSR* relates the fluid's circumferential velocity at the seal inlet to the rotor's surface velocity. Positive *PSR* denotes fluid rotation in the same direction as the rotor's spin direction, whereas negative *PSR* occurs when the fluid is injected against rotor rotation. Past test results for TOS labyrinth seals by Picardo [3] and Mehta [4] have shown that cross-coupled stiffness is largely proportional to positive *PSR*.

Stability can be characterized in terms of the whirl frequency ratio (*WFR*) as follows

$$WFR = \frac{k}{C\omega} \tag{4}$$

It relates the destabilizing influence of cross-coupled stiffness to the stabilizing influence of direct damping, and stability decreases as this ratio increases. Picardo [3] and Mehta [4] have also shown that *WFR* is approximately equal to *PSR* for TOS labyrinth seals. An additional parameter that is useful in comparing seal stability is called effective damping, defined as

$$C_{eff} = C - \frac{k}{\omega} \tag{5}$$

It also relates direct damping to cross-coupled stiffness. It is desirable to have a high positive value for effective damping. This is accomplished by having relatively low cross-coupled forces when compared to the available amount of direct damping.

Concerning TOR labyrinth seals, there has not been a considerable amount of published data on their performance. Childs and Scharrer [5] tested a TOR and TOS labyrinth seal at inlet pressures ranging from 3.08 to 8.25 bar, ω's from 0.5 to 8 kRPM, and various inlet swirl ratios. Results show that ω has a small impact on rotordynamic coefficients, which might be explained by relatively low testing speeds that do not allow significant shear forces to develop. All measured *K* values were negative, with the TOR seal having a larger magnitude than the TOS seal. The TOR seal also had slightly larger

magnitudes for all other rotordynamic coefficients. For positive *PSR's*, the TOS seal was marginally more stable as defined by *WFR*. The TOS seal had slightly higher leakage than the TOR seal. The *PSR* for these tests was not measured accurately with a pitot tube as it is on the current air seal test rig. Also, the current test rig runs at considerably higher inlet pressures up to 70 bar, and higher ω's up to 20.2 kRPM.

Hawkins [6] tested labyrinth rotors with honeycomb stators and compared their performance to labyrinth rotors with conventional smooth stators. Tests were run at ω's ranging from 3 to 16 kRPM, supply pressures from 3.03 bar to 8.25 bar, and three radial clearances of 0.203, 0.304, and 0.406 mm. Using *WFR*, results showed that the honeycomb-stator seal was more stable at low ω, but the smooth-stator seal was more stable at the minimum clearance and high ω. For the smooth-stator seal at the minimum clearance, *k* increased significantly with ω but remained relatively constant for the medium and high clearances. Also, *k* increased continuously with increasing *PSR's* for the smooth-stator seal. *C* did not depend on *PSR* for both stator surfaces. For the smooth-stator seal, direct damping was insensitive to rotor speed. *WFR* for the smooth-stator seal increased significantly at higher ω for the minimum clearance. This ω dependency for the rotordynamic coefficients is significantly more pronounced at higher ω's than for those tests run by Childs and Scharrer [5] in a lower ω range.

Picardo [3] tested a straight-tooth TOS labyrinth seal and Mehta [4] tested a similar slanted-tooth TOS labyrinth seal. Both tests were run at ω's ranging from 10.2 to 20.2 kRPM, supply pressures up to 70 bar, and a clearance of 0.2 mm. Their results agree with Hawkins' [6] smooth-stator TOR labyrinth seal in that *k* increases with increasing *PSR*. However, contrary to Hawkins [6], *k* was not speed dependent, and *C* increased with increasing *PSR*. Speed dependency was only observed for *K*, which began to decrease with an increase in ω. Hawkins [6] observed the same trend for the minimum-clearance smooth-stator TOR labyrinth seal, which became more pronounced as supply pressure was increased. Overall, Hawkins' [6] testing of the smooth-stator TOR labyrinth seal showed significant ω dependency for rotordynamic coefficients as compared to the results of Picardo [3] and Mehta [4] for a TOS labyrinth seal.

Using a magnetic bearing test rig, Kwanka [7] tested a TOR labyrinth seal at 750 RPM, with low pressure differentials of 0.25 and 1 bar, and a relatively high clearance of 0.5 mm. Although the testing was performed at a relatively low speed and pressure, k was also found to be a linear function of swirl velocity. However, speed dependency could not be evaluated as the tests were run at a single speed.

The scope of this research is centered on the performance of a TOR labyrinth seal. The seal's rotordynamic coefficients and leakage will be presented and compared to the performance of the TOS labyrinth seal tested by Picardo [3]. Tests will be run at nominally identical testing conditions, which include speeds ranging from 10.2 to 20.2 kRPM, a supply pressure of 70 bar, and a radial clearance of 0.1 mm. The stability characteristics of both seals will be compared by means of WFR and C_{eff}. An additional interest is to observe if speed dependency of the rotordynamic coefficients is more pronounced for the TOR seal, as suggested by Hawkins [6] for a small radial clearance. Lastly, the leakage performance of both seals will be compared.

2. TEST RIG DESCRIPTION

2.1 Test Section

Figure 5 contains a lateral section view of the annular gas seal test stand (AGSTS) that is focused on the test section. A top view and front view of the AGSTS are also shown in Figure 6. The stator houses the test seals and is discussed in greater detail in the next section. Two hydraulic shakers are attached to the stator's top side and are used to control the stator's position. Three pairs of pitch stabilizers support the stator axially and are adjusted to ensure alignment between the rotor and stator. The stator is also supported on its sides by horizontal cables and on its bottom by a vertical spring assembly. The rotor is supported by two hydrostatic bearings that are each mounted into a support pedestal. The bearings are supplied with water at 70 bar (1,015 psi). Most of the water is fed back into the main water pump's supply tank for reuse.

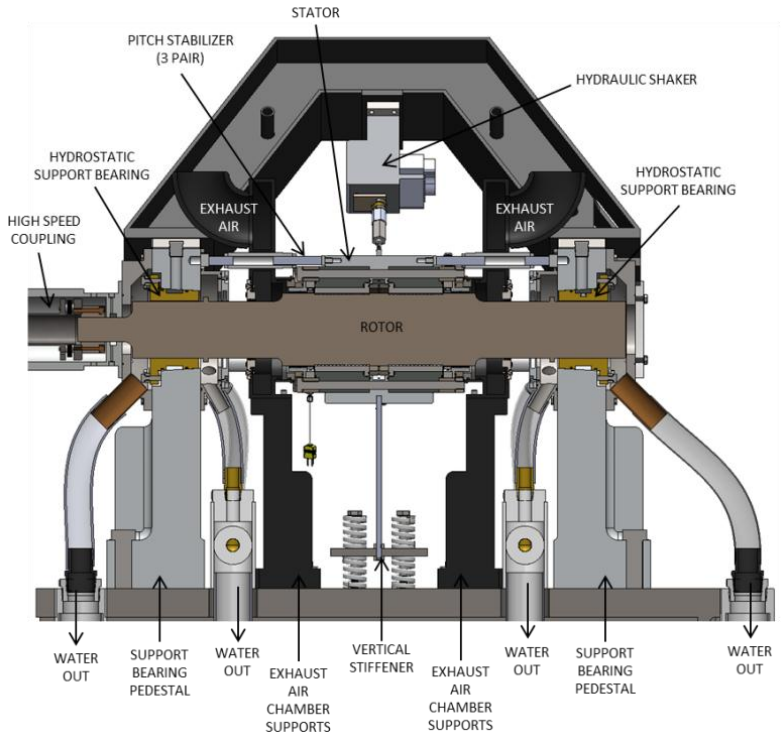

Figure 5. Lateral section view of the annular gas seal test stand (AGSTS)

Although not shown in this schematic, the test rotor is connected to a 7:1 speed increasing gearbox via a flexible disc coupling. The gearbox is driven by a 125 hp variable frequency drive electric motor. This drive system can drive the test rotor to a maximum speed of 29 kRPM, although most testing is performed up to a speed of only 20.2 kRPM. Also not shown, hoses are attached to the stator to allow for the input and output of high-pressure air. High-pressure air is supplied by the Oran W. Nicks Low Speed Wind Tunnel located near the Turbomachinery Laboratory.

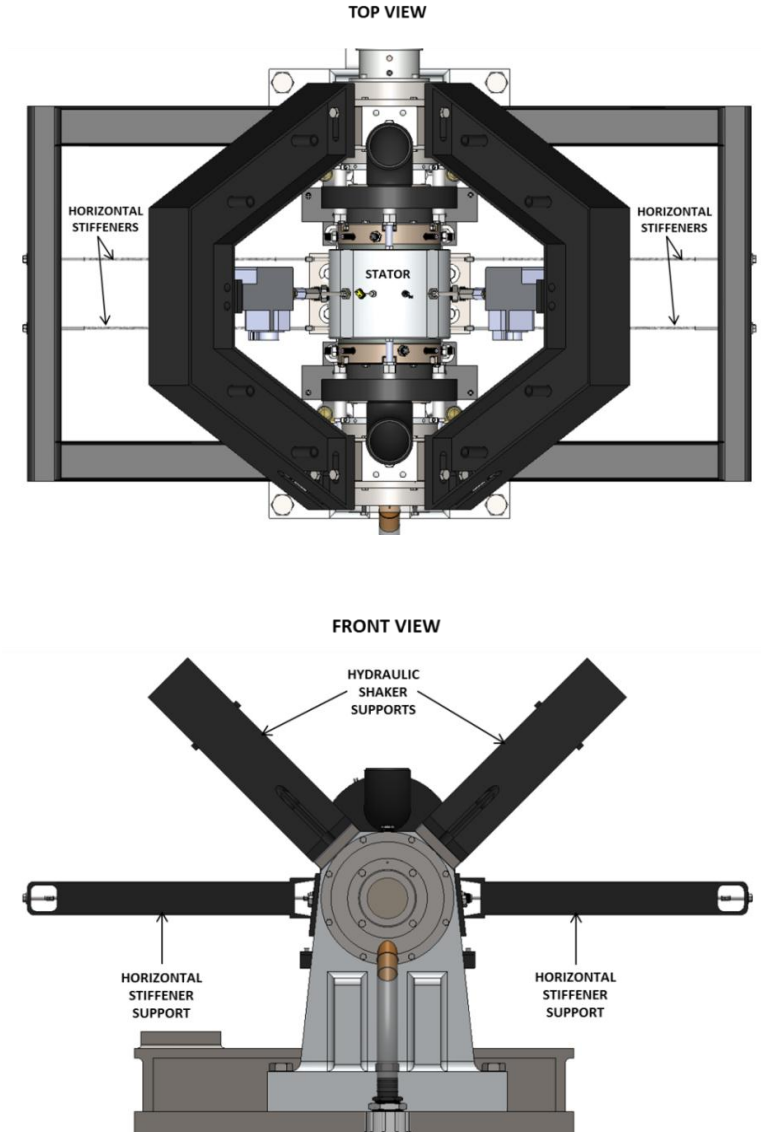

Figure 6. Top and front views of the annular gas seal test stand (AGSTS)

2.2 Stator Assembly

A section view of the assembled stator with TOR labyrinth test seals is shown in Figure 7. The stator contains two nominally identical test seals oriented back-to-back to minimize the net thrust caused by the pressure drop across each seal. High-pressure air enters at the stator's center annulus and flows through a preswirl ring, which is discussed later. The air then flows through both test seals and exits radially to a bleed valve, or axially through a swirl brake to the atmosphere. The swirl brake acts to reduce circumferential air flow, thus minimizing cross-coupled forces within the exit labyrinth seal. The bleed valve can be opened or closed to adjust the test seal's pressure ratio (*PR*), defined as

$$PR = \frac{P_{exit}}{P_{inlet}} \tag{6}$$

It is the ratio of the test seal's exit to inlet pressure. Depending on the clearance tested and the leakage of the test seal, PR's ranging from about 0.15 to 0.7 can be achieved.

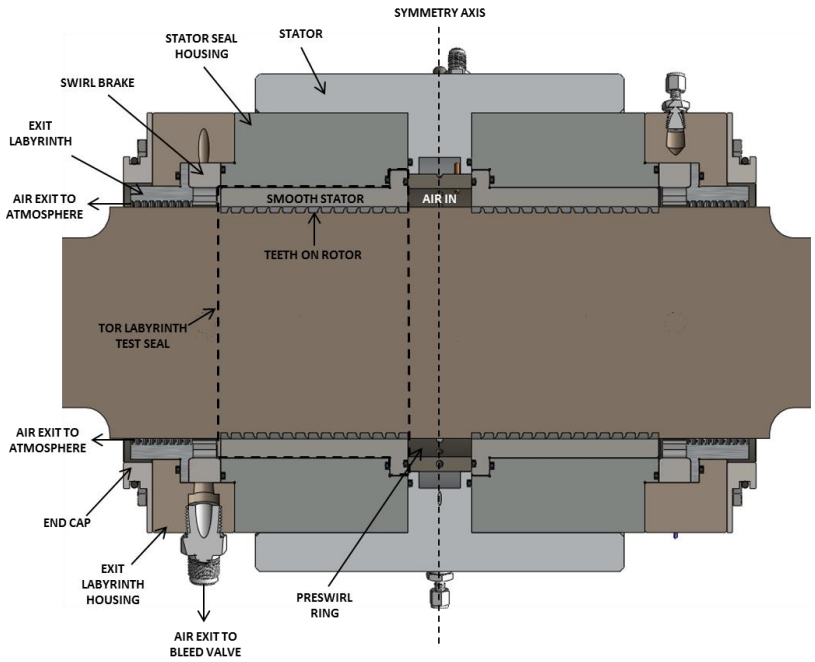

Figure 7. Lateral section view of assembled stator with TOR labyrinth test seals

2.3 Preswirl Rings

To analyze the effect of preswirl on the test seal's performance, preswirl is deliberately introduced into the stator via preswirl rings. Three separate stators are used that are each outfitted with their own preswirl ring. The preswirl rings vary only by hole angle, as shown in Figure 8. The zero preswirl ring has radial holes, whereas the medium and high preswirl rings have angled holes that induce both radial and circumferential velocity components. To determine the preswirl ratio during testing, the pitot tube setup of Figure 9 is used to measure the difference between

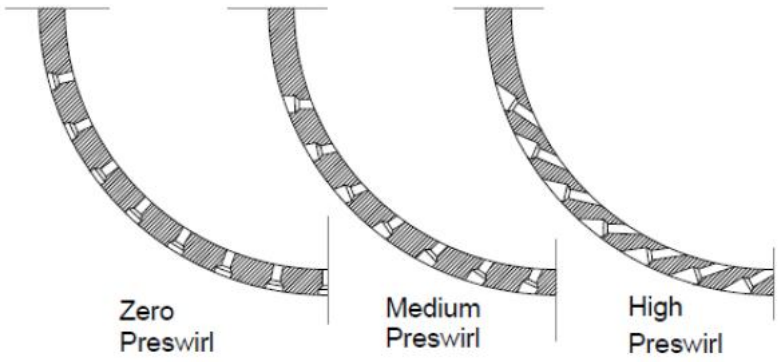

Figure 8. Preswirl ring cross-section for zero, medium, and high preswirl [8]

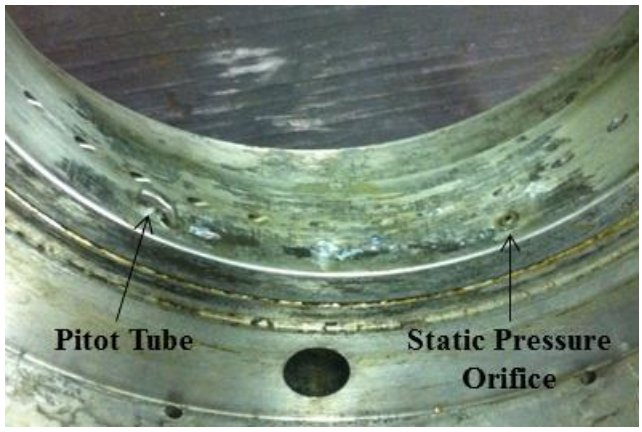

Figure 9. Preswirl ring showing pitot tube and static pressure orifice

stagnation and static pressure. The pitot tube is installed to aim as closely as possible in the circumferential direction. The stagnation and static pressures are fed into a differential transmitter, which outputs a voltage based on the pressure differential. From these measurements, according to Bernouilli, the circumferential air velocity of Equation (3) is calculated by

$$V_\theta(0) = \sqrt{\frac{2g\rho_w H_w}{\rho_a}} \tag{7}$$

where g is standard acceleration due to gravity, ρ_w is the density of water, H_w is the measured pressure differential in inches of water, and ρ_a is the air density at the seal inlet. The air density is calculated by employing the ideal gas law at the measured inlet temperature and pressure.

2.4 Seal Leakage

A turbine flow meter measures the volumetric flow rate (Q) of the air in Actual Cubic Feet per Minute (ACFM) and is located between the inlet air control valve and the test section. The temperature and pressure before and after the flow meter are measured to determine an average density (ρ) at the flow meter, which is accomplished by employing ideal gas law. Next, assuming that there is no leakage between the flow meter and the test section, the mass flow rate through each seal is determined by

$$\dot{m}_{uncorrected} = \frac{Q/2 \cdot \rho}{35.31466 \cdot 60} \tag{8}$$

where $\dot{m}_{uncorrected}$ is the mass flow rate through each seal in kg/s, without having corrected for differences between flow meter calibration conditions and testing conditions. The terms in the denominator are conversion factors. To compensate for differences between flow meter calibration conditions and testing conditions, the corrected flow rate through each seal is determined as follows

$$\dot{m}_{corrected} = \frac{Q}{3598.02}\left(\frac{T_{calib} + 273.15}{T_{test} + 273.15}\right)\left(\frac{P_{test}}{P_{calib}}\right) \tag{9}$$

where T_{calib} is the calibration temperature of approximately 13.5 °C, T_{test} and P_{test} are the measured average temperature and pressure across the flow meter during a test, and P_{calib} is the calibration pressure of approximately 70 bar-a.

During an actual test, all temperature, pressure, and flow rate measurements are taken before and after each shake of the stator. The measurements taken through the course of an entire test are then averaged. To ensure that the measurements do not vary considerably, testing is not run until a steady state temperature has been reached. Also, the inlet pressure is constantly monitored and set to the desired seal inlet pressure.

2.5 Test Seal

The TOR test seal is depicted in detail in Figure 10. The rotor has a nominal diameter of 114.3 mm (4.5 in) at the tooth tips. The smooth-stator seals have a nominal inner diameter of 114.5 mm (4.508 in), yielding a nominal radial clearance of 0.1 mm (4 mils).

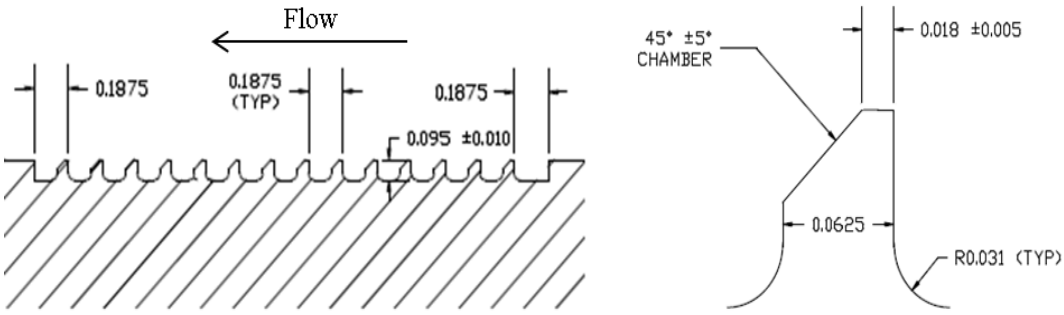

Figure 10. TOR test seal schematic (dimensions are in inches)

The inner diameters at the inlet and outlet of each of the two smooth stator seals were measured by a bore gage and are listed in Table 1. At both the inlet and outlet, three measurements were taken in increments of 60°, and the average of these was taken. As seen, the measured diameters are very close to the nominal diameter, with a maximum difference from the nominal diameter of 0.2 mils (0.005 mm).

Table 1. Measured inner diameters at the inlet and outlet of each smooth stator seal

Measured Inner Diameters - Smooth Stator No. 1				
Angle	Inlet		Outlet	
0	4.5081	(114.506 mm)	4.5080	(114.503 mm)
60	4.5081	(114.506 mm)	4.5080	(114.503 mm)
120	4.5080	(114.503 mm)	4.5081	(114.506 mm)
Average:	**4.5081**	**(114.506 mm)**	**4.5080**	**(114.503 mm)**

Measured Inner Diameters - Smooth Stator No. 2				
Angle	Inlet		Outlet	
0	4.5081	(114.506 mm)	4.5080	(114.503 mm)
60	4.5080	(114.503 mm)	4.5080	(114.503 mm)
120	4.5082	(114.508 mm)	4.5080	(114.503 mm)
Average:	**4.5081**	**(114.506 mm)**	**4.5080**	**(114.503 mm)**

2.6 Instrumentation

Figure 11 shows an array of instrumentation used to measure the static and dynamic performance of the test seals. The stator is connected to both hydraulic actuators (not shown) by a stinger and load cell. Two proximity probes are located in each loading direction (with one on the stator's drive end and the other on its non-drive end) and are used to measure relative position between the rotor and stator. This setup allows for the measurement of the stator position at two different axial locations, which is necessary to align the stator with the rotor.

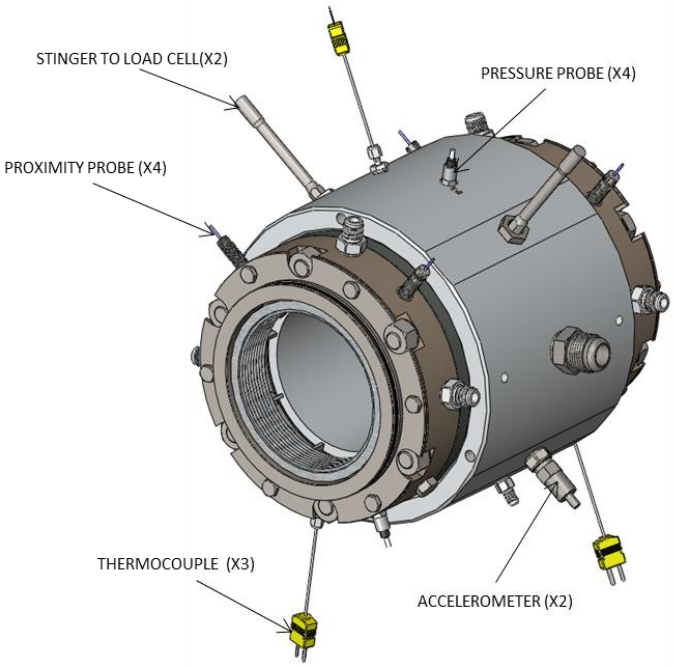

Figure 11. Stator assembly with instrumentation

An accelerometer is positioned 180° away from the proximity probes (in both loading directions) and measures the stator's absolute acceleration. There are four static pressures probes, two of which measure the pressure within the stator's inlet annulus (before entering the preswirl ring). The remaining two measure the pressure at the exit of each test seal. These pressure measurements are used to set the desired inlet pressure and pressure ratio, as well as to determine air density. Three thermocouples measure the seal's inlet temperature and the exit temperature of both seals. A turbine flow meter (not shown) measures the volumetric flow just upstream of the stator. A thermocouple and pressure transducer is placed before and after the flow meter to determine the average air density at the flow meter. Lastly, an optical tachometer (not shown) is located at the high-speed coupling to measure rotor speed.

2.7 Test Conditions

The TOR labyrinth seal test matrix of Table 2 consists of 1 radial clearance, 3 pressure ratios, 3 rotor speeds, and 3 inlet preswirl ratios, yielding a total of 27 testing conditions. At each of these test conditions, the stator is shaken and all dynamic and

static data are recorded. Prior to each test condition, the pressure ratio is set by adjusting the inlet and back pressure valves. The drive motor is then started and the desired rotor speed is set using a variable-frequency drive (VFD). All testing conditions were run in the seal's centered position by using the stator's proximity probes to set the seal concentric with the rotor.

Table 2. TOR Labyrinth seal testing conditions

TOR Laby Seal - Test Conditions			Preswirl		
Radial Clearance (mm)	Pressure Ratio (-)	Rotor Speed (RPM)	Zero	Medium Positive	High Positive
			Inlet Pressure (bar)		
0.1	0.4	10200	70	70	70
		15350	70	70	70
		20200	70	70	70
	0.5	10200	70	70	70
		15350	70	70	70
		20200	70	70	70
	0.6	10200	70	70	70
		15350	70	70	70
		20200	70	70	70

3. EXPERIMENTAL PROCEDURE

3.1 Parameter Identification

To identify the test seal's rotordynamic coefficients, the stator assembly is assumed to be a point mass whose general equation of motion is governed by Newton's Second Law

$$m_s \ddot{\boldsymbol{R}}_s = \boldsymbol{f} - \boldsymbol{f}_{seal} \ , \tag{10}$$

where m_s is the stator's effective mass, $\ddot{\boldsymbol{R}}_s$ is the stator's absolute acceleration, $\boldsymbol{f}$ is the excitation force, and $\boldsymbol{f}_{seal}$ is the seal's reaction force. Figure 12 shows the coordinate definitions for the test rig frame (X-Y) and horizontal/vertical frame (x_1-y_1). For testing performed prior to the vertical stiffener, the stator's effective mass was approximately equal in the horizontal and vertical direction. However, after installing the vertical stiffener to solve the stator's static instability problem, the stator's effective mass in the vertical direction became considerably higher than that of the horizontal direction. This fact necessitated the ability to define independent stator masses

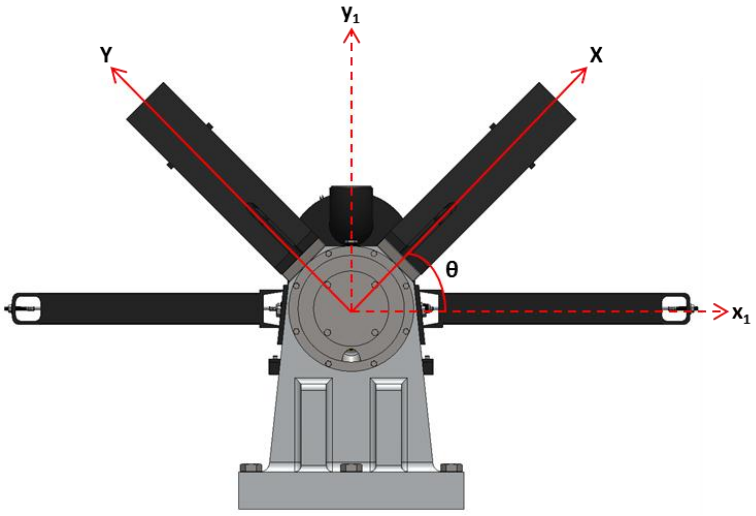

Figure 12. Schematic showing test rig frame (X-Y) and horizontal/vertical frame (x_1-y_1) as viewed from the non-drive end

in the horizontal and vertical directions when calculating rotordynamic coefficients. However, since all excitation forces, stator accelerations, and relative rotor-stator displacements are measured in the *X-Y* frame, they had to be transformed into the horizontal-vertical frame.

Following an analysis performed by Wilkes [9], this is accomplished by recognizing that vectors in the two coordinate systems of Figure 12 are related by

$$\begin{Bmatrix} v_{x_1} \\ v_{y_1} \end{Bmatrix} = \begin{bmatrix} \cos\theta & \sin\theta \\ -\sin\theta & \cos\theta \end{bmatrix} \begin{Bmatrix} v_X \\ v_Y \end{Bmatrix} = R_z(\theta) \begin{Bmatrix} v_X \\ v_Y \end{Bmatrix} \tag{11}$$

where v_{x_1} and v_{y_1} are orthogonal vectors in the x_1-y_1 frame, v_X and v_Y are orthogonal vectors in the X-Y frame, and θ is the angle between both frames. For the air seal rig, $\theta = -45°$ and is negative because the rotation defined by Equation (11) is clockwise.

To account for unequal stator masses in the x_1-y_1 frame, Newton's Second Law can be employed in this frame (rather than the *X-Y* frame) as follows

$$\begin{bmatrix} m_{x_1} & 0 \\ 0 & m_{y_1} \end{bmatrix} \begin{Bmatrix} \ddot{x}_1 \\ \ddot{y}_1 \end{Bmatrix} = \begin{Bmatrix} f_{x1} \\ f_{y1} \end{Bmatrix} - \begin{Bmatrix} f_{seal_{x1}} \\ f_{seal_{y1}} \end{Bmatrix} \tag{12}$$

where m_{x1} and m_{y1} are the stator's effective masses, $\ddot{x}_1$ and $\ddot{y}_1$ are the stator's acceleration components, f_{x1} and f_{y1} are the excitation force components, and $f_{seal_{x1}}$ and $f_{seal_{y1}}$ are the seal reaction force components, all transformed into the x_1-y_1 frame. To transform the stator's accelerations, excitation forces, and seal forces of Equation (12) back into the *X-Y* frame, the relationship of Equation (11) is applied to obtain

$$\begin{bmatrix} m_{x_1} & 0 \\ 0 & m_{y_1} \end{bmatrix} R_z \begin{Bmatrix} \ddot{X} \\ \ddot{Y} \end{Bmatrix} = R_z \begin{Bmatrix} f_X \\ f_Y \end{Bmatrix} - R_z \begin{Bmatrix} f_{seal_X} \\ f_{seal_Y} \end{Bmatrix} \tag{13}$$

Multiplying through by $R_z^T(\theta)$ yields

$$R_z^T \begin{bmatrix} m_{x_1} & 0 \\ 0 & m_{y_1} \end{bmatrix} R_z \begin{Bmatrix} \ddot{X} \\ \ddot{Y} \end{Bmatrix} = \begin{Bmatrix} f_X \\ f_Y \end{Bmatrix} - \begin{Bmatrix} f_{seal_X} \\ f_{seal_Y} \end{Bmatrix} \tag{14}$$

Next, substitute the definition of $R_z(\theta)$ to obtain

$$\begin{bmatrix} \cos\theta & -\sin\theta \\ \sin\theta & \cos\theta \end{bmatrix}_{\theta=-45°} \begin{bmatrix} m_{x_1} & 0 \\ 0 & m_{y_1} \end{bmatrix} \begin{bmatrix} \cos\theta & \sin\theta \\ -\sin\theta & \cos\theta \end{bmatrix} \begin{Bmatrix} \ddot{X} \\ \ddot{Y} \end{Bmatrix} = \begin{Bmatrix} f_X \\ f_Y \end{Bmatrix} - \begin{Bmatrix} f_{seal_X} \\ f_{seal_Y} \end{Bmatrix} \tag{15}$$

By substituting , the final time-domain equation of motion reduces to

$$[M_s] \begin{Bmatrix} \ddot{X} \\ \ddot{Y} \end{Bmatrix} = \begin{Bmatrix} f_X \\ f_Y \end{Bmatrix} - \begin{Bmatrix} f_{seal_X} \\ f_{seal_Y} \end{Bmatrix} \tag{16}$$

$$\text{where: } [M_s] = \frac{1}{2} \begin{bmatrix} m_{x_1} + m_{y_1} & m_{y_1} - m_{x_1} \\ m_{y_1} - m_{x_1} & m_{x_1} + m_{y_1} \end{bmatrix}$$

Note that this equation has stator masses defined in the horizontal/vertical frame, but accelerations, excitation forces, and seal forces defined in the test rig frame. Rearranging this equation and substituting Equation (1) for the seal reaction forces produces

$$[M_s] \begin{Bmatrix} \ddot{X} \\ \ddot{Y} \end{Bmatrix} = \begin{Bmatrix} f_X \\ f_Y \end{Bmatrix} - \begin{bmatrix} K_{xx} & K_{xy} \\ K_{yx} & K_{yy} \end{bmatrix} \begin{Bmatrix} X \\ Y \end{Bmatrix} - \begin{bmatrix} C_{xx} & C_{xy} \\ C_{yx} & C_{yy} \end{bmatrix} \begin{Bmatrix} \dot{X} \\ \dot{Y} \end{Bmatrix} \tag{17}$$

Next, by taking a Fourier transform, Equation (17) becomes

$$\begin{Bmatrix} \boldsymbol{F_X} \\ \boldsymbol{F_Y} \end{Bmatrix} - [M_s] \begin{Bmatrix} \boldsymbol{A_X} \\ \boldsymbol{A_Y} \end{Bmatrix} = \begin{bmatrix} \boldsymbol{H_{XX}} & \boldsymbol{H_{XY}} \\ \boldsymbol{H_{YX}} & \boldsymbol{H_{YY}} \end{bmatrix} \begin{Bmatrix} \boldsymbol{D_X} \\ \boldsymbol{D_Y} \end{Bmatrix} \tag{18}$$

where $\boldsymbol{F_{ij}}$, $\boldsymbol{A_{ij}}$, and $\boldsymbol{D_{ij}}$ are the Fourier transforms of the excitation forces, stator accelerations, and relative rotor/stator displacements, respectively. $\boldsymbol{H_{ij}}$ is the complex dynamic stiffness and can be related to the seal's rotordynamic coefficients by

$$\boldsymbol{H_{ij}} = K_{ij} + \boldsymbol{j}\Omega C_{ij} \tag{19}$$

where $\boldsymbol{j} = \sqrt{-1}$ and it is assumed that the virtual mass contribution is negligible for a gas labyrinth seal. The subscripts *i* and *j* represent the excitation force direction and reaction force direction, respectively. To obtain four independent equations to solve for the four unknown complex dynamic stiffness coefficients, two multi-frequency excitations are sequentially applied to the stator in the *X* and *Y* directions. Measurements are recorded

simultaneously in both directions during each excitation to capture direct and cross-coupled terms. Combining both sets of measurements results in

$$\begin{bmatrix} \boldsymbol{F_{XX}} & \boldsymbol{F_{XY}} \\ \boldsymbol{F_{YX}} & \boldsymbol{F_{YY}} \end{bmatrix} - [M_s] \begin{bmatrix} \boldsymbol{A_{XX}} & \boldsymbol{A_{XY}} \\ \boldsymbol{A_{YX}} & \boldsymbol{A_{YY}} \end{bmatrix} = \begin{bmatrix} \boldsymbol{H_{XX}} & \boldsymbol{H_{XY}} \\ \boldsymbol{H_{YX}} & \boldsymbol{H_{YY}} \end{bmatrix} \begin{bmatrix} \boldsymbol{D_{XX}} & \boldsymbol{D_{XY}} \\ \boldsymbol{D_{YX}} & \boldsymbol{D_{YY}} \end{bmatrix} \tag{20}$$

The complex dynamic stiffness coefficients are then solved for by inverting the displacement matrix to the left-hand side of the equation. Lastly, the rotordynamic coefficients are determined from the complex dynamic stiffness coefficients as follows

$$K_{ii} = \mathrm{Re}\left(\boldsymbol{H_{ii}}\right) \tag{21}$$

$$K_{ij} = \mathrm{Re}\left(\boldsymbol{H_{ij}}\right) \tag{22}$$

$$C_{ii} = \frac{\mathrm{Im}\left(\boldsymbol{H_{ii}}\right)}{\Omega} \tag{23}$$

$$C_{ij} = \frac{\mathrm{Im}\left(\boldsymbol{H_{ij}}\right)}{\Omega} \tag{24}$$

During a test the seal is excited about its centered position and the displacement amplitude is kept small when compared to the clearance. For this case, the rotordynamic coefficients can be simplified even further to $K_{xx}=K_{yy}=K$, $K_{xy}=-K_{yx}=k$, $C_{xx}=C_{yy}=C$, and $C_{xy}=-C_{yx}=c$. The experimental rotordynamic coefficients are found to be almost identical in the X and Y directions, but are not exactly equal. Hence average values determined by

$$K = \left(\frac{K_{XX} + K_{YY}}{2} \right) \tag{25}$$

$$k = \left(\frac{K_{XY} + K_{YX}}{2} \right) \tag{26}$$

$$C = \left(\frac{C_{XX} + C_{YY}}{2} \right) \tag{27}$$

$$c = \left(\frac{C_{XY} + C_{YX}}{2} \right) \tag{28}$$

3.2 Baseline Data

As discussed earlier, the test seals lie within a stator that is connected to pitch stabilizers, horizontal stiffening cables, a vertical spring assembly, and many other assembly components. When the stator is excited, the rotordynamic coefficients obtained are representative of the entire system. Also, although minimal, the exit labyrinth seals contribute stiffness and damping that must be accounted for. Baselines are needed to isolate the stiffness and damping contribution from the test seals alone. A dry shake, in which the fully assembled stator is excited without air, cannot be used as a baseline due to the presence of exit labyrinth seals. More appropriately, the stator is assembled without test seals but with the exit labyrinth seals installed. It is then pressurized to back pressures (or test seal exit pressures) that match those that are run during full testing. The rotor is also spun at the desired testing speeds, and the stator is shaken with an identical waveform that is used during full testing. Next, the stator is reassembled with test seals and retested at identical conditions. To obtain the complex dynamic stiffness coefficients for the test seals alone, the baseline coefficients are subtracted from those that are measured for a full test. Assuming that both test seals are identical, the complex dynamic stiffness coefficients are halved to obtain rotordynamic coefficients for one test seal.

To illustrate this procedure, Figure 13 shows plots of the real and imaginary parts of $\boldsymbol{H}_{ij}$ versus excitation frequency for the baseline test at a 500 psi (34.5 bar) back pressure and 20.2 kRPM. This baseline mimics a full test performed at 1,000 psi (69 bar) inlet, 0.5 *PR*, and 20.2 kRPM. Next, plots of the real and imaginary parts of $\boldsymbol{H}_{ij}$ for the full TOR labyrinth seal test (prior to subtracting baseline) at these conditions and positive high preswirl are depicted in Figure 14. Lastly, Figure 15 shows the results for the TOR labyrinth seal test after subtracting the baseline. Note that due to an erratic trend observed while testing labyrinth seals, data above 225 Hz has been truncated.

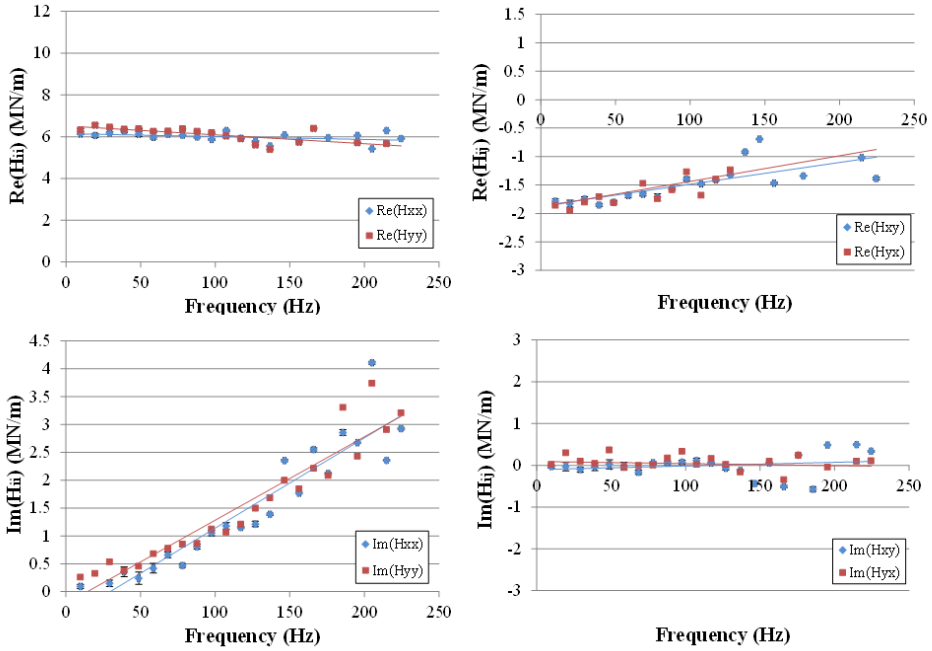

Figure 13. Complex dynamic stiffness coefficients for baseline - 500 psi back pressure, 20.2 kRPM

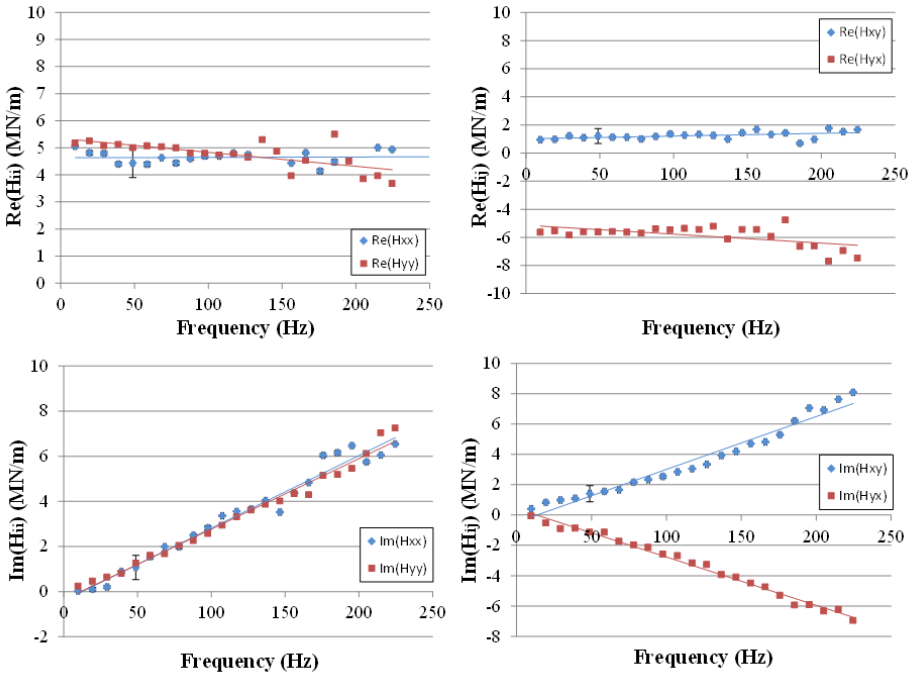

Figure 14. Complex dynamic stiffness coefficients for TOR labyrinth test prior to subtracting baseline data - 0.5 PR, 20.2 kRPM, positive high preswirl

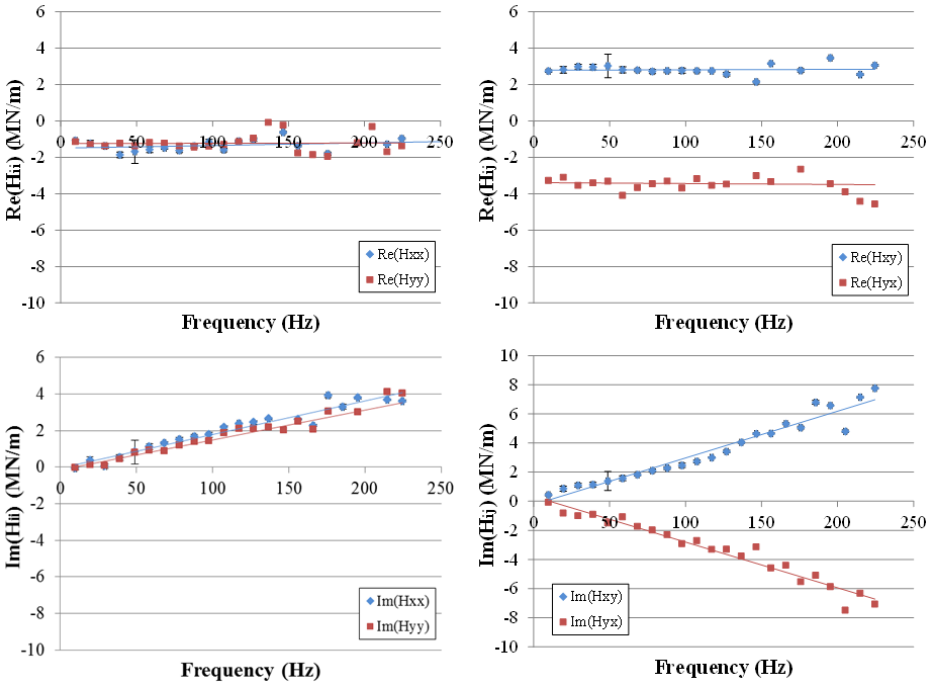

Figure 15. Complex dynamic stiffness coefficients for TOR labyrinth with subtracted baseline - 0.5 PR, 20.2 kRPM, positive high preswirl

3.3 Static Uncertainty

The static measurements of temperatures, pressures, flow rate, and rotor speed are all taken by sensors that have their own calibration curve. This curve relates the voltage output of the sensor to the parameter being measured and is approximated by a linear curve fit. Since this curve fit is not perfect, there is a small amount of error when converting sensor voltage to the parameter of interest. Also, the analog-to-digital converter (A/C) used to feed the sensor signals into the computer introduces a small amount of measurement error. Taking these errors into consideration, Kurtin et al.[10] performed an uncertainty analysis, the results of which are shown in Table 3.

Table 3. Static uncertainties

Stator Pressure	Flowmeter Pressure Differential	Temperatures	Pitot Tube Differential Pressure	Volumetric Flow Rate	Rotor Speed
0.838 psi	5.004 psi	5.613 °F	1.276 in-H_2O	0.547 ACFM	2.807 RPM

3.4 Dynamic Repeatability

The stator is excited via a Zonic hydraulic shaker and controller. The controller sends voltage waveform commands to a servo valve, which is built into the shaker head. As the waveform is applied, the servo valve opens and closes to control the amount of hydraulic fluid acting to cause a force. The waveform is executed from a computer and consists of an ensemble of pseudo-random frequencies [11] ranging from 10 Hz to 350 Hz in increments of 10 Hz. The waveform is sent from the computer to the Zonic controller via a digital-to-analog converter.

While the waveform is executing, LabVIEW dynamic data acquisition cards record the stator acceleration, stator position, and excitation force readings at a sampling rate of 10 kHz. The waveform occurs over a 0.1024 second interval and is executed 320 times sequentially along both axes. The time-domain measurements are converted into the frequency domain by using an FFT. Next, measurements from the 320 excitations are divided into 5 groups of 64 in both directions. The 5 groups from both directions are then combined to form 25 complex dynamic stiffness matrices. The standard deviation of these matrices yields the repeatability values of the dynamic data. The repeatability values are represented graphically by error bars. This repeatability analysis is performed for both the baseline testing and full testing.

4. DISCUSSION OF RESULTS

For the TOR labyrinth seal, the test matrix of Table 2 was carried out to examine the effects of *PSR*, *PR*, and ω on rotordynamic and leakage performance. As shown, all of these tests were performed at a 70 bar inlet pressure and 0.1 mm radial clearance. For ease of analysis, the results are presented in a 3 by 3 graphical format where rotor speed changes column by column, pressure ratio varies row by row, and each graph is plotted as a function of preswirl ratio. This follows the format presented by Picardo [3] and Mehta [4] for TOS labyrinth seals, as the TOR labyrinth rotordynamic coefficients were also found to be frequency independent. The TOR labyrinth seal test data is displayed alone in the following sections. Comparisons will then be made to Picardo's [3] TOS labyrinth seal, which was retested at medium preswirl and identical conditions to the TOR labyrinth seal.

4.1 Direct Stiffness

Figure 16 shows direct stiffness for the TOR labyrinth seal plotted against preswirl ratio, rotor speed, and pressure ratio. *K* decreases significantly with increasing rotor speed, a trend also observed by Picardo [3] and Mehta [4] for TOS labyrinth seals. However, contrary to their results, *K* starts out positive and becomes negative as rotor speed increases. Although not significant, *K* tends to decrease from the lowest to highest preswirl ratio. Pressure ratio does not have a large impact on *K*. Lastly, the magnitude of *K* is small when compared to hole-pattern seals and especially when compared to bearings.

Note that the preswirl ratios shown on each plot represent tests run with the zero, medium, and high preswirl stators. However, the measured preswirl ratios change with rotor speed and their range becomes relatively small at 20.2 kRPM. Also at this speed, the first preswirl ratio approaches that of the second preswirl ratio, which is a peculiar trend since the zero preswirl stator injects air radially only. This trend was also seen by Picardo [3] for tests run at a small clearance. For tests run at a high radial clearance of

0.2 mm, this trend is not as pronounced. Therefore, it could be a result of higher shaft-induced swirl near the Pitot tube for small-clearance testing.

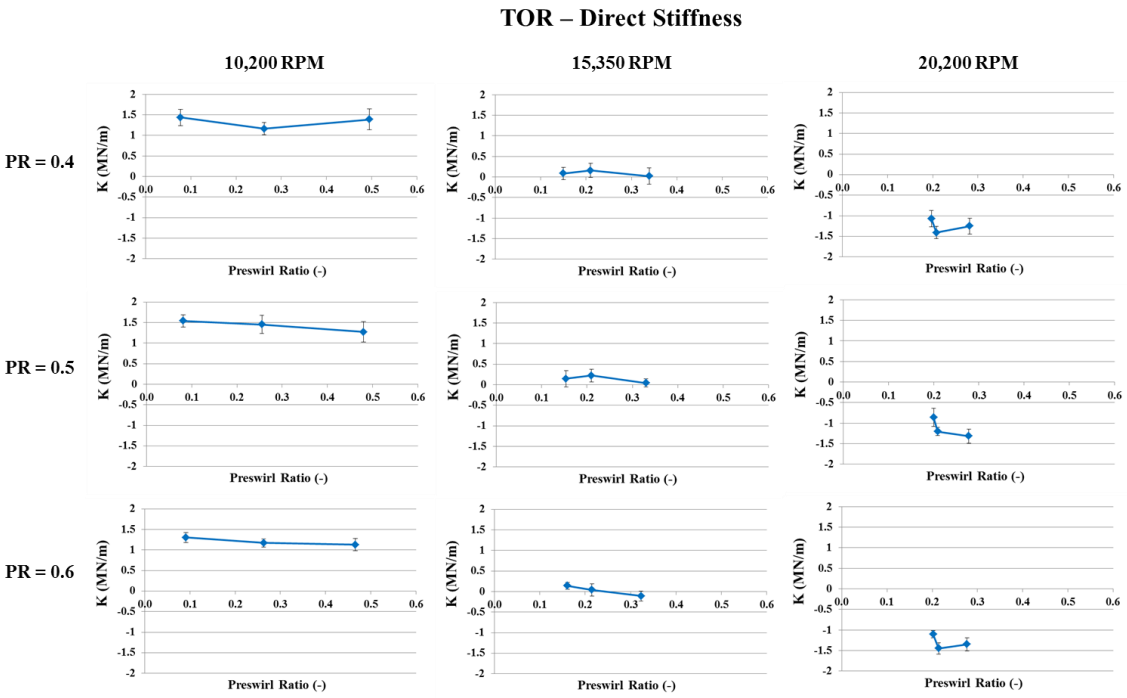

Figure 16. TOR direct stiffness versus *PSR*, ω, and *PR* - 70 bar supply pressure and 0.1 mm radial clearance

4.2 Cross-Coupled Stiffness

The cross-coupled stiffness for the TOR labyrinth seal is illustrated in Figure 17. Results show a fairly linear relationship between *k* and preswirl ratio and a negligible influence of pressure ratio on *k*. These trends were also seen by Picardo [3] and Mehta [4]. However, the TOR results exhibit a more pronounced dependence of *k* on rotor speed, since *k* increases significantly with rotor speed. Picardo [3] observes this for small clearance testing as well, but to a lesser extent. Also noticed in Figure 17, *k* is close to zero at 10.2 kRPM for the first preswirl condition, but this is not the case at higher rotor speeds. Although the zero preswirl stator was used for these data points, *k* is measured to be relatively high at 15.35 kRPM and 20.2 kRPM. Picardo [3] also reported this for the same clearance, but the magnitude of *k* is higher for the TOR labyrinth seal.

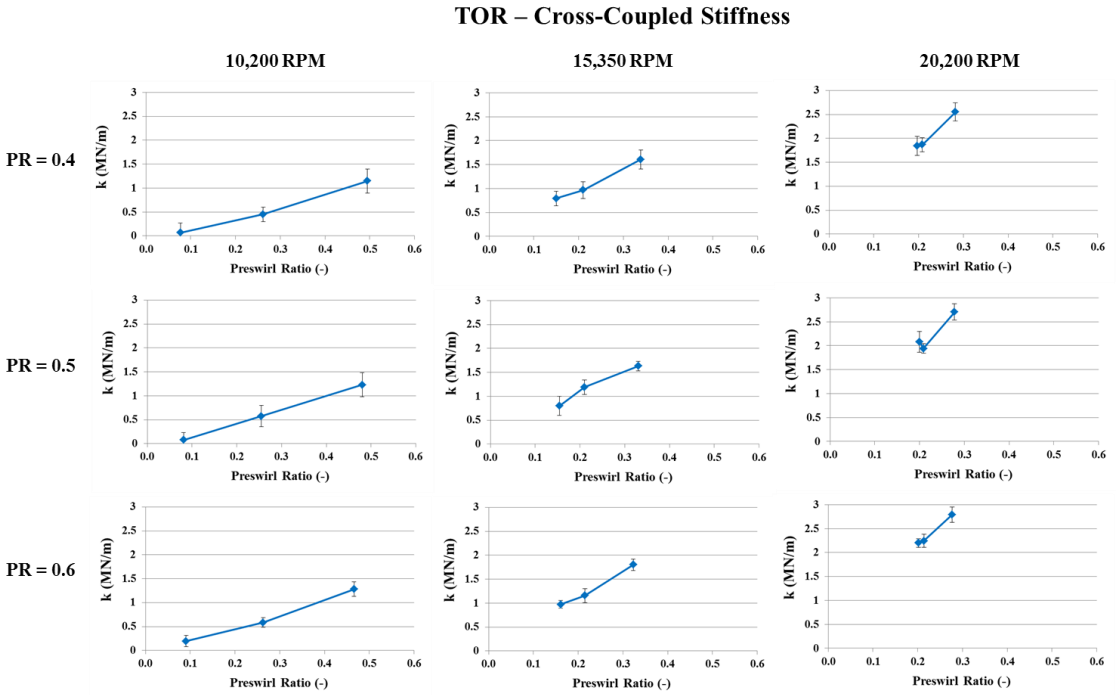

Figure 17. TOR cross-coupled stiffness versus *PSR*, ω, and *PR* - 70 bar supply pressure and 0.1 mm radial clearanceDirect Damping

Figure 18 shows the variation of direct damping with preswirl and rotor speed. Increases in preswirl ratio lead to an increase in *C*, a trend also observed by Picardo [3] and Mehta [4] at both small and large clearances. *C* also grows as rotor speed is increased, which Picardo [3] showed for the small clearance testing as well, though this trend is slightly more pronounced for the TOR labyrinth seal. Pressure ratio does not influence direct damping significantly.

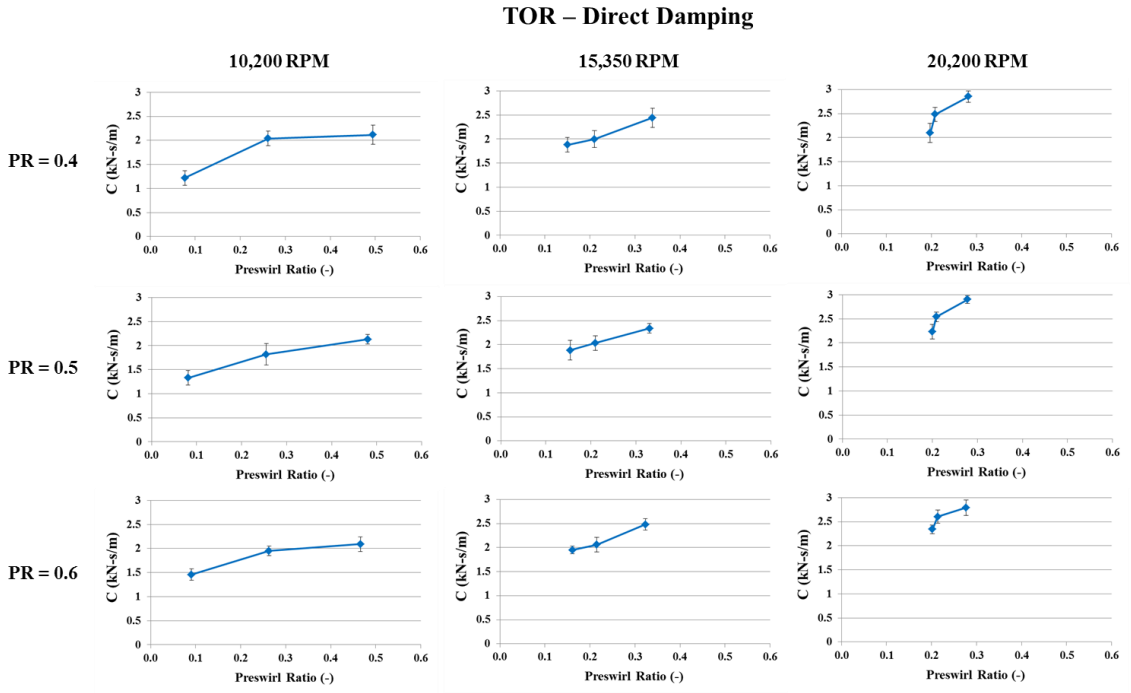

Figure 18. TOR direct damping versus *PSR*, ω, and *PR* - 70 bar supply pressure and 0.1 mm radial clearance

4.3 Cross-Coupled Damping

Plots of cross-coupled damping can be seen in Figure 19. As with Picardo [3] and Mehta [4], cross-coupled damping increases with rotor speed but changes in pressure ratio shows little influence. The effect of preswirl ratio is not as clear, but cross-coupled damping increases from the first to last preswirl ratio. Although not considered as important, cross-coupled damping for the TOR labyrinth seal increases at a faster rate than what Picardo [3] reported at the same clearance for a TOS labyrinth. This continues the trend of a more pronounced rotor speed dependency for the TOR rotordynamic coefficients.

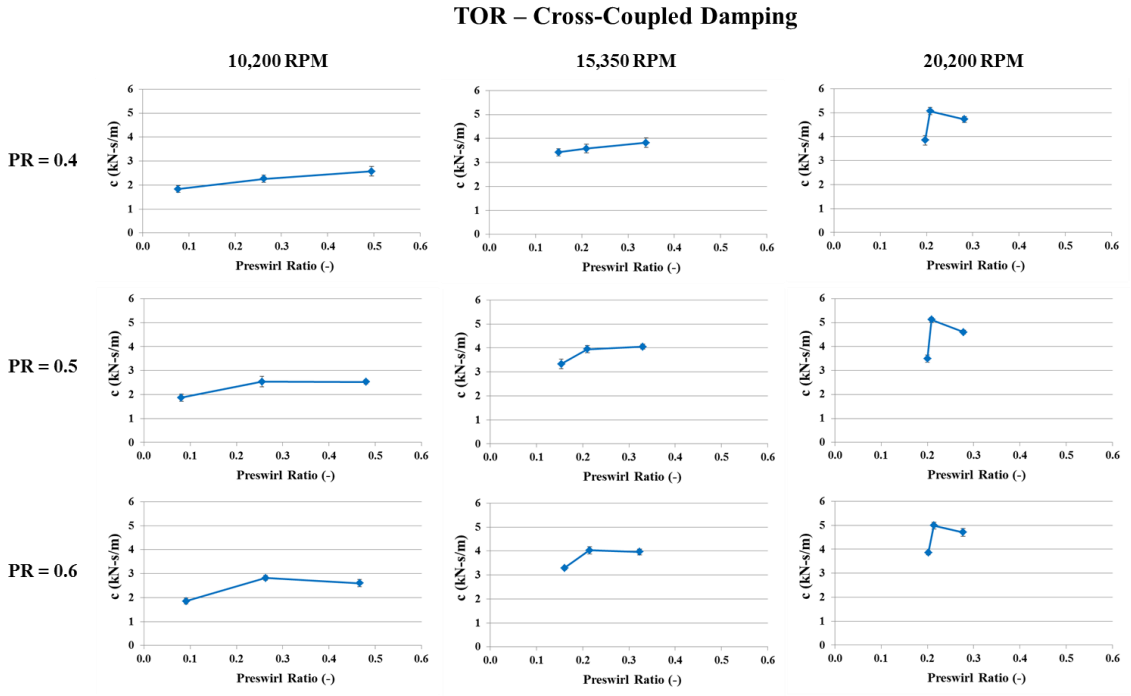

Figure 19. TOR cross-coupled damping versus *PSR*, ω, and *PR* - 70 bar supply pressure and 0.1 mm radial clearance

4.4 Effective Damping

As defined in Equation (5), effective damping is plotted in Figure 20 and is the best measure of stability for seals. There is a slight decrease with an increase in pressure ratio. Also, effective damping first increases and then decreases with preswirl ratio at the lowest and highest rotor speed. There is not much variation with ω, but this is due to the fact that direct damping and cross-coupled stiffness both increase with rotor speed at about the same rate. The stability of TOS and TOR labyrinth seals will be compared later on in the following section.

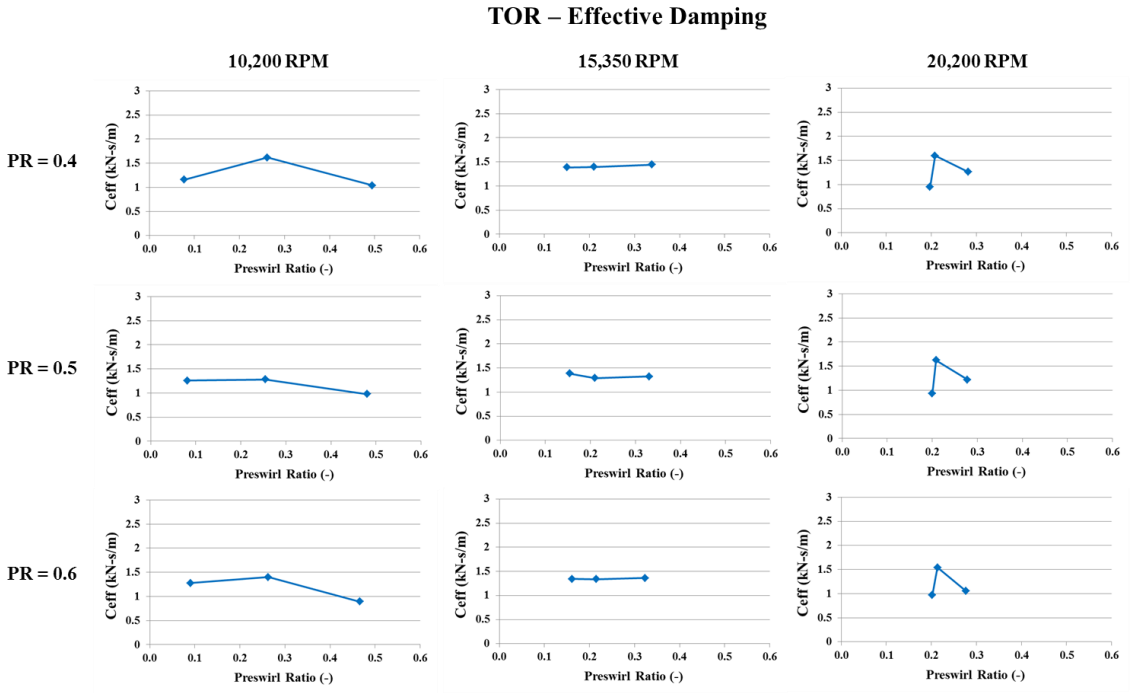

Figure 20. TOR effective damping versus *PSR*, ω, and *PR* - 70 bar supply pressure and 0.1 mm radial clearance

4.5 Whirl Frequency Ratio (WFR)

WFR is shown in Figure **21** and is defined by Equation (4). This is a more useful parameter for defining the stability of fluid-film bearings, but holds almost no value when trying to compare the stability of annular seals. The results for the TOR labyrinth seal show that *WFR* increases linearly with preswirl ratio at 10.2 kRPM and 15.35 kRPM. Also, at 10.2 kRPM *WFR* is approximately equal to preswirl ratio, but this trend does not hold as rotor speed increases. This is most likely due to higher shaft-induced swirl within the seal at higher rotor speeds, causing cross-coupled stiffness to be a function of both preswirl and shaft-induced swirl. Pressure ratio imparts little influence on *WFR*.

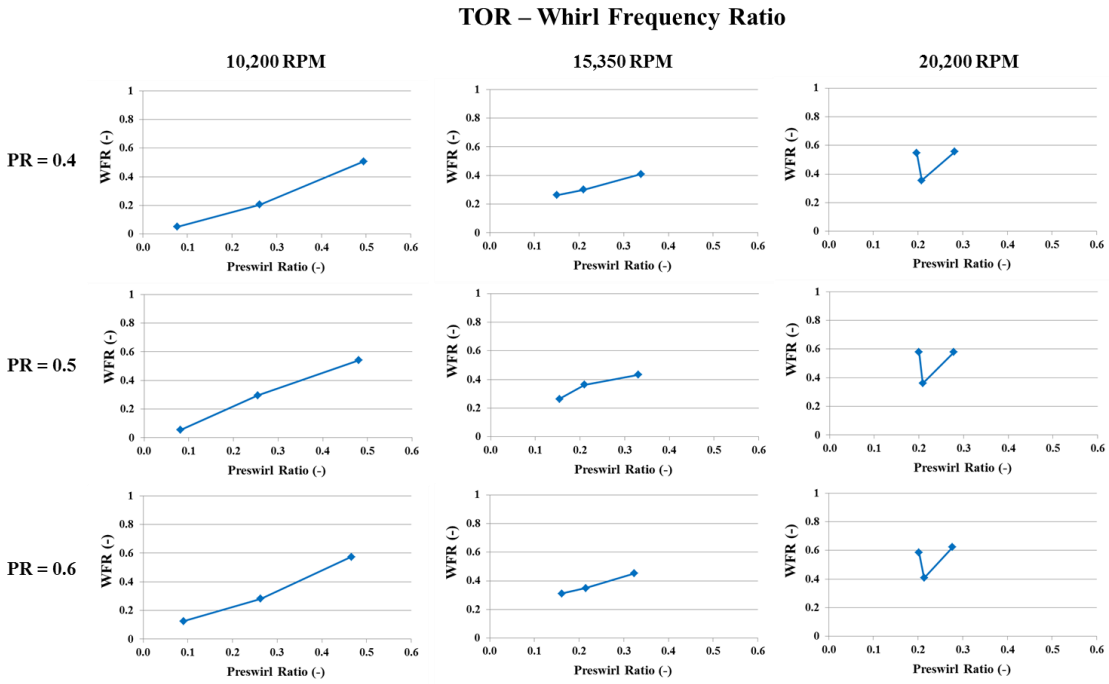

Figure 21. TOR whirl frequency ratio versus *PSR*, ω, and *PR* - 70 bar supply pressure and 0.1 mm radial clearance

4.6 Leakage

Figure **22** shows the TOR labyrinth seal mass flow leakage as calculated by Equation (23), from the measured volumetric flow rate, temperatures, and pressures. The leakage slightly decreases with increasing ω due to the centrifugal growth of the rotor. Also, although not expected, the leakage slightly increases from zero to medium preswirl, and then reduces from medium to high preswirl. Picardo [3] and Mehta [4] also saw a similar trend, but the increase from zero to medium preswirl was not as pronounced. Lastly, as expected the leakage decreases as the pressure ratio increases.

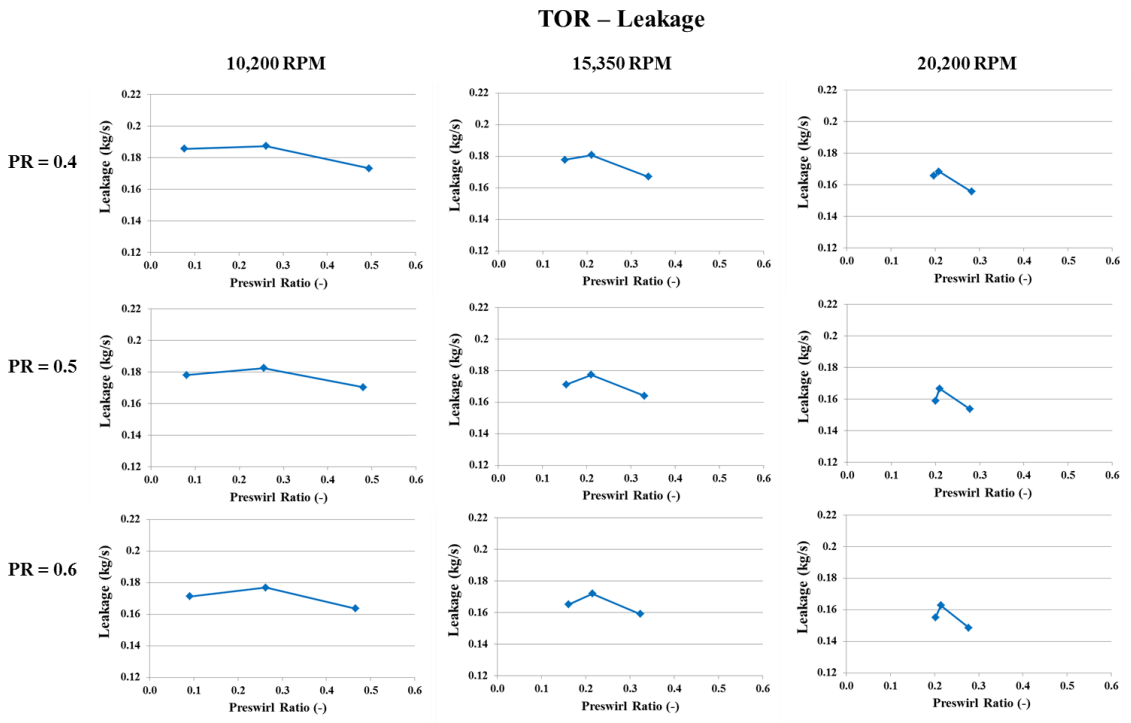

Figure 22. TOR leakage versus *PSR*, ω, and *PR* - 70 bar supply pressure and 0.1 mm radial clearance

5. TOR AND TOS LABYRINTH SEAL COMPARISONS

In this section, comparisons between the TOR test seal and Picardo's [3] TOS seal will be presented. As Picardo's tests were run about a decade prior to the TOR tests, Picardo's seals were remade and tested again on the current AGSTS. Tests were rerun at medium preswirl and identical conditions to those run for the TOR, which were previously shown in Table 2. The retests yielded very similar rotordynamic coefficients and leakage rates to the original tests run by Picardo [3].

A comparison of critical dimensions between the TOR and TOS seals is provided in Table 4. Although both test seals have roughly the same diameter, the TOR seal is shorter in overall length by about 17%. The TOR seal also has fewer number of teeth (14), shorter teeth, and a smaller tooth-cavity axial length. The profile shape of the TOR teeth is also considerably different, as can be seen in Figure 23. The TOR teeth have a sharp vertical leading edge followed by a chamfered trailing edge, whereas Picardo's [3] TOS teeth had a triangular profile.

Table 4. Comparison of critical dimensions between the TOR and TOS test seals

	TOR	TOS
Diameter (mm)	114.3	114.3
Total Length (mm)	71.44	85.73
L/D (-)	0.62	0.75
Rad. Clearance (mm)	0.1	0.1
No. of Teeth (-)	14	20
Tooth Height (mm)	2.41	4.29
Cavity Length (mm)	3.18	4.29

TOR Tooth Profile **TOS Tooth Profile [3]**

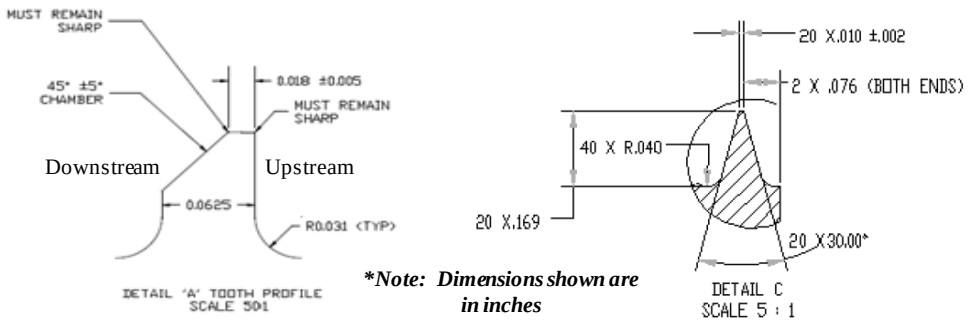

Figure 23. Tooth profile comparison between the TOR and TOS test seals

In the following subsections, all stiffness coefficients were non-dimensionalized and damping coefficients were normalized to account for the difference in overall seal length. The non-dimensional direct and cross-coupled stiffness coefficients are taken from Childs [2] as

$$K^* = K\left(\frac{C_r}{\Delta P \cdot D_s \cdot L}\right) \tag{29}$$

$$k^* = k\left(\frac{C_r}{\Delta P \cdot D_s \cdot L}\right) \tag{30}$$

where K^* and k^* are non-dimensional direct and cross-coupled stiffness, respectively. C_r is the seal radial clearance, ΔP is the pressure drop across the seal, D_s is the seal diameter, and L is the seal length. Normalized direct and effective damping coefficients are defined by

$$C^* = C\left(\frac{C_r}{\Delta P \cdot D_s \cdot L}\right) \tag{31}$$

$$C^*_{eff} = C_{eff}\left(\frac{C_r}{\Delta P \cdot D_s \cdot L}\right) \tag{32}$$

where C^* and C^*_{eff} are normalized direct and effective damping, respectively. Note that the unit of normalized damping is seconds. Measured leakage rates have also been non-dimensionalized via a flow coefficient defined by

$$\Phi = \frac{\dot{m}}{\pi D_s C_r} \sqrt{\frac{R_a T_{in}}{2 P_{in} \Delta P}} \tag{33}$$

where $\dot{m}$ is the seal mass leakage rate, R_a is the ideal gas constant of air, T_{in} is the seal inlet temperature, and P_{in} is the seal inlet pressure.

In the plots of the following subsections, the data is reported differently than the prior section since the comparisons are being made at only medium preswirl. Data are plotted versus rotor speed on each graph, while the pressure ratio changes from graph to graph.

5.1 TOR vs. TOS - Non-Dimensional Direct Stiffness

Comparisons of K^* are shown in Figure 24. Contrary to the TOS seal, K^* for the TOR seal starts out positive at 10.2 kRPM and becomes negative as ω increases. The magnitude of K^* for the TOR is always larger than that of the TOS, but the difference reduces with increasing ω. *PR* imparts little impact on K^*. Also, as expected for labyrinth seals, the magnitude of K^* for both seals is small when compared to hole-pattern and smooth seals.

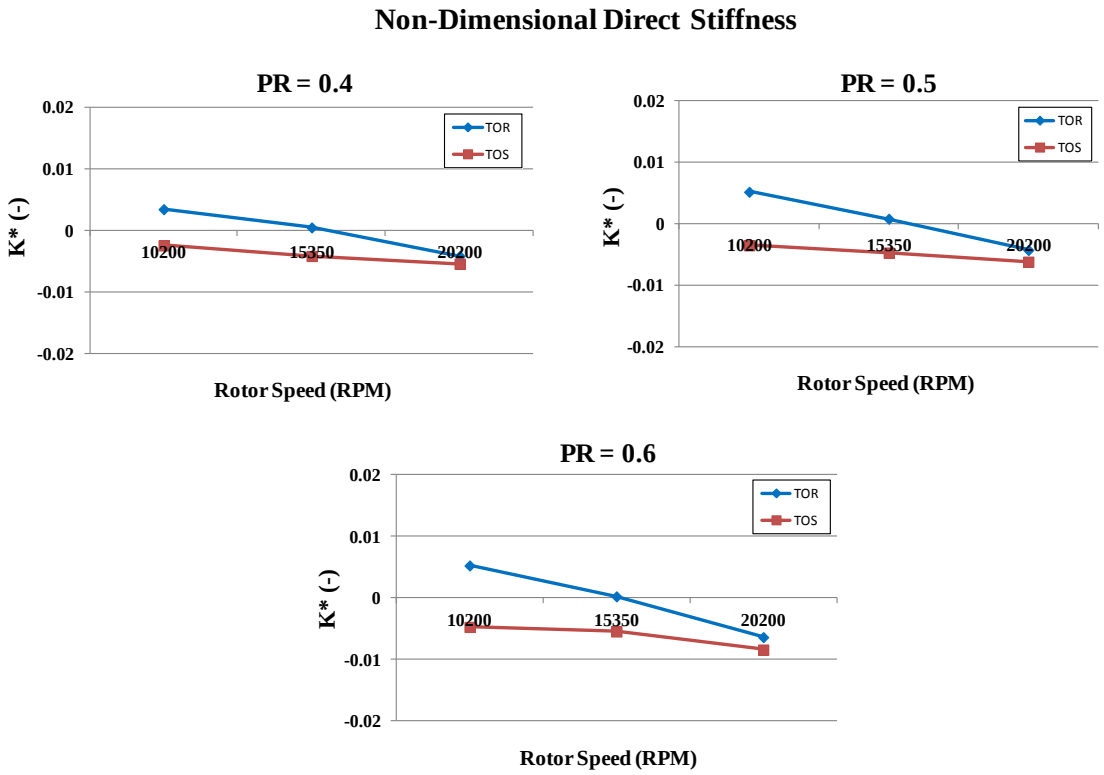

Figure 24. TOR vs. TOS - Non-dimensional direct stiffness versus ω and *PR* at 70 bar supply pressure and medium preswirl

5.2 TOR vs. TOS - Non-Dimensional Cross-Coupled Stiffness

Figure 25 shows comparisons of k^*, which (along with direct damping) is of prime importance when assessing the stability seals. k^* for the TOR seal is only slightly higher than the TOS seal at 10.2 kRPM, but becomes twice as large as the TOS seal at the highest ω of 20.2 kRPM. Increases in *PR* lead to increased k^* because pressure drop is included in Equation (30). *PR* has little influence on dimensional cross-coupled stiffness. As the pressure drop decreases with increased *PR*, the denominator of Equation (30) decreases and the magnitude of k^* increases.

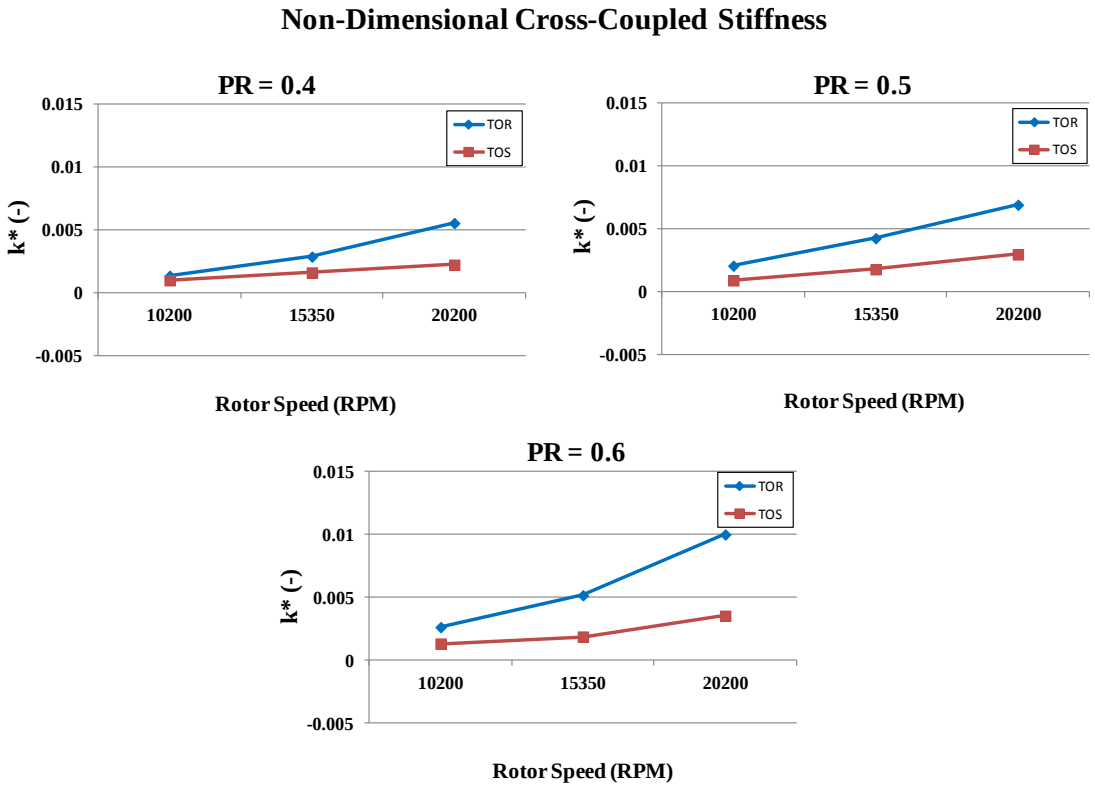

Figure 25. TOR vs. TOS - Non-dimensional cross-coupled stiffness versus ω and *PR* at 70 bar supply pressure and medium preswirl

5.3 TOR vs. TOS - Normalized Direct Damping

The remaining factor needed to assess the stability of seals is direct damping. Plots of C^* are shown in Figure 26. Results show that C^* for the TOR seal is higher than the TOS seal by a factor of about 2 at all speeds. In general, C^* increases with ω at about the same rate for both seals. The next subsection will present final stability comparisons between the seals by combining the effects of cross-coupled stiffness and direct damping to determine effective damping.

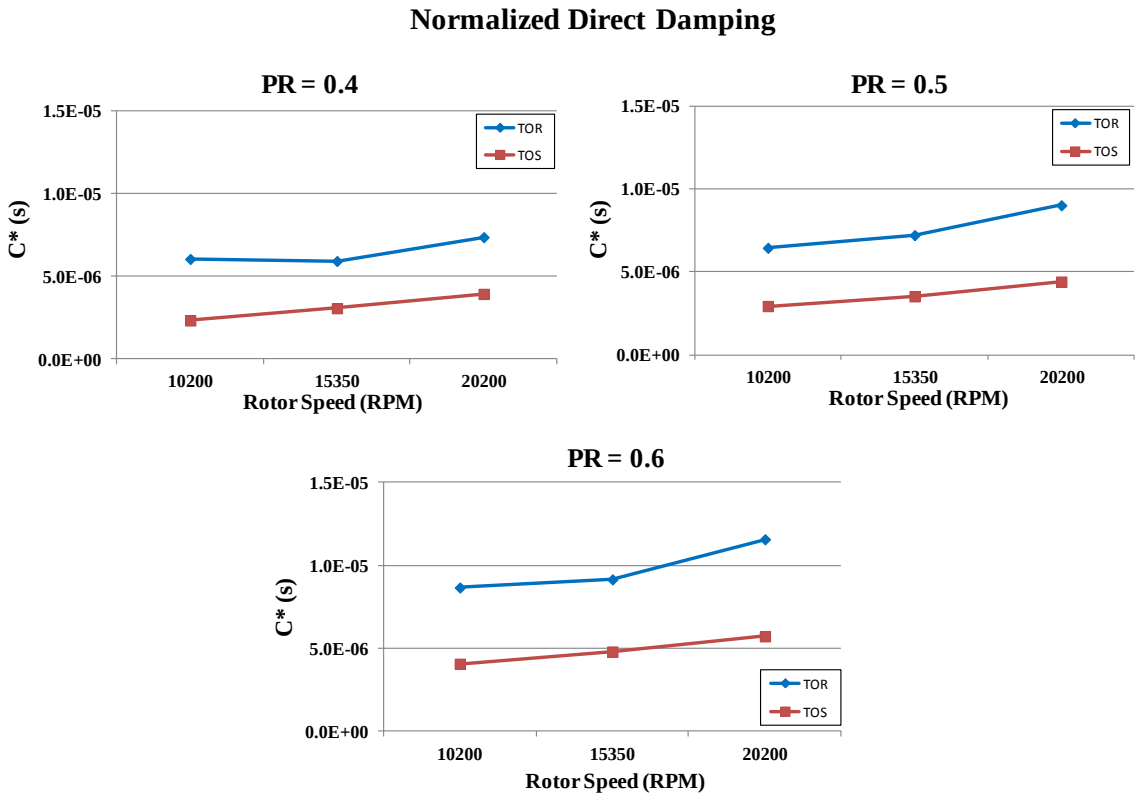

Figure 26. TOR vs. TOS - Normalized direct damping versus ω and *PR* at 70 bar supply pressure and medium preswirl

5.4 TOR vs. TOS - Normalized Effective Damping

The best measure of stability for seals is C_{eff}, which was defined earlier by Equation (5). C_{eff} considers both k (destabilizing) and C (stabilizing) to determine an effective damping contribution from the seal. C_{eff} was normalized via Equation (31) and is plotted for both seals in Figure 27.

The results show that the TOR seal has higher effective damping than the TOS seal across all ω. This is predominantly because the TOR C measurements were higher than those measured for the TOS seal. C_{eff}^{*} tends to slightly increase with increasing ω and *PR* for both seals.

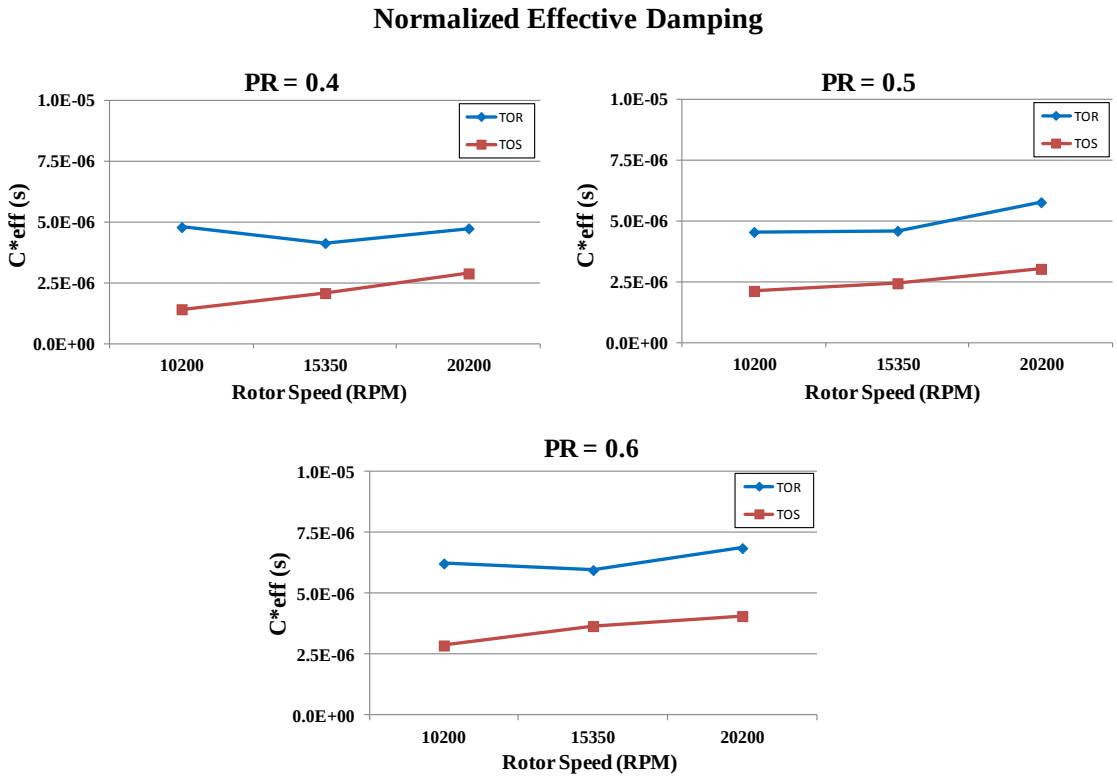

Figure 27. TOR vs. TOS - Normalized effective damping versus ω and *PR* at 70 bar supply pressure and medium preswirl

5.5 TOR vs. TOS - Leakage Flow Coefficient

Leakage data has been presented in terms of Φ and is shown in Figure 28. Φ for the TOR seal is approximately 5-15% less than that of the TOS seal. The difference in Φ between both seals tends to decrease with increasing *PR*. For both test seals, Φ decreases with increasing ω because $\dot{m}$ decreases due to shaft centrifugal growth.

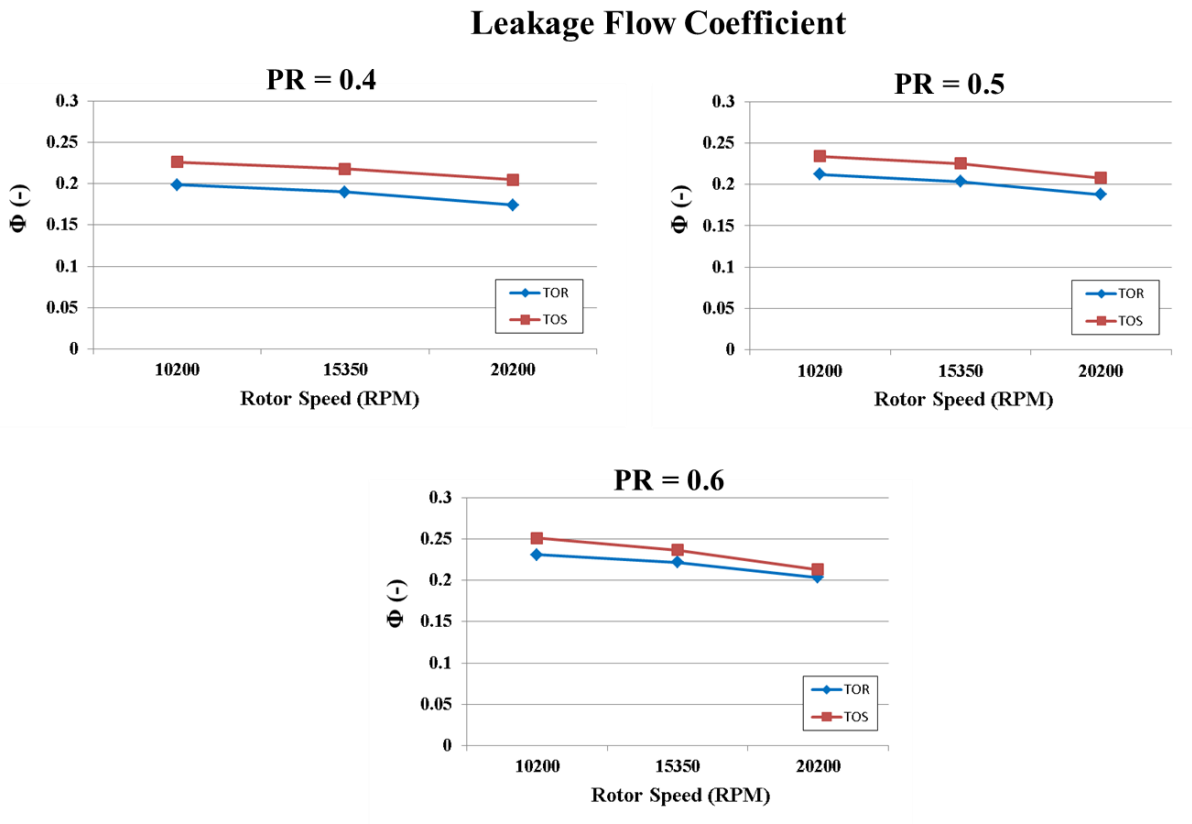

Figure 28. TOR vs. TOS - Leakage flow coefficient versus ω and *PR* at 70 bar supply pressure and medium preswirl

6. PREDICTIONS VERSUS MEASUREMENTS

Predictions of rotordynamic coefficients and leakage rates for the TOR and TOS test seals were generated by XLLaby, which is based on a 1-control volume model derived by Childs and Scharrer [9]. An example screenshot of the inputs from XLLaby is shown in Figure 29 for the TOR seal, and Figure 30 for the TOS seal. For simplicity, predictions were only generated for medium preswirl and 0.5 pressure ratio. Note that the predictions assume that the test fluid (air) is an ideal gas, the rotor and stator surfaces are smooth, and the temperature and viscosity of the air remains constant during each test sequence.

Select units: SI Units

Select Leakage Model: Gamal Model

Use High Mach number: ☑

Seal Radius	57.3532	mm	Ratio of Specific Heats	1.4	--
Tooth Location	Rotor	--	Gas Constant	286.9	J/kg/K
Number of Teeth	14	--	Compressibility Factor	1	--
Axial Cavity Length	3.175	mm	Kinematic Viscosity	1.51E-05	m^2/s
Tooth Height	2.413	mm	Reservoir Temperature	288	K
Stator Friction Constant	0.079	--	Reservoir Pressure	70	bar
Stator Friction Exponent	-0.25	--	Sump Pressure	35	bar
Rotor Friction Constant	0.079	--	Inlet Tangential Velocity Ratio	0.255	--
Rotor Friction Exponent	-0.25	--	Use Correction Factors?	No	--
			Whirl Speed	10200	rpm

Figure 29. Screenshot of XLLaby inputs used to generate predictions for the TOR test seal

Select units: SI Units

Select Leakage Model: Gamal Model

Use High Mach number: ☑

Seal Radius	57.3532	mm	Ratio of Specific Heats	1.4	--
Tooth Location	Stator	--	Gas Constant	286.9	J/kg/K
Number of Teeth	20	--	Compressibility Factor	1	--
Axial Cavity Length	4.2926	mm	Kinematic Viscosity	1.51E-05	m^2/s
Tooth Height	4.2926	mm	Reservoir Temperature	288	K
Stator Friction Constant	0.079	--	Reservoir Pressure	70	bar
Stator Friction Exponent	-0.25	--	Sump Pressure	35	bar
Rotor Friction Constant	0.079	--	Inlet Tangential Velocity Ratio	0.294	--
Rotor Friction Exponent	-0.25	--	Use Correction Factors?	No	--
			Whirl Speed	10200	rpm

Figure 30. Screenshot of XLLaby inputs used to generate predictions for the TOS test seal

6.1 Predictions vs. Measurements - Direct and Cross-Coupled Stiffness

XLLaby predictions for *K* and *k* are plotted against measurements in Figure 31. *K* is vastly under-predicted for the TOR seal for all ω. For the TOS seal, *K* is accurately predicted at 10.2 kRPM but is under-predicted as ω increases. Note that for both seals, *K* is too small to influence critical speed locations.

At lower ω, *k* is under-predicted for the TOR seal more so than the TOS seal. However, at the highest ω, *k* is just slightly under-predicted for both seals. Also at the highest ω, XLLaby agrees with measurements in that it predicts the TOR *k* to be twice that of the TOS seal.

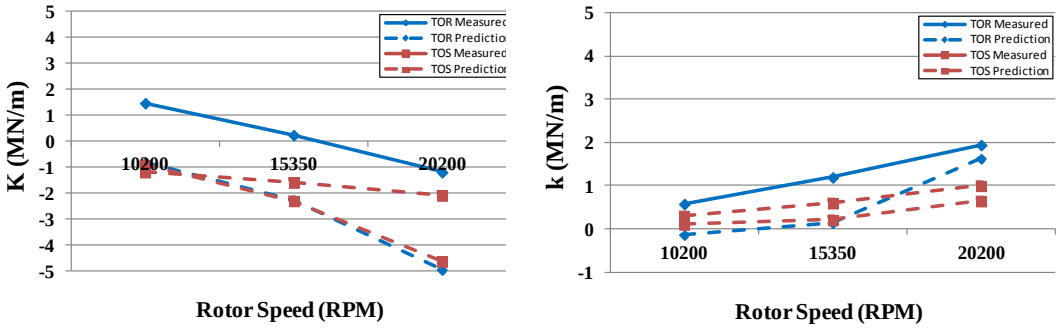

Figure 31. XLLaby predictions versus measurements of *K* and *k* for the TOR and TOS seal - Medium preswirl and PR=0.5

6.2 Predictions vs. Measurements - Direct and Effective Damping

Figure 32 shows comparisons between XLLaby predictions and measurements for *C* and C_{eff}. For both the TOR and TOS seals, *C* and C_{eff} are under-predicted by a factor of roughly 2. However, XLLaby predicts the TOR seal to have higher *C* than the TOS seal. Also, since XLLaby predicts higher C_{eff} for the TOR seal, predictions agree with measurements that the TOR seal is more stable than the TOS seal.

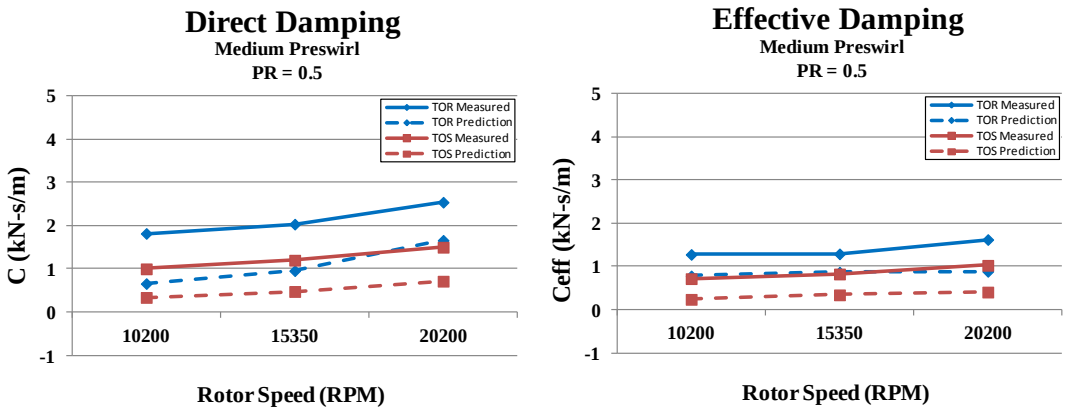

Figure 32. XLLaby predictions versus measurements of *C* and *Ceff* for the TOR and TOS seal - Medium preswirl and PR=0.5

6.3 Predictions vs. Measurements - Leakage Mass Flow Rate

XLLaby predictions for seal leakage mass flow rates are plotted against measurements in Figure 33. The TOR seal leakage rate is over-predicted by roughly 15% at the highest ω, whereas the TOS leakage rate is under-predicted by roughly 20% at the lowest ω. XLLaby predicts the TOR leakage rate to be higher than that of the TOS seal. This does not agree with measurements since the measured TOR leakage rate was actually lower than the TOS leakage rate.

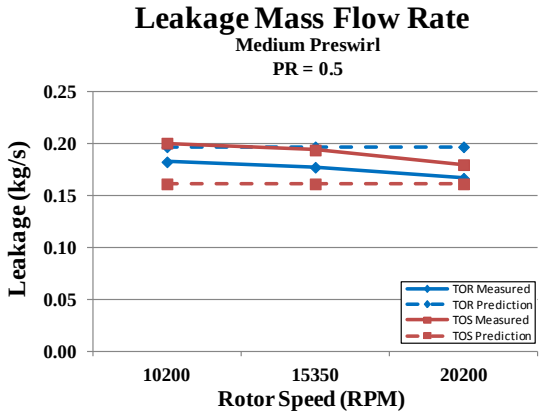

Figure 33. XLLaby predictions versus measurements of leakage mass flow for the TOR and TOS seal - Medium preswirl and PR=0.5

7. SUMMARY AND CONCLUSIONS

Experimental results show that at the lowest rotor speed, The TOR labyrinth cross-coupling stiffness was just slightly higher than the TOS labyrinth. At higher rotor speeds, this gap increased as the TOR labyrinth cross-coupling increased at a higher rate. However, at all rotor speeds, measurements of direct damping were greater for the TOR labyrinth leading to higher effective damping across all speeds. Due to this finding, the TOR labyrinth was deemed to be more stable than the TOS labyrinth. The TOR labyrinth leaked approximately 5-10% less than the TOS labyrinth at all test conditions.

The XLLaby 1-CVM prediction code underpredicted cross-coupling stiffness and direct damping for both seals, but agreed with measurements in that it predicted the TOR labyrinth to have higher C_{eff} values. Leakage rate was overpredicted for the TOR labyrinth and underpredicted for the TOS labyrinth.

To expand on this work, further CFD investigations are needed to investigate the shortcomings of the 1-control volume and to examine the effects of tooth design on the rotordynamic and leakage performance of both test seals. These effects include tooth count, tooth height, tooth shape and axial cavity length.

REFERENCES

[1] Kirk, G. (1987), "A Method for Calculating Labyrinth Seal Inlet Swirl Velocity," Rotating Machinery Dynamics, 2, ASME, pp. 345-350.

[2] Childs, D. (1993), *Turbomachinery Rotordynamics – Phenomena, Modeling and Analysis*, John Wiley & Sons, New York.

[3] Picardo, A.M. (2003), "High Pressure Testing of See-Through Labyrinth Seals," MS Thesis, Department of Mechanical Engineering, Texas A&M University, College Station.

[4] Mehta, N.J. (2012), "Comparison of a Slanted-Tooth See-Through Labyrinth Seal to a Straight-Tooth See-Through Labyrinth Seal for Rotordynamic Coefficients and Leakage," MS Thesis, Department of Mechanical Engineering, Texas A&M University, College Station.

[5] Childs, D., and Scharrer, J. (1986), "Experimental Rotordynamic Coefficient Results for Teeth-on-Rotor and Teeth-on-Stator Labyrinth Gas Seals," Journal of Engineering for Gas Turbines and Power, 108, pp. 599-604.

[6] Hawkins, L., Childs, D., and Hale, K. (1988), "Experimental Results for Labyrinth Gas Seals With Honeycomb Stators: Comparisons to Smooth Stator Seals and Theoretical Predictions," *ASME, J. of Tribology*, 111 (1), pp. 161-168.

[7] Kwanka, K. (1997), "Rotordynamic Impact of Swirl Brakes on Labyrinth Seals with Smooth or Honeycomb Stators," Paper number 97-GT-232, Transactions of the ASME International Gas Turbine & Aeroengine Congress & Exhibition.

[8] Childs, D., and Wade, J. (2004), "Rotordynamic-Coefficient and Leakage

Characteristics for Hole-Pattern-Stator Annular Gas Seals-Measurements Versus Predictions," ASME J. of Tribology, **126**, pp. 326-333

[9] Wilkes, J. (2011), Private Correspondence

[10] Kurtin, K.A., Childs, D.W., San Andres, L.A., and Hale, R.K. (1993), "Experimental Versus Theoretical Characteristics of a High-Speed Hybrid (Combination Hydrostatic and Hydrodynamic) Bearing," ASME J. of Tribology, 115, pp. 160-169.

[11] Stanway, R., Burrows, C., and Holmes, R. (1978), "Pseudo-random Binary Sequence Forcing in Journal and Squeeze Film Bearings," Proceedings of the ASME Annual meeting, 78-AM-2A-1

[12] Childs, D., and Scharrer, J. (1986), "Iwatsubo-Based Solution for Labyrinth Seals: Comparison to Experimental Results," Journal of Engineering for Gas Turbines and Power, Transactions of the ASME, 108, pp. 325-331.

APPENDIX

Table 5. Raw data for TOR labyrinth seal at 10,200 rpm, 0.4 PR, and zero preswirl

Freq	Re Hxx	Re Hxy	Re Hyx	Re Hyy	Im Hxx	Im Hxy	Im Hyx	Im Hyy	Re eHxx	Re eHxy	Re eHyx	Re eHyy	Im eHxx	Im eHxy	Im eHyx	Im eHyy
Hz	N/m	N/m	N/m	N/m	N/m	N/m	N/m	N/m	N/m	N/m	N/m	N/m	N/m	N/m	N/m	N/m
9.8	1.7E+06	-2.0E+05	-9.2E+05	2.1E+06	4.0E+04	3.4E+05	-2.4E+05	-2.0E+05	-9.7E+04	-1.7E+05	-7.4E+04	-1.2E+05	-1.1E+05	-8.7E+04	-7.7E+04	-1.0E+05
19.5	1.2E+06	8.6E+04	-5.9E+05	1.9E+06	-2.7E+05	4.5E+05	1.0E+05	-1.0E+05	-3.0E+05	-9.8E+04	-2.0E+05	-1.1E+05	-3.4E+05	-1.0E+05	-2.7E+05	-7.8E+04
29.3	1.6E+06	7.4E+04	-1.0E+06	2.1E+06	1.9E+05	3.6E+05	-2.3E+05	-2.4E+04	-7.3E+04	-1.1E+05	-8.3E+04	-1.1E+05	-1.4E+05	-1.3E+05	-6.7E+04	-1.2E+05
39.1	1.4E+06	2.3E+05	-1.1E+06	2.0E+06	9.4E+04	6.6E+05	-8.9E+04	1.7E+05	-1.7E+05	-1.1E+05	-2.1E+05	-1.4E+05	-1.4E+05	-6.3E+04	-6.4E+04	-6.2E+04
48.8	1.4E+06	3.9E+05	-7.9E+05	1.9E+06	5.9E+04	5.8E+05	-4.8E+05	3.0E+05	-1.6E+05	-8.4E+04	-1.9E+05	-7.8E+04	-1.7E+05	-1.0E+05	-1.9E+05	-9.1E+04
58.6	1.3E+06	2.8E+05	-7.3E+05	2.0E+06	8.9E+04	7.8E+05	-7.1E+05	2.5E+05	-2.3E+05	-5.3E+04	-2.5E+05	-8.3E+04	-2.7E+05	-1.1E+05	-2.3E+05	-1.0E+05
68.4	1.2E+06	3.4E+05	-8.9E+05	1.8E+06	3.8E+05	6.0E+05	-6.0E+05	2.7E+05	-1.5E+05	-8.2E+04	-9.1E+04	-9.1E+04	-8.9E+04	-7.9E+04	-6.7E+04	-5.7E+04
78.1	1.0E+06	-3.7E+05	-7.8E+04	1.4E+06	1.4E+06	3.0E+05	-6.8E+05	1.1E+06	-1.3E+05	-8.0E+04	-1.6E+05	-7.7E+04	-2.5E+05	-8.1E+04	-2.0E+05	-8.5E+04
87.9	1.6E+06	-7.9E+04	-6.3E+05	2.0E+06	1.2E+06	1.0E+06	-1.4E+06	8.5E+05	-9.1E+04	-6.2E+04	-1.0E+05	-7.7E+04	-9.9E+04	-6.1E+04	-1.6E+05	-7.3E+04
97.7	1.4E+06	-1.5E+05	-8.4E+05	1.7E+06	8.3E+05	1.0E+06	-1.6E+06	8.2E+05	-8.2E+04	-6.7E+04	-6.6E+04	-7.2E+04	-1.0E+05	-6.4E+04	-1.4E+05	-7.5E+04
107.4	1.4E+06	4.2E+04	-6.9E+05	1.9E+06	1.4E+06	1.2E+06	-1.9E+06	1.3E+06	-7.0E+04	-4.6E+04	-7.4E+04	-5.5E+04	-5.9E+04	-7.3E+04	-4.2E+04	-5.6E+04
117.2	1.8E+06	-1.1E+05	-1.1E+06	2.0E+06	1.4E+06	1.4E+06	-1.8E+06	1.3E+06	-5.2E+04	-5.1E+04	-2.9E+04	-5.9E+04	-4.2E+04	-4.7E+04	-5.5E+04	-5.0E+04
127.0	2.0E+06	-1.6E+05	-1.3E+06	2.2E+06	1.4E+06	1.7E+06	-1.8E+06	1.3E+06	-3.6E+04	-5.7E+04	-8.0E+04	-6.3E+04	-4.8E+04	-4.3E+04	-5.3E+04	-4.7E+04
136.7	2.2E+06	-3.6E+05	-1.8E+06	2.5E+06	1.5E+06	2.0E+06	-1.9E+06	1.2E+06	-4.2E+04	-5.5E+04	-5.4E+04	-5.8E+04	-5.2E+04	-5.8E+04	-4.1E+04	-6.7E+04
146.5	1.8E+06	1.3E+05	4.4E+04	2.6E+06	4.6E+05	2.7E+06	-1.0E+06	1.1E+06	-4.0E+04	-4.5E+04	-4.1E+04	-6.7E+04	-3.2E+04	-5.2E+04	-3.7E+04	-4.6E+04
156.3	9.9E+05	9.6E+05	-3.3E+05	1.4E+06	2.9E+06	1.4E+06	-3.2E+06	2.4E+06	-7.2E+04	-8.3E+04	-6.7E+04	-8.5E+04	-6.3E+04	-8.0E+04	-9.5E+04	-9.4E+04
166.0	3.3E+05	1.9E+06	2.2E+05	9.4E+05	1.5E+06	2.7E+06	-2.5E+06	3.1E+06	-1.4E+05	-8.0E+04	-1.1E+05	-1.2E+05	-1.1E+05	-1.0E+05	-1.3E+05	-9.4E+04
175.8	2.4E+06	3.6E+05	-1.7E+06	2.9E+06	2.0E+06	2.2E+06	-2.6E+06	2.3E+06	-9.4E+04	-8.1E+04	-6.6E+04	-7.1E+04	-8.1E+04	-9.5E+04	-3.9E+04	-7.0E+04
185.5	1.2E+06	2.2E+06	5.2E+05	-3.3E+05	1.6E+06	3.6E+06	-2.3E+06	9.1E+05	-4.1E+04	-5.4E+04	-5.9E+04	-7.0E+04	-4.8E+04	-5.1E+04	-5.8E+04	-5.2E+04
195.3	2.8E+06	9.2E+05	-1.5E+06	2.3E+06	2.0E+06	3.3E+06	-2.9E+06	1.5E+06	-6.0E+04	-7.9E+04	-4.9E+04	-6.6E+04	-7.8E+04	-7.9E+04	-5.3E+04	-5.3E+04
205.1	3.2E+06	2.3E+06	-9.7E+05	3.1E+06	2.8E+05	1.7E+06	-4.0E+06	1.0E+06	-6.0E+04	-7.2E+04	-5.5E+04	-6.4E+04	-8.5E+04	-7.0E+04	-8.0E+04	-8.2E+04
214.8	1.5E+06	1.4E+05	-2.0E+06	1.8E+06	2.1E+06	3.4E+06	-3.0E+06	2.2E+06	-5.3E+04	-5.9E+04	-2.7E+04	-5.2E+04	-5.1E+04	-5.9E+04	-3.0E+04	-4.9E+04
224.6	1.6E+06	5.7E+05	-1.9E+06	2.2E+06	2.1E+06	4.0E+06	-3.1E+06	2.5E+06	-4.7E+04	-5.8E+04	-2.8E+04	-8.7E+04	-3.9E+04	-8.3E+04	-3.8E+04	-6.5E+04

Table 6. Raw data for TOR labyrinth seal at 15,350 rpm, 0.4 PR, and zero preswirl

Freq	Re Hxx	Re Hxy	Re Hyx	Re Hyy	Im Hxx	Im Hxy	Im Hyx	Im Hyy	Re eHxx	Re eHxy	Re eHyx	Re eHyy	Im eHxx	Im eHxy	Im eHyx	Im eHyy
Hz	N/m	N/m	N/m	N/m	N/m	N/m	N/m	N/m	N/m	N/m	N/m	N/m	N/m	N/m	N/m	N/m
9.8	4.1E+05	4.5E+04	-1.6E+06	1.0E+06	-1.6E+05	6.8E+05	-1.6E+05	-2.9E+04	-9.2E+04	-1.4E+05	-8.1E+04	-1.9E+05	-1.2E+05	-1.5E+05	-6.7E+04	-6.3E+04
19.5	1.4E+05	6.6E+05	-1.2E+06	7.8E+05	-3.1E+05	5.8E+05	-4.6E+05	1.1E+05	-2.3E+05	-8.9E+04	-1.4E+05	-8.0E+04	-2.3E+05	-7.6E+04	-2.0E+05	-5.5E+04
29.3	1.3E+05	5.9E+05	-1.6E+06	1.0E+06	1.1E+05	6.6E+05	-6.5E+05	8.4E+04	-6.4E+04	-7.8E+04	-9.4E+04	-9.1E+04	-1.2E+05	-9.0E+04	-7.2E+04	-5.3E+04
39.1	7.8E+04	7.2E+05	-1.6E+06	7.0E+05	1.3E+05	1.1E+06	-5.8E+05	1.9E+05	-2.3E+05	-5.4E+04	-1.5E+05	-9.4E+04	-7.5E+04	-7.7E+04	-5.5E+04	-5.8E+04
48.8	4.2E+05	7.3E+05	-1.5E+06	6.8E+05	2.0E+05	1.1E+06	-1.1E+06	3.2E+05	-1.5E+05	-5.4E+04	-1.3E+05	-8.0E+04	-1.6E+05	-7.1E+04	-1.7E+05	-9.9E+04
58.6	4.3E+04	5.9E+05	-1.6E+06	8.0E+05	6.4E+05	1.3E+06	-1.6E+06	5.5E+05	-1.5E+05	-8.3E+04	-1.9E+05	-9.8E+04	-1.8E+05	-9.0E+04	-2.5E+05	-7.0E+04
68.4	1.8E+05	7.3E+05	-1.7E+06	6.8E+05	6.2E+05	1.5E+06	-1.6E+06	3.0E+05	-1.0E+05	-6.2E+04	-6.8E+04	-7.6E+04	-8.0E+04	-5.9E+04	-5.7E+04	-7.1E+04
78.1	3.6E+04	8.2E+05	-1.6E+06	7.7E+05	8.7E+05	1.6E+06	-1.5E+06	5.5E+05	-1.4E+05	-6.8E+04	-1.2E+05	-7.1E+04	-1.7E+05	-7.2E+04	-1.8E+05	-6.3E+04
87.9	2.7E+05	7.5E+05	-2.0E+06	5.1E+05	8.9E+05	1.7E+06	-2.1E+06	6.3E+05	-8.8E+04	-5.3E+04	-6.0E+04	-9.2E+04	-9.2E+04	-4.9E+04	-9.0E+04	-4.2E+04
97.7	8.0E+04	7.0E+05	-2.1E+06	2.4E+05	7.1E+05	1.8E+06	-2.3E+06	7.1E+05	-5.1E+04	-3.8E+04	-8.7E+04	-6.6E+04	-7.5E+04	-4.4E+04	-8.5E+04	-4.6E+04
107.4	-2.0E+05	8.3E+05	-2.0E+06	3.6E+05	9.6E+05	2.0E+06	-2.3E+06	1.2E+06	-9.5E+04	-4.1E+04	-6.3E+04	-6.6E+04	-3.5E+04	-4.5E+04	-4.6E+04	-4.8E+04
117.2	-2.6E+04	7.6E+05	-2.1E+06	2.9E+05	1.4E+06	2.0E+06	-2.2E+06	1.3E+06	-7.5E+04	-4.8E+04	-5.1E+04	-6.2E+04	-4.5E+04	-6.3E+04	-8.4E+04	-4.0E+04
127.0	-2.9E+05	1.4E+05	-1.8E+06	-7.2E+04	2.0E+06	2.0E+06	-2.0E+06	1.8E+06	-6.7E+04	-4.9E+04	-7.7E+04	-6.3E+04	-4.8E+04	-5.8E+04	-4.4E+04	-4.8E+04
136.7	8.1E+05	-2.4E+04	-2.4E+06	1.3E+06	2.0E+06	3.4E+06	-2.9E+06	1.8E+06	-6.3E+04	-4.5E+04	-4.7E+04	-7.9E+04	-4.1E+04	-6.9E+04	-4.8E+04	-5.6E+04
146.5	2.3E+05	6.6E+05	-6.8E+05	1.3E+06	5.1E+05	4.1E+06	-2.1E+06	1.5E+06	-5.1E+04	-7.0E+04	-4.3E+04	-8.2E+04	-4.7E+04	-6.0E+04	-3.9E+04	-4.5E+04
156.3	-7.8E+05	2.2E+06	-5.4E+05	-2.1E+05	2.1E+06	4.0E+06	-3.5E+06	2.0E+06	-4.0E+04	-6.3E+04	-7.7E+04	-9.2E+04	-6.1E+04	-6.2E+04	-7.8E+04	-9.3E+04
166.0	-4.6E+05	2.4E+06	-8.9E+05	-7.6E+05	2.3E+06	4.1E+06	-4.0E+06	2.9E+06	-5.3E+04	-5.2E+04	-5.3E+04	-7.1E+04	-7.5E+04	-5.4E+04	-5.4E+04	-4.5E+04
175.8	3.0E+04	-4.6E+05	-4.3E+05	4.6E+06	2.3E+06	1.9E+05	-4.2E+06	8.8E+06	-8.8E+04	-1.0E+05	-8.8E+04	-1.9E+05	-1.1E+05	-8.3E+04	-1.9E+05	-1.0E+05
185.5	-5.8E+04	2.9E+06	-5.2E+05	-1.3E+06	2.4E+06	5.3E+06	-3.9E+06	1.2E+06	-4.3E+04	-5.0E+04	-4.6E+04	-6.9E+04	-4.9E+04	-5.5E+04	-6.7E+04	-4.4E+04
195.3	1.5E+06	1.9E+06	-2.5E+06	1.2E+06	2.7E+06	5.2E+06	-4.5E+06	1.8E+06	-6.2E+04	-6.9E+04	-3.2E+04	-7.5E+04	-6.6E+04	-8.6E+04	-4.6E+04	-5.0E+04
205.1	2.1E+06	3.2E+06	-2.0E+06	2.0E+06	1.2E+06	3.3E+06	-5.8E+06	1.4E+06	-6.4E+04	-5.8E+04	-5.5E+04	-7.4E+04	-6.1E+04	-6.2E+04	-6.1E+04	-6.1E+04
214.8	3.1E+05	1.3E+06	-3.1E+06	6.2E+05	2.1E+06	5.0E+06	-4.7E+06	2.6E+06	-3.2E+04	-5.2E+04	-2.3E+04	-6.4E+04	-3.6E+04	-5.6E+04	-3.4E+04	-5.2E+04
224.6	2.3E+05	1.3E+06	-3.0E+06	9.8E+05	2.8E+06	5.7E+06	-5.0E+06	2.8E+06	-4.8E+04	-8.5E+04	-3.3E+04	-9.0E+04	-4.1E+04	-1.2E+05	-4.1E+04	-5.4E+04

Table 7. Raw data for TOR labyrinth seal at 20,200 rpm, 0.4 PR, and zero preswirl

Freq	Re Hxx	Re Hxy	Re Hyx	Re Hyy	Im Hxx	Im Hxy	Im Hyx	Im Hyy	Re eHxx	Re eHxy	Re eHyx	Re eHyy	Im eHxx	Im eHxy	Im eHyx	Im eHyy
Hz	N/m	N/m	N/m	N/m	N/m	N/m	N/m	N/m	N/m	N/m	N/m	N/m	N/m	N/m	N/m	N/m
9.8	-1.1E+06	1.7E+06	-2.7E+06	-9.7E+05	5.8E+04	2.1E+05	-2.2E+05	9.8E+04	-1.0E+05	-8.6E+04	-5.2E+04	-1.3E+05	-1.2E+05	-1.3E+05	-7.3E+04	-1.2E+05
19.5	-1.1E+06	1.8E+06	-2.7E+06	-9.5E+05	1.2E+05	4.5E+05	-1.1E+06	2.3E+05	-1.8E+05	-9.9E+04	-1.8E+05	-9.2E+04	-2.3E+05	-1.1E+05	-1.6E+05	-7.5E+04
29.3	-1.0E+06	1.7E+06	-2.8E+06	-7.6E+05	2.4E+05	6.6E+05	-9.3E+05	2.2E+05	-4.1E+04	-8.8E+04	-7.0E+04	-1.5E+05	-7.7E+04	-1.2E+05	-6.6E+04	-1.1E+05
39.1	-1.2E+06	1.9E+06	-3.1E+06	-1.0E+06	2.6E+05	1.1E+06	-9.3E+05	5.6E+05	-2.1E+05	-6.2E+04	-1.5E+05	-1.0E+05	-8.0E+04	-8.4E+04	-1.2E+05	-5.1E+04
48.8	-1.6E+06	2.1E+06	-3.0E+06	-1.2E+06	4.8E+05	1.2E+06	-1.3E+06	7.6E+05	-1.4E+06	-3.1E+05	-3.9E+05	-1.1E+05	-1.3E+06	-3.8E+05	-3.6E+05	-1.0E+05
58.6	-1.4E+06	1.9E+06	-2.4E+06	-8.3E+05	1.1E+06	1.4E+06	-1.3E+06	1.0E+06	-1.7E+05	-8.3E+04	-9.7E+04	-9.1E+04	-2.0E+05	-8.4E+04	-2.6E+05	-4.5E+04
68.4	-1.3E+06	1.8E+06	-3.0E+06	-9.0E+05	8.7E+05	1.8E+06	-1.9E+06	9.6E+05	-8.4E+04	-6.3E+04	-9.1E+04	-8.5E+04	-6.4E+04	-5.2E+04	-7.8E+04	-7.8E+04
78.1	-1.4E+06	1.9E+06	-3.1E+06	-9.2E+05	1.2E+06	1.9E+06	-1.9E+06	1.2E+06	-8.0E+04	-6.5E+04	-8.9E+04	-8.3E+04	-1.7E+05	-5.6E+04	-1.9E+05	-7.6E+04
87.9	-1.0E+06	1.9E+06	-3.0E+06	-8.6E+05	1.4E+06	2.1E+06	-2.5E+06	1.5E+06	-6.2E+04	-5.1E+04	-4.3E+04	-5.2E+04	-1.3E+05	-5.9E+04	-7.3E+04	-5.7E+04
97.7	-1.1E+06	1.8E+06	-3.3E+06	-1.0E+06	1.2E+06	2.1E+06	-2.8E+06	1.5E+06	-3.8E+05	-2.9E+05	-3.0E+05	-2.2E+05	-4.5E+05	-2.7E+05	-3.6E+05	-1.9E+05
107.4	-1.5E+06	2.0E+06	-3.0E+06	-8.0E+05	1.6E+06	2.5E+06	-2.9E+06	2.0E+06	-5.7E+04	-6.0E+04	-1.1E+05	-8.2E+04	-1.1E+05	-7.1E+04	-6.4E+04	-6.2E+04
117.2	-9.9E+05	1.8E+06	-3.2E+06	-6.9E+05	1.8E+06	2.9E+06	-3.1E+06	2.2E+06	-4.3E+04	-5.7E+04	-3.5E+04	-6.8E+04	-4.0E+04	-4.9E+04	-6.2E+04	-4.1E+04
127.0	-8.9E+05	1.6E+06	-3.2E+06	-3.9E+05	2.2E+06	3.3E+06	-3.2E+06	2.3E+06	-5.6E+04	-5.8E+04	-6.8E+04	-7.1E+04	-5.3E+04	-7.4E+04	-4.5E+04	-6.3E+04
136.7	-6.5E+05	1.6E+06	-3.9E+06	2.3E+04	2.2E+06	3.8E+06	-3.5E+06	2.1E+06	-5.3E+04	-5.7E+04	-6.4E+04	-7.5E+04	-3.7E+04	-6.4E+04	-5.4E+04	-5.3E+04
146.5	-1.2E+06	2.2E+06	-2.0E+06	7.2E+04	8.6E+05	4.6E+06	-2.8E+06	1.9E+06	-4.4E+04	-4.7E+04	-8.0E+04	-8.9E+04	-5.6E+04	-7.6E+04	-5.6E+04	-8.0E+04
156.3	-2.9E+06	4.2E+06	-1.5E+06	-1.9E+06	3.5E+06	3.6E+06	-5.3E+06	2.9E+06	-4.8E+04	-6.4E+04	-7.5E+04	-9.2E+04	-1.1E+05	-1.1E+05	-1.2E+05	-1.0E+05
166.0	-2.4E+06	4.1E+06	-2.1E+06	-1.9E+06	2.6E+06	4.6E+06	-4.7E+06	3.6E+06	-7.7E+04	-7.2E+04	-9.2E+04	-1.2E+05	-7.3E+04	-6.5E+04	-9.4E+04	-5.9E+04
175.8	-8.6E+05	-1.0E+06	-2.7E+06	4.0E+06	4.9E+06	3.2E+06	-7.0E+06	5.0E+06	-2.2E+05	-1.4E+05	-3.3E+05	-2.0E+05	-8.0E+04	-1.4E+05	-1.6E+05	-2.3E+05
185.5	-1.1E+06	3.8E+06	-1.3E+06	-2.6E+06	3.0E+06	6.6E+06	-5.3E+06	1.9E+06	-5.6E+04	-5.2E+04	-6.8E+04	-8.9E+04	-5.2E+04	-6.9E+04	-8.6E+04	-5.3E+04
195.3	3.6E+05	3.1E+06	-3.5E+06	4.3E+04	3.6E+06	6.8E+06	-5.9E+06	2.5E+06	-6.8E+04	-8.9E+04	-6.7E+04	-9.4E+04	-8.6E+04	-1.0E+05	-5.9E+04	-8.0E+04
205.1	9.0E+05	4.4E+06	-3.2E+06	7.8E+05	1.8E+06	4.9E+06	-7.2E+06	2.0E+06	-9.3E+04	-6.6E+04	-8.5E+04	-1.1E+05	-7.3E+04	-6.8E+04	-7.2E+04	-7.7E+04
214.8	-8.3E+05	2.5E+06	-4.4E+06	-6.5E+05	2.7E+06	6.7E+06	-6.1E+06	3.3E+06	-4.0E+04	-6.5E+04	-3.0E+04	-7.5E+04	-4.4E+04	-7.2E+04	-4.0E+04	-4.6E+04
224.6	-8.3E+05	2.6E+06	-4.1E+06	-1.8E+05	3.3E+06	7.3E+06	-6.5E+06	3.6E+06	-4.0E+04	-9.5E+04	-3.1E+04	-9.5E+04	-4.1E+04	-5.7E+04	-4.6E+04	-7.2E+04

Table 8. Raw data for TOR labyrinth seal at 10,200 rpm, 0.5 PR, and zero preswirl

Freq	Re Hxx	Re Hxy	Re Hyx	Re Hyy	Im Hxx	Im Hxy	Im Hyx	Im Hyy	Re eHxx	Re eHxy	Re eHyx	Re eHyy	Im eHxx	Im eHxy	Im eHyx	Im eHyy
Hz	N/m	N/m	N/m	N/m	N/m	N/m	N/m	N/m	N/m	N/m	N/m	N/m	N/m	N/m	N/m	N/m
9.8	1.8E+06	2.6E+05	-1.1E+06	1.9E+06	-5.3E+04	4.1E+05	-1.4E+04	-1.3E+05	-8.9E+04	-1.5E+05	-6.9E+04	-7.8E+04	-6.8E+04	-1.1E+05	-9.8E+04	-8.9E+04
19.5	1.8E+06	4.9E+05	-8.0E+05	1.6E+06	4.4E+05	4.1E+05	-4.0E+05	-1.8E+05	-3.1E+05	-1.8E+05	-2.2E+05	-1.3E+05	-2.1E+05	-1.7E+05	-2.3E+05	-1.3E+05
29.3	1.5E+06	2.9E+05	-9.7E+05	1.7E+06	2.2E+05	3.9E+05	-1.7E+05	6.7E+04	-1.1E+05	-7.9E+04	-1.2E+05	-6.7E+04	-9.2E+04	-1.5E+05	-9.1E+04	-1.1E+05
39.1	1.3E+06	2.0E+05	-8.3E+05	1.7E+06	3.6E+05	4.3E+05	-5.0E+05	3.4E+05	-1.4E+05	-1.0E+05	-1.5E+05	-4.5E+04	-1.2E+05	-9.8E+04	-1.2E+05	-6.2E+04
48.8	1.5E+06	2.4E+05	-8.2E+05	1.5E+06	2.0E+05	6.8E+05	-5.1E+05	2.4E+05	-5.3E+05	-8.1E+04	-4.0E+05	-1.0E+05	-1.9E+05	-1.0E+05	-2.0E+05	-6.5E+04
58.6	1.4E+06	1.4E+05	-1.1E+06	1.9E+06	3.1E+05	6.1E+05	-2.7E+05	3.7E+05	-1.9E+05	-7.6E+04	-3.5E+05	-6.6E+04	-2.2E+05	-6.9E+04	-2.6E+05	-1.3E+05
68.4	1.3E+06	2.8E+05	-9.9E+05	1.6E+06	4.6E+05	7.3E+05	-7.8E+05	2.8E+05	-7.0E+04	-7.6E+04	-1.4E+05	-6.4E+04	-1.3E+05	-7.6E+04	-9.8E+04	-6.3E+04
78.1	1.3E+06	-1.1E+05	-3.3E+05	1.2E+06	1.2E+06	3.9E+05	-7.6E+05	7.6E+05	-1.1E+05	-4.8E+04	-1.0E+05	-7.8E+04	-1.8E+05	-7.6E+04	-2.0E+05	-6.8E+04
87.9	1.6E+06	-7.7E+04	-4.7E+05	1.6E+06	1.2E+06	1.0E+06	-1.3E+06	8.2E+05	-9.9E+04	-6.3E+04	-1.4E+05	-6.5E+04	-1.6E+05	-7.2E+04	-1.2E+05	-6.7E+04
97.7	1.8E+06	-1.2E+05	-8.8E+05	1.5E+06	1.0E+06	1.1E+06	-1.7E+06	6.7E+05	-1.0E+05	-5.5E+04	-1.1E+05	-6.0E+04	-7.1E+04	-4.4E+04	-9.6E+04	-8.0E+04
107.4	1.4E+06	2.2E+05	-4.7E+05	1.6E+06	1.1E+06	1.1E+06	-1.7E+06	1.0E+06	-1.2E+05	-4.7E+04	-8.3E+04	-4.6E+04	-7.5E+04	-5.2E+04	-5.0E+04	-5.9E+04
117.2	1.8E+06	-4.1E+04	-1.0E+06	1.7E+06	1.3E+06	1.3E+06	-2.0E+06	1.3E+06	-3.1E+04	-4.5E+04	-5.7E+04	-4.6E+04	-3.5E+04	-3.6E+04	-4.3E+04	-6.9E+04
127.0	2.0E+06	-5.8E+04	-1.3E+06	1.8E+06	1.3E+06	1.8E+06	-1.8E+06	1.2E+06	-6.9E+04	-4.9E+04	-8.0E+04	-4.0E+04	-7.6E+04	-4.1E+04	-6.0E+04	-5.0E+04
136.7	2.1E+06	-3.1E+05	-1.7E+06	2.2E+06	1.3E+06	2.0E+06	-1.9E+06	1.2E+06	-5.2E+04	-3.8E+04	-3.3E+04	-3.3E+04	-3.1E+04	-4.7E+04	-4.5E+04	-4.3E+04
146.5	1.3E+06	1.6E+05	1.3E+05	2.3E+06	5.4E+04	2.7E+06	-1.1E+06	1.0E+06	-6.1E+04	-4.3E+04	-4.6E+04	-4.5E+04	-4.6E+04	-6.6E+04	-5.2E+04	-4.8E+04
156.3	8.8E+05	1.3E+06	9.2E+03	9.2E+05	3.8E+06	8.9E+05	-4.1E+06	2.9E+06	-6.2E+04	-7.0E+04	-5.5E+04	-5.9E+04	-7.1E+04	-7.7E+04	-5.1E+04	-5.0E+04
166.0	3.3E+05	1.8E+06	4.6E+04	1.3E+06	1.5E+06	2.0E+06	-2.7E+06	3.5E+06	-5.8E+04	-5.9E+04	-5.8E+04	-7.1E+04	-9.9E+04	-5.4E+04	-1.0E+05	-6.2E+04
175.8	2.0E+06	4.6E+05	-6.3E+05	2.1E+06	2.0E+06	1.9E+06	-3.1E+06	3.3E+06	-5.7E+04	-4.6E+04	-7.8E+04	-5.0E+04	-3.4E+04	-6.0E+04	-2.7E+04	-7.8E+04
185.5	1.0E+06	2.5E+06	6.2E+05	-1.1E+06	1.1E+06	3.8E+06	-1.8E+06	7.0E+05	-7.6E+04	-4.6E+04	-6.2E+04	-4.4E+04	-4.8E+04	-4.2E+04	-5.4E+04	-4.8E+04
195.3	2.7E+06	1.2E+06	-1.5E+06	2.0E+06	1.9E+06	3.5E+06	-2.7E+06	1.7E+06	-4.1E+04	-6.7E+04	-4.2E+04	-7.4E+04	-5.2E+04	-6.6E+04	-5.2E+04	-5.1E+04
205.1	3.3E+06	2.3E+06	-1.0E+06	3.1E+06	3.1E+05	1.8E+06	-3.9E+06	1.0E+06	-5.4E+04	-4.5E+04	-5.9E+04	-5.9E+04	-8.8E+04	-6.3E+04	-5.5E+04	-7.4E+04
214.8	1.4E+06	3.3E+05	-1.9E+06	1.8E+06	1.4E+06	3.5E+06	-2.8E+06	2.2E+06	-3.9E+04	-5.1E+04	-3.4E+04	-5.2E+04	-2.8E+04	-5.4E+04	-2.7E+04	-6.5E+04
224.6	1.7E+06	7.7E+05	-1.8E+06	2.1E+06	2.1E+06	4.0E+06	-3.0E+06	2.4E+06	-4.2E+04	-5.4E+04	-2.8E+04	-6.4E+04	-4.2E+04	-7.1E+04	-5.0E+04	-6.2E+04

Table 9. Raw data for TOR labyrinth seal at 15,350 rpm, 0.5 PR, and zero preswirl

Freq	Re Hxx	Re Hxy	Re Hyx	Re Hyy	Im Hxx	Im Hxy	Im Hyx	Im Hyy	Re eHxx	Re eHxy	Re eHyx	Re eHyy	Im eHxx	Im eHxy	Im eHyx	Im eHyy
Hz	N/m	N/m	N/m	N/m	N/m	N/m	N/m	N/m	N/m	N/m	N/m	N/m	N/m	N/m	N/m	N/m
9.8	5.2E+05	5.8E+05	-1.6E+06	7.5E+05	1.2E+04	2.8E+05	-1.5E+05	6.2E+04	-6.6E+04	-6.9E+04	-8.7E+04	-9.5E+04	-1.0E+05	-7.4E+04	-9.1E+04	-5.6E+04
19.5	5.2E+05	5.1E+05	-1.4E+06	7.1E+05	2.3E+05	5.0E+05	-5.6E+05	5.7E+04	-1.6E+05	-1.2E+05	-1.7E+05	-1.4E+05	-2.1E+05	-1.1E+05	-2.2E+05	-7.8E+04
29.3	4.6E+05	7.1E+05	-1.5E+06	5.4E+05	2.4E+05	8.9E+05	-7.2E+05	-1.5E+05	-1.2E+05	-1.0E+05	-1.1E+05	-6.8E+04	-7.4E+04	-8.5E+04	-7.1E+04	-6.5E+04
39.1	2.2E+05	8.1E+05	-1.7E+06	6.5E+05	3.0E+05	8.3E+05	-1.1E+06	3.2E+05	-1.7E+05	-6.2E+04	-1.8E+05	-3.9E+04	-1.4E+05	-6.5E+04	-1.9E+05	-7.4E+04
48.8	4.0E+05	7.9E+05	-1.8E+06	5.6E+05	4.4E+05	1.1E+06	-1.6E+06	2.9E+05	-2.1E+05	-9.3E+04	-3.6E+05	-5.3E+04	-1.7E+05	-5.7E+04	-2.3E+05	-7.0E+04
58.6	-1.8E+04	9.4E+05	-2.0E+06	6.8E+05	8.7E+05	1.3E+06	-1.1E+06	4.1E+05	-1.7E+05	-5.0E+04	-2.3E+05	-6.5E+04	-2.5E+05	-8.2E+04	-1.9E+05	-7.1E+04
68.4	1.6E+05	9.8E+05	-1.8E+06	6.5E+05	6.0E+05	1.6E+06	-1.5E+06	5.0E+05	-7.2E+04	-4.7E+04	-1.1E+05	-7.5E+04	-8.6E+04	-6.5E+04	-1.6E+05	-8.2E+04
78.1	2.3E+05	1.0E+06	-1.6E+06	4.8E+05	9.2E+05	1.5E+06	-1.6E+06	5.9E+05	-1.0E+05	-7.6E+04	-1.2E+05	-7.6E+04	-1.6E+05	-4.0E+04	-1.1E+05	-8.5E+04
87.9	2.3E+05	1.1E+06	-1.7E+06	2.7E+05	9.6E+05	1.7E+06	-2.0E+06	7.1E+05	-9.0E+04	-6.4E+04	-1.4E+05	-4.4E+04	-1.1E+05	-5.4E+04	-7.3E+04	-5.0E+04
97.7	2.8E+05	9.2E+05	-2.0E+06	1.6E+05	9.3E+05	1.8E+06	-2.3E+06	6.9E+05	-7.5E+04	-5.2E+04	-6.3E+04	-4.6E+04	-5.8E+04	-6.3E+04	-9.5E+04	-7.4E+04
107.4	-2.0E+05	1.1E+06	-1.7E+06	1.9E+05	1.1E+06	1.9E+06	-2.2E+06	1.3E+06	-7.6E+04	-4.8E+04	-8.3E+04	-5.2E+04	-1.1E+05	-3.9E+04	-3.8E+04	-6.8E+04
117.2	1.4E+05	9.3E+05	-2.0E+06	2.5E+05	1.4E+06	2.1E+06	-2.4E+06	1.4E+06	-5.8E+04	-3.9E+04	-4.5E+04	-4.0E+04	-3.5E+04	-4.4E+04	-4.7E+04	-4.9E+04
127.0	1.8E+05	6.9E+05	-2.2E+06	-2.7E+04	1.8E+06	2.0E+06	-2.3E+06	1.5E+06	-9.6E+04	-4.9E+04	-8.4E+04	-6.0E+04	-9.4E+04	-5.3E+04	-7.7E+04	-6.0E+04
136.7	8.8E+05	3.6E+04	-2.2E+06	1.1E+06	2.1E+06	3.4E+06	-3.0E+06	2.0E+06	-4.9E+04	-5.2E+04	-4.6E+04	-4.6E+04	-5.5E+04	-4.9E+04	-3.5E+04	-5.1E+04
146.5	1.9E+05	8.5E+05	-6.1E+05	1.2E+06	4.9E+05	4.1E+06	-2.2E+06	1.5E+06	-7.6E+04	-4.2E+04	-5.0E+04	-4.6E+04	-3.3E+04	-6.4E+04	-4.3E+04	-6.1E+04
156.3	-1.4E+06	2.6E+06	1.7E+04	-4.7E+05	2.4E+06	3.9E+06	-4.0E+06	2.3E+06	-4.9E+04	-5.1E+04	-5.0E+04	-5.9E+04	-6.5E+04	-6.4E+04	-5.7E+04	-7.7E+04
166.0	-4.6E+05	2.4E+06	-9.5E+05	3.8E+05	2.4E+06	3.4E+06	-4.3E+06	3.9E+06	-7.9E+04	-4.8E+04	-5.8E+04	-4.8E+04	-9.9E+04	-5.5E+04	-7.2E+04	-6.4E+04
175.8	1.8E+06	-5.2E+05	-3.2E+06	4.7E+06	3.2E+06	3.6E+06	-5.7E+06	3.1E+06	-6.7E+04	-5.6E+04	-1.1E+05	-9.2E+04	-4.0E+04	-5.9E+04	-6.4E+04	-9.1E+04
185.5	7.1E+04	3.4E+06	-4.8E+05	-1.9E+06	1.8E+06	5.5E+06	-3.4E+06	1.0E+06	-7.2E+04	-4.9E+04	-6.5E+04	-4.8E+04	-6.4E+04	-4.7E+04	-5.9E+04	-5.3E+04
195.3	1.6E+06	2.3E+06	-2.5E+06	9.7E+05	2.7E+06	5.4E+06	-4.5E+06	1.9E+06	-6.6E+04	-5.9E+04	-5.4E+04	-6.2E+04	-4.3E+04	-6.7E+04	-5.7E+04	-6.7E+04
205.1	2.3E+06	3.6E+06	-2.1E+06	1.9E+06	1.0E+06	3.5E+06	-5.7E+06	1.5E+06	-6.6E+04	-5.9E+04	-6.1E+04	-6.2E+04	-9.9E+04	-5.5E+04	-5.6E+04	-7.0E+04
214.8	2.8E+05	1.6E+06	-3.1E+06	5.9E+05	2.0E+06	5.2E+06	-4.6E+06	2.8E+06	-3.9E+04	-5.1E+04	-3.0E+04	-3.7E+04	-3.7E+04	-6.0E+04	-2.4E+04	-5.2E+04
224.6	4.8E+05	1.8E+06	-3.0E+06	8.7E+05	2.7E+06	5.8E+06	-4.9E+06	2.9E+06	-5.2E+04	-4.8E+04	-3.9E+04	-7.4E+04	-4.5E+04	-9.9E+04	-4.1E+04	-7.6E+04

Table 10. Raw data for TOR labyrinth seal at 20,200 rpm, 0.5 PR, and zero preswirl

Freq	Re Hxx	Re Hxy	Re Hyx	Re Hyy	Im Hxx	Im Hxy	Im Hyx	Im Hyy	Re eHxx	Re eHxy	Re eHyx	Re eHyy	Im eHxx	Im eHxy	Im eHyx	Im eHyy
Hz	N/m	N/m	N/m	N/m	N/m	N/m	N/m	N/m	N/m	N/m	N/m	N/m	N/m	N/m	N/m	N/m
9.8	-6.0E+05	2.0E+06	-2.8E+06	-8.8E+05	-4.9E+04	3.5E+05	-2.3E+05	1.3E+05	-5.7E+04	-9.3E+04	-6.7E+04	-5.8E+04	-1.0E+05	-4.6E+04	-9.5E+04	-6.5E+04
19.5	-6.9E+05	1.9E+06	-2.8E+06	-9.8E+05	4.3E+05	6.3E+05	-7.7E+05	-3.0E+04	-1.9E+05	-9.0E+04	-1.4E+05	-8.7E+04	-2.1E+05	-8.7E+04	-1.6E+05	-1.1E+05
29.3	-8.4E+05	2.0E+06	-2.9E+06	-9.7E+05	2.4E+05	5.7E+05	-9.1E+05	2.4E+05	-1.0E+05	-6.6E+04	-1.0E+05	-1.1E+05	-6.0E+04	-7.6E+04	-4.7E+04	-6.7E+04
39.1	-1.3E+06	2.2E+06	-2.9E+06	-9.5E+05	3.5E+05	9.4E+05	-8.8E+05	5.4E+05	-1.6E+05	-5.2E+04	-1.1E+05	-6.3E+04	-1.4E+05	-5.6E+04	-1.1E+05	-6.7E+04
48.8	-5.6E+05	2.1E+06	-2.6E+06	-1.1E+06	-2.7E+05	1.3E+06	-1.4E+06	7.3E+05	-8.1E+05	-3.0E+05	-2.5E+05	-9.5E+04	-4.7E+05	-3.0E+05	-4.2E+05	-1.3E+05
58.6	-1.1E+06	2.1E+06	-3.5E+06	-7.9E+05	9.3E+05	1.4E+06	-1.4E+06	1.0E+06	-2.0E+05	-5.3E+04	-2.9E+05	-1.1E+05	-1.8E+05	-8.1E+04	-2.1E+05	-1.1E+05
68.4	-9.7E+05	2.0E+06	-3.3E+06	-8.4E+05	9.4E+05	1.7E+06	-1.9E+06	1.0E+06	-8.2E+04	-4.6E+04	-9.9E+04	-7.5E+04	-8.2E+04	-4.9E+04	-1.2E+05	-8.4E+04
78.1	-1.2E+06	2.2E+06	-2.8E+06	-1.1E+06	1.5E+06	1.8E+06	-1.8E+06	1.1E+06	-8.2E+04	-8.4E+04	-7.9E+04	-6.0E+04	-1.2E+05	-5.9E+04	-1.6E+05	-9.3E+04
87.9	-8.9E+05	2.1E+06	-3.0E+06	-1.0E+06	1.4E+06	2.0E+06	-2.3E+06	1.4E+06	-9.5E+04	-5.6E+04	-9.6E+04	-4.1E+04	-1.0E+05	-5.5E+04	-7.5E+04	-6.9E+04
97.7	-9.5E+05	2.0E+06	-3.4E+06	-1.0E+06	1.4E+06	2.2E+06	-2.7E+06	1.4E+06	-2.4E+05	-1.5E+05	-1.6E+05	-1.4E+05	-2.3E+05	-1.8E+05	-1.6E+05	-1.7E+05
107.4	-1.2E+06	2.3E+06	-3.1E+06	-8.9E+05	1.6E+06	2.5E+06	-2.6E+06	1.8E+06	-1.1E+05	-3.9E+04	-6.9E+04	-4.6E+04	-1.0E+05	-7.0E+04	-6.8E+04	-6.1E+04
117.2	-8.2E+05	2.1E+06	-3.3E+06	-7.9E+05	1.8E+06	2.8E+06	-3.1E+06	2.2E+06	-6.3E+04	-6.3E+04	-6.6E+04	-5.1E+04	-2.9E+04	-5.2E+04	-4.1E+04	-5.8E+04
127.0	-6.4E+05	1.9E+06	-3.2E+06	-4.4E+05	2.3E+06	3.3E+06	-3.2E+06	2.3E+06	-8.4E+04	-3.5E+04	-9.7E+04	-3.9E+04	-9.0E+04	-6.6E+04	-6.4E+04	-6.6E+04
136.7	-4.3E+05	1.8E+06	-3.8E+06	7.2E+03	2.1E+06	3.9E+06	-3.6E+06	2.1E+06	-4.8E+04	-3.5E+04	-4.3E+04	-5.3E+04	-3.8E+04	-4.4E+04	-5.1E+04	-5.6E+04
146.5	-1.3E+06	2.4E+06	-1.9E+06	-4.4E+04	7.6E+05	4.5E+06	-2.8E+06	1.8E+06	-5.0E+04	-4.3E+04	-4.9E+04	-4.0E+04	-3.3E+04	-4.4E+04	-5.4E+04	-6.0E+04
156.3	-3.7E+06	4.9E+06	-5.5E+05	-2.5E+06	5.1E+06	2.4E+06	-6.5E+06	3.8E+06	-8.7E+04	-4.4E+04	-6.4E+04	-4.4E+04	-1.4E+05	-1.4E+05	-1.2E+05	-1.3E+05
166.0	-2.3E+06	4.0E+06	-2.0E+06	-1.3E+06	2.5E+06	4.6E+06	-4.7E+06	3.0E+06	-7.3E+04	-3.6E+04	-9.1E+04	-5.1E+04	-8.1E+04	-5.5E+04	-9.0E+04	-8.8E+04
175.8	1.8E+05	1.6E+05	-4.2E+06	2.7E+06	4.5E+06	1.6E+06	-6.6E+06	8.4E+06	-1.1E+05	-1.6E+05	-1.7E+05	-2.9E+05	-1.4E+05	-7.4E+04	-2.6E+05	-9.1E+04
185.5	-1.1E+06	4.3E+06	-1.3E+06	-3.2E+06	2.7E+06	7.1E+06	-4.8E+06	1.9E+06	-9.9E+04	-5.8E+04	-9.1E+04	-6.8E+04	-7.1E+04	-6.8E+04	-7.8E+04	-7.6E+04
195.3	7.9E+05	3.7E+06	-3.6E+06	-4.7E+04	3.6E+06	6.9E+06	-5.9E+06	2.8E+06	-5.7E+04	-8.5E+04	-4.7E+04	-5.1E+04	-6.1E+04	-6.4E+04	-6.5E+04	-7.7E+04
205.1	1.4E+06	5.0E+06	-3.3E+06	7.4E+05	1.8E+06	5.0E+06	-7.1E+06	2.1E+06	-5.4E+04	-4.8E+04	-6.5E+04	-5.7E+04	-1.0E+05	-7.4E+04	-5.4E+04	-6.9E+04
214.8	-5.1E+05	2.9E+06	-4.4E+06	-6.5E+05	2.6E+06	6.6E+06	-6.1E+06	3.5E+06	-5.7E+04	-5.9E+04	-3.3E+04	-5.6E+04	-4.9E+04	-5.1E+04	-4.7E+04	-7.3E+04
224.6	-4.5E+05	3.3E+06	-4.1E+06	-3.6E+05	3.2E+06	7.4E+06	-6.6E+06	3.6E+06	-5.0E+04	-7.0E+04	-4.1E+04	-4.8E+04	-5.3E+04	-7.3E+04	-4.7E+04	-6.2E+04

Table 11. Raw data for TOR labyrinth seal at 10,200 rpm, 0.6 PR, and zero preswirl

Freq	Re Hxx	Re Hxy	Re Hyx	Re Hyy	Im Hxx	Im Hxy	Im Hyx	Im Hyy	Re eHxx	Re eHxy	Re eHyx	Re eHyy	Im eHxx	Im eHxy	Im eHyx	Im eHyy
Hz	N/m	N/m	N/m	N/m	N/m	N/m	N/m	N/m	N/m	N/m	N/m	N/m	N/m	N/m	N/m	N/m
9.8	1.2E+06	7.8E+04	-6.7E+05	1.7E+06	3.0E+04	2.5E+05	-1.4E+05	1.5E+04	-1.2E+05	-1.6E+05	-1.0E+05	-1.7E+05	-1.3E+05	-1.8E+05	-9.1E+04	-1.0E+05
19.5	1.1E+06	6.5E+05	-1.1E+06	1.5E+06	3.1E+05	3.0E+05	1.4E+04	-1.4E+05	-1.8E+05	-1.3E+05	-2.2E+05	-9.9E+04	-1.9E+05	-1.9E+05	-2.7E+05	-9.0E+04
29.3	1.3E+06	4.0E+05	-8.9E+05	1.5E+06	3.5E+05	3.9E+05	-3.7E+05	-1.7E+04	-9.4E+04	-1.2E+05	-8.1E+04	-1.1E+05	-4.7E+04	-1.2E+05	-7.8E+04	-1.0E+05
39.1	1.2E+06	3.6E+05	-7.6E+05	1.4E+06	1.6E+05	4.4E+05	-3.3E+05	2.7E+05	-1.1E+05	-7.5E+04	-1.3E+05	-9.4E+04	-1.0E+05	-9.4E+04	-2.1E+05	-5.7E+04
48.8	1.5E+06	4.9E+05	-6.3E+05	1.3E+06	-3.4E+04	5.3E+05	-3.2E+05	3.7E+05	-3.9E+05	-9.5E+04	-2.3E+05	-8.1E+04	-4.7E+05	-1.4E+05	-3.5E+05	-6.2E+04
58.6	1.5E+06	4.4E+05	-9.7E+05	1.6E+06	4.1E+05	5.4E+05	-9.0E+05	3.6E+05	-3.1E+05	-9.5E+04	-1.0E+05	-1.0E+05	-3.2E+05	-1.1E+05	-2.2E+05	-9.7E+04
68.4	1.2E+06	4.3E+05	-8.2E+05	1.5E+06	3.8E+05	4.4E+05	-9.2E+05	2.9E+05	-7.2E+04	-8.6E+04	-1.9E+05	-7.5E+04	-1.7E+05	-6.6E+04	-1.1E+05	-5.0E+04
78.1	9.1E+05	1.0E+05	-6.2E+05	1.1E+06	8.8E+05	3.4E+05	-6.0E+05	6.2E+05	-2.4E+05	-1.2E+05	-1.6E+05	-1.1E+05	-1.9E+05	-8.0E+04	-1.0E+05	-7.0E+04
87.9	1.3E+06	5.1E+04	-5.8E+05	1.4E+06	1.0E+06	1.1E+06	-1.3E+06	8.9E+05	-1.8E+05	-9.7E+04	-1.2E+05	-9.0E+04	-7.6E+04	-8.5E+04	-1.0E+05	-5.1E+04
97.7	1.3E+06	-1.9E+04	-7.8E+05	1.3E+06	8.1E+05	1.1E+06	-1.7E+06	7.8E+05	-6.0E+04	-8.6E+04	-6.7E+04	-8.1E+04	-7.8E+04	-7.5E+04	-1.2E+05	-9.3E+04
107.4	1.2E+06	2.5E+05	-7.1E+05	1.3E+06	1.0E+06	1.3E+06	-1.7E+06	1.2E+06	-8.9E+04	-8.4E+04	-8.9E+04	-7.1E+04	-8.7E+04	-8.2E+04	-7.0E+04	-6.9E+04
117.2	1.4E+06	9.6E+04	-1.1E+06	1.4E+06	1.2E+06	1.3E+06	-1.8E+06	1.3E+06	-3.5E+04	-8.0E+04	-5.0E+04	-6.2E+04	-8.0E+04	-7.1E+04	-7.5E+04	-5.1E+04
127.0	1.6E+06	5.0E+04	-1.1E+06	1.6E+06	1.4E+06	1.7E+06	-1.8E+06	1.2E+06	-4.6E+04	-7.2E+04	-6.1E+04	-6.7E+04	-6.8E+04	-6.7E+04	-7.2E+04	-4.7E+04
136.7	1.7E+06	-1.4E+05	-1.5E+06	1.8E+06	1.4E+06	2.1E+06	-1.9E+06	1.0E+06	-4.6E+04	-8.7E+04	-6.2E+04	-6.0E+04	-5.3E+04	-7.9E+04	-3.7E+04	-4.5E+04
146.5	8.8E+05	3.6E+05	3.7E+05	1.9E+06	3.5E+03	2.9E+06	-1.2E+06	9.9E+05	-1.1E+05	-1.0E+05	-6.7E+04	-8.8E+04	-9.4E+04	-1.1E+05	-9.9E+04	-7.1E+04
156.3	3.7E+05	1.7E+06	2.5E+05	3.1E+05	3.7E+06	1.1E+06	-4.1E+06	2.7E+06	-8.4E+04	-1.1E+05	-8.5E+04	-1.2E+05	-1.1E+05	-9.6E+04	-7.0E+04	-8.3E+04
166.0	2.8E+05	1.7E+06	-2.0E+04	1.8E+06	2.2E+06	1.6E+06	-3.4E+06	3.5E+06	-2.0E+05	-1.3E+05	-2.3E+05	-1.7E+05	-1.8E+05	-1.6E+05	-2.1E+05	-1.3E+05
175.8	1.7E+06	5.6E+05	-4.5E+05	2.0E+06	1.8E+06	2.3E+06	-2.7E+06	2.6E+06	-1.1E+05	-1.0E+05	-8.2E+04	-1.1E+05	-9.1E+04	-1.3E+05	-8.2E+04	-7.8E+04
185.5	1.1E+06	2.2E+06	2.3E+05	-5.9E+05	1.2E+06	3.6E+06	-2.2E+06	1.1E+06	-7.3E+04	-8.7E+04	-6.7E+04	-6.5E+04	-6.9E+04	-9.2E+04	-6.3E+04	-5.7E+04
195.3	2.2E+06	1.4E+06	-1.2E+06	1.7E+06	1.9E+06	3.7E+06	-2.9E+06	1.7E+06	-5.8E+04	-1.1E+05	-5.5E+04	-7.3E+04	-7.6E+04	-9.6E+04	-7.6E+04	-7.4E+04
205.1	3.0E+06	2.6E+06	-1.1E+06	2.5E+06	4.4E+05	2.1E+06	-4.1E+06	1.1E+06	-7.0E+04	-8.1E+04	-5.7E+04	-7.6E+04	-7.1E+04	-8.6E+04	-4.7E+04	-6.9E+04
214.8	1.2E+06	6.8E+05	-1.8E+06	1.4E+06	1.3E+06	3.5E+06	-2.8E+06	2.3E+06	-5.1E+04	-6.4E+04	-3.1E+04	-6.0E+04	-3.2E+04	-6.9E+04	-3.5E+04	-5.8E+04
224.6	1.2E+06	9.2E+05	-1.6E+06	1.8E+06	2.1E+06	4.1E+06	-3.1E+06	2.6E+06	-5.8E+04	-8.1E+04	-4.5E+04	-7.2E+04	-4.9E+04	-9.6E+04	-3.7E+04	-1.0E+05

Table 12. Raw data for TOR labyrinth seal at 15,350 rpm, 0.6 PR, and zero preswirl

Freq	Re Hxx	Re Hxy	Re Hyx	Re Hyy	Im Hxx	Im Hxy	Im Hyx	Im Hyy	Re eHxx	Re eHxy	Re eHyx	Re eHyy	Im eHxx	Im eHxy	Im eHyx	Im eHyy
Hz	N/m	N/m	N/m	N/m	N/m	N/m	N/m	N/m	N/m	N/m	N/m	N/m	N/m	N/m	N/m	N/m
9.8	1.9E+05	8.7E+05	-1.6E+06	4.3E+05	9.0E+04	4.0E+05	-3.6E+05	-1.2E+05	-7.4E+04	-1.5E+05	-6.7E+04	-1.2E+05	-6.9E+04	-1.0E+05	-8.3E+04	-9.2E+04
19.5	3.5E+05	8.5E+05	-2.1E+06	5.0E+05	2.7E+05	5.6E+05	-3.5E+05	-8.6E+04	-1.6E+05	-7.8E+04	-2.4E+05	-9.8E+04	-1.6E+05	-1.0E+05	-2.2E+05	-8.0E+04
29.3	1.0E+05	9.9E+05	-1.6E+06	2.8E+05	1.6E+05	6.7E+05	-5.2E+05	-1.6E+04	-8.0E+04	-1.1E+05	-7.0E+04	-1.1E+05	-7.7E+04	-1.2E+05	-5.4E+04	-7.5E+04
39.1	1.9E+05	1.0E+06	-1.9E+06	2.0E+05	9.7E+04	1.0E+06	-9.1E+05	2.5E+05	-1.4E+05	-1.2E+05	-8.8E+04	-8.4E+04	-6.9E+04	-1.0E+05	-1.2E+05	-6.1E+04
48.8	1.6E+05	1.1E+06	-1.8E+06	2.4E+05	-1.9E+05	9.4E+05	-6.8E+05	4.2E+05	-1.8E+05	-8.5E+04	-2.4E+05	-8.1E+04	-3.1E+05	-9.8E+04	-2.6E+05	-5.9E+04
58.6	7.6E+04	1.0E+06	-1.6E+06	4.2E+05	6.5E+05	1.3E+06	-1.0E+06	7.1E+05	-2.5E+05	-1.2E+05	-1.6E+05	-9.8E+04	-1.9E+05	-9.8E+04	-2.2E+05	-7.9E+04
68.4	2.5E+05	1.1E+06	-1.7E+06	4.4E+05	6.8E+05	1.4E+06	-1.4E+06	6.9E+05	-7.4E+04	-7.3E+04	-1.3E+05	-7.5E+04	-1.1E+05	-8.5E+04	-8.8E+04	-6.7E+04
78.1	1.8E+05	1.2E+06	-1.6E+06	3.7E+05	7.4E+05	1.6E+06	-1.4E+06	6.8E+05	-2.1E+05	-7.2E+04	-1.5E+05	-7.4E+04	-2.4E+05	-1.0E+05	-9.2E+04	-7.4E+04
87.9	1.0E+05	1.3E+06	-1.7E+06	1.9E+05	8.3E+05	1.7E+06	-1.8E+06	8.6E+05	-1.2E+05	-8.6E+04	-1.1E+05	-8.3E+04	-7.1E+04	-7.4E+04	-1.3E+05	-7.2E+04
97.7	1.1E+05	1.2E+06	-1.9E+06	4.0E+03	9.2E+05	1.7E+06	-2.2E+06	8.5E+05	-4.0E+04	-7.9E+04	-4.0E+04	-7.5E+04	-6.1E+04	-9.0E+04	-1.1E+05	-5.9E+04
107.4	-2.0E+05	1.3E+06	-1.6E+06	5.3E+04	1.2E+06	1.8E+06	-2.3E+06	1.5E+06	-8.9E+04	-7.3E+04	-1.1E+05	-6.0E+04	-1.0E+05	-8.7E+04	-6.4E+04	-5.0E+04
117.2	4.4E+04	1.0E+06	-2.1E+06	1.7E+05	1.4E+06	2.0E+06	-2.5E+06	1.5E+06	-3.7E+04	-6.8E+04	-4.7E+04	-5.8E+04	-5.9E+04	-8.0E+04	-7.5E+04	-5.0E+04
127.0	-2.4E+03	9.2E+05	-2.1E+06	-5.4E+04	1.8E+06	2.2E+06	-2.4E+06	1.4E+06	-5.8E+04	-8.3E+04	-7.6E+04	-6.0E+04	-9.4E+04	-7.0E+04	-5.7E+04	-4.8E+04
136.7	5.2E+05	2.7E+05	-2.2E+06	8.9E+05	2.1E+06	3.5E+06	-2.9E+06	1.9E+06	-4.9E+04	-9.4E+04	-5.9E+04	-6.7E+04	-5.5E+04	-8.5E+04	-3.7E+04	-5.7E+04
146.5	5.0E+02	1.1E+06	-4.5E+05	9.7E+05	4.8E+05	4.2E+06	-2.1E+06	1.6E+06	-6.7E+04	-6.5E+04	-5.8E+04	-7.3E+04	-6.1E+04	-8.1E+04	-6.3E+04	-5.7E+04
156.3	-1.7E+06	3.0E+06	1.7E+05	-9.1E+05	2.6E+06	3.8E+06	-4.1E+06	2.2E+06	-4.7E+04	-7.5E+04	-5.7E+04	-8.1E+04	-7.1E+04	-9.7E+04	-6.3E+04	-6.1E+04
166.0	-2.0E+05	2.3E+06	-1.2E+06	4.5E+05	2.7E+06	3.7E+06	-4.2E+06	3.0E+06	-1.1E+05	-7.2E+04	-8.3E+04	-7.3E+04	-6.8E+04	-8.8E+04	-6.1E+04	-6.4E+04
175.8	1.5E+06	8.0E+05	-2.7E+06	2.4E+06	2.8E+06	4.0E+06	-4.7E+06	2.7E+06	-5.8E+04	-7.5E+04	-5.2E+04	-8.0E+04	-5.8E+04	-7.9E+04	-5.5E+04	-5.5E+04
185.5	2.4E+05	3.2E+06	-7.9E+05	-1.4E+06	2.0E+06	5.2E+06	-3.8E+06	1.5E+06	-4.8E+04	-7.3E+04	-5.0E+04	-7.3E+04	-6.1E+04	-7.5E+04	-7.5E+04	-5.2E+04
195.3	1.5E+06	2.5E+06	-2.2E+06	8.3E+05	2.7E+06	5.3E+06	-4.5E+06	2.1E+06	-5.7E+04	-8.1E+04	-4.0E+04	-1.0E+05	-6.0E+04	-8.5E+04	-4.9E+04	-6.9E+04
205.1	2.1E+06	3.8E+06	-1.9E+06	1.6E+06	1.2E+06	3.8E+06	-5.7E+06	1.5E+06	-5.6E+04	-9.1E+04	-7.7E+04	-8.3E+04	-6.2E+04	-7.1E+04	-6.9E+04	-6.1E+04
214.8	1.9E+05	1.8E+06	-2.9E+06	4.3E+05	2.0E+06	5.3E+06	-4.6E+06	2.8E+06	-4.1E+04	-9.4E+04	-2.8E+04	-7.6E+04	-5.4E+04	-1.1E+05	-4.6E+04	-6.0E+04
224.6	3.3E+05	2.0E+06	-2.6E+06	7.0E+05	2.7E+06	5.8E+06	-5.0E+06	3.0E+06	-5.0E+04	-1.2E+05	-6.2E+04	-1.2E+05	-5.3E+04	-1.0E+05	-3.6E+04	-9.3E+04

Table 13. Raw data for TOR labyrinth seal at 20,200 rpm, 0.6 PR, and zero preswirl

Freq	Re Hxx	Re Hxy	Re Hyx	Re Hyy	Im Hxx	Im Hxy	Im Hyx	Im Hyy	Re eHxx	Re eHxy	Re eHyx	Re eHyy	Im eHxx	Im eHxy	Im eHyx	Im eHyy
Hz	N/m	N/m	N/m	N/m	N/m	N/m	N/m	N/m	N/m	N/m	N/m	N/m	N/m	N/m	N/m	N/m
9.8	-1.1E+06	2.0E+06	-2.9E+06	-1.1E+06	-7.7E+04	5.2E+05	-1.7E+05	-5.6E+03	-9.8E+04	-1.7E+05	-6.8E+04	-9.8E+04	-9.5E+04	-1.1E+05	-6.7E+04	-8.9E+04
19.5	-1.1E+06	2.1E+06	-3.5E+06	-9.6E+05	3.3E+05	7.9E+05	-5.6E+05	-1.1E+05	-1.9E+05	-7.9E+04	-1.7E+05	-8.5E+04	-1.6E+05	-1.2E+05	-2.0E+05	-7.9E+04
29.3	-1.2E+06	2.2E+06	-2.9E+06	-1.1E+06	4.0E+05	7.1E+05	-8.4E+05	1.8E+05	-9.2E+04	-1.2E+05	-8.1E+04	-8.5E+04	-6.8E+04	-1.0E+05	-8.1E+04	-8.4E+04
39.1	-1.3E+06	2.3E+06	-3.0E+06	-1.3E+06	3.0E+05	1.2E+06	-8.8E+05	4.9E+05	-1.1E+05	-5.5E+04	-7.2E+04	-1.0E+05	-1.2E+05	-7.0E+04	-1.4E+05	-6.5E+04
48.8	-1.4E+06	2.2E+06	-3.1E+06	-1.3E+06	-4.9E+05	1.3E+06	-1.2E+06	7.0E+05	-1.0E+06	-3.7E+05	-2.5E+05	-1.1E+05	-4.6E+05	-3.7E+05	-4.9E+05	-1.1E+05
58.6	-1.4E+06	2.2E+06	-2.8E+06	-1.0E+06	8.2E+05	1.5E+06	-1.1E+06	9.7E+05	-2.3E+05	-8.3E+04	-1.7E+05	-1.1E+05	-2.9E+05	-1.2E+05	-2.0E+05	-7.7E+04
68.4	-1.1E+06	2.2E+06	-2.9E+06	-1.0E+06	9.5E+05	1.8E+06	-1.7E+06	1.0E+06	-1.1E+05	-8.0E+04	-1.5E+05	-8.1E+04	-1.1E+05	-7.5E+04	-8.8E+04	-6.5E+04
78.1	-1.3E+06	2.3E+06	-2.8E+06	-1.1E+06	1.1E+06	2.0E+06	-1.7E+06	1.2E+06	-1.9E+05	-8.3E+04	-8.9E+04	-8.1E+04	-1.7E+05	-8.0E+04	-9.9E+04	-7.9E+04
87.9	-9.3E+05	2.4E+06	-2.8E+06	-1.2E+06	1.4E+06	2.2E+06	-2.2E+06	1.4E+06	-1.1E+05	-7.9E+04	-1.2E+05	-8.9E+04	-7.4E+04	-6.9E+04	-1.4E+05	-5.3E+04
97.7	-1.3E+06	2.3E+06	-3.0E+06	-1.3E+06	1.6E+06	2.2E+06	-2.6E+06	1.5E+06	-1.8E+05	-2.2E+05	-1.2E+05	-1.5E+05	-2.1E+05	-2.4E+05	-2.1E+05	-1.5E+05
107.4	-1.3E+06	2.5E+06	-2.8E+06	-1.1E+06	1.7E+06	2.6E+06	-2.9E+06	2.0E+06	-1.0E+05	-6.0E+04	-1.1E+05	-5.9E+04	-8.9E+04	-6.6E+04	-8.3E+04	-5.3E+04
117.2	-8.1E+05	2.2E+06	-3.2E+06	-9.5E+05	1.9E+06	2.8E+06	-3.2E+06	2.1E+06	-8.4E+04	-7.0E+04	-5.3E+04	-7.2E+04	-7.1E+04	-7.2E+04	-7.8E+04	-4.9E+04
127.0	-7.3E+05	2.1E+06	-3.2E+06	-7.3E+05	2.2E+06	3.4E+06	-3.1E+06	2.0E+06	-5.2E+04	-6.8E+04	-7.3E+04	-7.8E+04	-6.8E+04	-6.9E+04	-5.6E+04	-5.5E+04
136.7	-6.2E+05	1.9E+06	-3.5E+06	-4.5E+05	2.3E+06	4.0E+06	-3.5E+06	2.0E+06	-4.7E+04	-8.0E+04	-5.6E+04	-7.3E+04	-6.2E+04	-7.3E+04	-6.0E+04	-6.1E+04
146.5	-1.4E+06	2.5E+06	-1.6E+06	-5.4E+05	8.4E+05	4.7E+06	-2.7E+06	1.8E+06	-5.4E+04	-7.6E+04	-5.3E+04	-6.9E+04	-6.5E+04	-6.6E+04	-6.5E+04	-5.1E+04
156.3	-3.9E+06	4.9E+06	-1.5E+05	-2.9E+06	5.9E+06	2.2E+06	-7.3E+06	4.3E+06	-1.1E+05	-9.1E+04	-9.0E+04	-8.3E+04	-1.3E+05	-1.4E+05	-1.1E+05	-1.1E+05
166.0	-2.1E+06	4.1E+06	-1.9E+06	-1.4E+06	2.9E+06	4.4E+06	-4.9E+06	3.5E+06	-8.9E+04	-8.9E+04	-9.2E+04	-7.1E+04	-8.7E+04	-8.3E+04	-6.6E+04	-7.3E+04
175.8	-3.1E+04	-1.3E+06	-4.4E+06	6.0E+06	5.3E+06	2.2E+06	-8.2E+06	7.5E+06	-1.2E+05	-1.2E+05	-9.7E+04	-1.8E+05	-1.6E+05	-1.6E+05	-2.6E+05	-1.9E+05
185.5	-8.0E+05	4.2E+06	-1.4E+06	-2.6E+06	3.1E+06	6.8E+06	-5.0E+06	2.3E+06	-6.0E+04	-8.0E+04	-5.7E+04	-7.3E+04	-6.5E+04	-7.7E+04	-6.4E+04	-5.0E+04
195.3	7.9E+05	3.9E+06	-3.3E+06	-3.5E+05	3.5E+06	6.8E+06	-6.1E+06	2.6E+06	-7.9E+04	-1.0E+05	-4.7E+04	-9.5E+04	-5.7E+04	-1.1E+05	-6.7E+04	-9.0E+04
205.1	1.3E+06	5.1E+06	-3.3E+06	2.1E+05	1.7E+06	5.1E+06	-7.4E+06	2.3E+06	-9.9E+04	-1.1E+05	-6.5E+04	-7.4E+04	-9.5E+04	-1.0E+05	-8.6E+04	-7.6E+04
214.8	-5.8E+05	3.0E+06	-4.3E+06	-8.4E+05	2.4E+06	6.6E+06	-6.1E+06	3.6E+06	-5.1E+04	-9.0E+04	-4.0E+04	-8.8E+04	-5.9E+04	-9.8E+04	-3.8E+04	-5.3E+04
224.6	-4.9E+05	3.4E+06	-3.8E+06	-5.2E+05	3.2E+06	7.6E+06	-6.8E+06	3.6E+06	-4.3E+04	-1.1E+05	-4.8E+04	-7.1E+04	-5.7E+04	-7.7E+04	-3.5E+04	-8.3E+04

Table 14. Raw data for TOR labyrinth seal at 10,200 rpm, 0.4 PR, and medium preswirl

Freq	Re Hxx	Re Hxy	Re Hyx	Re Hyy	Im Hxx	Im Hxy	Im Hyx	Im Hyy	Re eHxx	Re eHxy	Re eHyx	Re eHyy	Im eHxx	Im eHxy	Im eHyx	Im eHyy
Hz	N/m	N/m	N/m	N/m	N/m	N/m	N/m	N/m	N/m	N/m	N/m	N/m	N/m	N/m	N/m	N/m
9.8	1.5E+06	2.6E+05	-1.5E+06	2.3E+06	-2.0E+04	4.4E+04	-9.8E+04	2.9E+05	-1.3E+05	-2.0E+05	-1.5E+05	-1.6E+05	-1.9E+05	-2.1E+05	-1.1E+05	-1.3E+05
19.5	1.5E+06	5.1E+05	-1.5E+06	1.9E+06	5.8E+05	2.6E+05	-7.1E+05	2.8E+05	-2.5E+05	-1.3E+05	-1.2E+05	-1.5E+05	-2.2E+05	-1.8E+05	-2.1E+05	-8.3E+04
29.3	1.4E+06	8.1E+05	-1.9E+06	1.9E+06	3.3E+05	4.5E+05	-5.5E+05	6.4E+05	-1.0E+05	-1.8E+05	-1.3E+05	-1.5E+05	-1.4E+05	-1.7E+05	-5.8E+04	-1.2E+05
39.1	8.3E+04	8.4E+05	-5.9E+05	1.8E+06	1.0E+06	6.7E+05	-8.2E+05	2.4E+05	-3.5E+05	-5.9E+04	-3.5E+05	-9.8E+04	-2.7E+05	-9.9E+04	-2.6E+05	-6.7E+04
48.8	1.6E+06	8.4E+05	-1.7E+06	1.6E+06	2.4E+05	7.0E+05	-5.6E+05	1.6E+05	-2.0E+05	-6.3E+04	-1.7E+05	-6.6E+04	-1.7E+05	-9.4E+04	-1.5E+05	-7.7E+04
58.6	1.1E+06	9.0E+05	-1.8E+06	1.5E+06	3.3E+05	6.5E+05	-4.5E+05	5.0E+05	-1.8E+05	-7.7E+04	-1.4E+05	-1.4E+05	-2.5E+05	-9.0E+04	-2.5E+05	-1.3E+05
68.4	7.8E+05	8.5E+05	-1.5E+06	1.2E+06	4.8E+05	5.4E+05	-5.7E+05	3.6E+05	-1.3E+05	-7.3E+04	-8.3E+04	-7.0E+04	-1.0E+05	-1.0E+05	-9.4E+04	-8.2E+04
78.1	6.4E+05	1.6E+04	-9.6E+05	1.2E+06	1.2E+06	1.4E+05	-3.4E+05	1.6E+06	-1.6E+05	-6.5E+04	-1.2E+05	-1.4E+05	-2.1E+05	-9.1E+04	-1.5E+05	-8.6E+04
87.9	1.5E+06	1.1E+05	-1.1E+06	1.7E+06	1.3E+06	1.0E+06	-1.5E+06	1.2E+06	-4.8E+04	-6.2E+04	-5.3E+04	-7.5E+04	-6.9E+04	-5.8E+04	-9.9E+04	-5.3E+04
97.7	1.4E+06	1.5E+05	-1.3E+06	1.7E+06	1.1E+06	1.1E+06	-1.8E+06	1.0E+06	-6.4E+04	-6.3E+04	-9.4E+04	-8.8E+04	-9.3E+04	-7.4E+04	-1.0E+05	-6.0E+04
107.4	9.8E+05	1.7E+05	-1.1E+06	1.7E+06	1.4E+06	1.1E+06	-1.8E+06	1.4E+06	-7.5E+04	-7.3E+04	-7.9E+04	-7.2E+04	-4.4E+04	-5.7E+04	-6.2E+04	-4.5E+04
117.2	1.6E+06	-1.1E+05	-1.6E+06	2.1E+06	1.4E+06	1.4E+06	-1.9E+06	1.4E+06	-5.5E+04	-5.4E+04	-3.9E+04	-7.2E+04	-2.8E+04	-5.5E+04	-6.6E+04	-5.5E+04
127.0	1.8E+06	-1.9E+05	-1.7E+06	2.3E+06	1.5E+06	1.7E+06	-2.0E+06	1.2E+06	-5.4E+04	-6.1E+04	-5.0E+04	-7.6E+04	-4.5E+04	-6.2E+04	-4.4E+04	-6.5E+04
136.7	1.3E+06	-1.2E+06	-3.1E+06	1.5E+06	2.2E+06	2.9E+06	-1.4E+06	2.1E+06	-6.0E+04	-6.5E+04	-5.3E+04	-8.1E+04	-6.8E+04	-8.8E+04	-1.1E+05	-6.0E+04
146.5	1.4E+06	-2.3E+05	-8.7E+05	2.1E+06	2.2E+05	2.7E+06	-1.1E+06	1.0E+06	-3.0E+04	-5.3E+04	-3.4E+04	-6.4E+04	-4.7E+04	-5.8E+04	-4.4E+04	-5.0E+04
156.3	-2.7E+05	2.1E+06	5.3E+05	7.8E+04	2.0E+06	2.3E+06	-2.5E+06	1.9E+06	-5.1E+04	-6.7E+04	-5.8E+04	-9.5E+04	-5.0E+04	-1.0E+05	-6.0E+04	-7.7E+04
166.0	7.9E+05	2.9E+05	-1.8E+06	2.5E+06	1.2E+06	3.2E+06	-2.2E+06	1.3E+06	-1.9E+05	-1.1E+05	-1.5E+05	-1.3E+05	-1.4E+05	-1.4E+05	-1.5E+05	-1.1E+05
175.8	1.6E+06	9.8E+04	-1.7E+06	3.1E+06	1.9E+06	2.6E+06	-2.8E+06	2.0E+06	-8.4E+04	-8.5E+04	-8.8E+04	-8.4E+04	-1.1E+05	-8.9E+04	-7.6E+04	-7.8E+04
185.5	8.9E+05	1.8E+06	8.8E+04	-4.5E+05	2.2E+06	3.0E+06	-3.4E+06	2.1E+06	-5.0E+04	-5.4E+04	-6.9E+04	-7.9E+04	-5.1E+04	-5.4E+04	-8.0E+04	-5.5E+04
195.3	2.4E+06	7.6E+05	-1.8E+06	1.9E+06	1.9E+06	3.3E+06	-3.4E+06	1.6E+06	-6.2E+04	-7.6E+04	-3.8E+04	-7.9E+04	-4.8E+04	-5.8E+04	-4.7E+04	-5.6E+04
205.1	2.9E+06	2.2E+06	-1.3E+06	2.9E+06	-7.7E+04	1.3E+06	-4.4E+06	7.4E+05	-6.5E+04	-5.5E+04	-5.0E+04	-8.6E+04	-4.6E+04	-6.7E+04	-6.7E+04	-6.0E+04
214.8	1.0E+06	-9.8E+05	-2.2E+06	1.2E+06	2.4E+06	3.1E+06	-3.6E+06	2.2E+06	-2.9E+04	-6.6E+04	-3.4E+04	-7.6E+04	-4.5E+04	-5.4E+04	-3.0E+04	-6.8E+04
224.6	1.2E+06	-5.9E+05	-2.0E+06	1.6E+06	2.2E+06	3.7E+06	-3.9E+06	2.3E+06	-3.9E+04	-7.1E+04	-3.3E+04	-8.4E+04	-2.3E+04	-7.1E+04	-3.7E+04	-4.8E+04

Table 15. Raw data for TOR labyrinth seal at 15,350 rpm, 0.4 PR, and medium preswirl

Freq	Re Hxx	Re Hxy	Re Hyx	Re Hyy	Im Hxx	Im Hxy	Im Hyx	Im Hyy	Re eHxx	Re eHxy	Re eHyx	Re eHyy	Im eHxx	Im eHxy	Im eHyx	Im eHyy
Hz	N/m	N/m	N/m	N/m	N/m	N/m	N/m	N/m	N/m	N/m	N/m	N/m	N/m	N/m	N/m	N/m
9.8	4.4E+05	8.3E+05	-1.6E+06	1.2E+06	-2.0E+05	4.4E+05	-1.1E+05	2.8E+05	-1.3E+05	-1.7E+05	-1.2E+05	-1.1E+05	-1.6E+05	-1.7E+05	-1.1E+05	-8.3E+04
19.5	3.7E+04	1.0E+06	-1.4E+06	6.8E+05	5.9E+04	4.5E+05	-7.7E+05	3.1E+05	-2.0E+05	-7.5E+04	-1.6E+05	-9.9E+04	-1.5E+05	-1.0E+05	-1.4E+05	-9.1E+04
29.3	1.3E+05	9.3E+05	-2.0E+06	8.3E+05	2.7E+05	5.5E+05	-8.3E+05	6.6E+05	-9.7E+04	-1.5E+05	-1.1E+05	-1.2E+05	-8.9E+04	-5.5E+04	-4.8E+04	-8.2E+04
39.1	7.0E+04	1.0E+06	-1.9E+06	7.5E+05	9.1E+05	1.0E+06	-1.2E+06	4.3E+05	-3.0E+05	-7.1E+04	-2.4E+05	-8.2E+04	-1.9E+05	-9.9E+04	-1.6E+05	-6.7E+04
48.8	2.9E+05	1.0E+06	-1.8E+06	5.9E+05	3.8E+05	1.1E+06	-1.2E+06	3.0E+05	-1.1E+05	-7.3E+04	-1.2E+05	-7.5E+04	-1.7E+05	-6.1E+04	-1.0E+05	-8.1E+04
58.6	4.9E+05	9.4E+05	-2.1E+06	6.3E+05	4.2E+05	1.5E+06	-1.2E+06	8.1E+05	-1.4E+05	-7.8E+04	-1.5E+05	-6.8E+04	-1.2E+05	-1.1E+05	-1.8E+05	-7.1E+04
68.4	2.3E+03	1.2E+06	-1.7E+06	5.1E+05	5.8E+05	1.5E+06	-1.7E+06	6.4E+05	-9.9E+04	-7.4E+04	-7.0E+04	-9.5E+04	-8.9E+04	-4.9E+04	-9.1E+04	-4.9E+04
78.1	1.5E+05	1.0E+06	-1.9E+06	6.5E+05	9.4E+05	1.6E+06	-1.7E+06	9.0E+05	-1.3E+05	-4.1E+04	-1.1E+05	-6.7E+04	-1.1E+05	-9.2E+04	-1.3E+05	-6.7E+04
87.9	7.1E+04	1.1E+06	-2.1E+06	3.9E+05	7.0E+05	1.6E+06	-2.1E+06	7.5E+05	-4.1E+04	-5.2E+04	-4.4E+04	-7.9E+04	-5.6E+04	-6.3E+04	-9.1E+04	-5.7E+04
97.7	-1.0E+05	9.7E+05	-2.3E+06	1.9E+05	8.1E+05	1.5E+06	-2.5E+06	9.5E+05	-6.6E+04	-4.8E+04	-7.4E+04	-7.2E+04	-8.1E+04	-7.8E+04	-1.0E+05	-7.1E+04
107.4	-6.0E+05	7.5E+05	-1.8E+06	2.5E+05	1.3E+06	1.7E+06	-2.5E+06	1.5E+06	-6.1E+04	-5.1E+04	-8.1E+04	-5.9E+04	-5.9E+04	-7.0E+04	-5.3E+04	-8.0E+04
117.2	-2.2E+05	5.0E+05	-2.1E+06	4.0E+05	1.5E+06	1.8E+06	-2.3E+06	1.6E+06	-4.6E+04	-5.1E+04	-5.1E+04	-7.4E+04	-4.0E+04	-5.6E+04	-4.9E+04	-5.2E+04
127.0	-1.8E+05	-1.4E+05	-1.6E+06	3.3E+05	2.3E+06	1.9E+06	-2.4E+06	2.1E+06	-8.0E+04	-7.8E+04	-5.3E+04	-7.8E+04	-5.3E+04	-9.5E+04	-8.6E+04	-7.6E+04
136.7	-1.0E+04	-1.1E+06	-3.2E+06	3.3E+05	3.1E+06	4.1E+06	-2.4E+06	2.7E+06	-5.9E+04	-7.9E+04	-6.7E+04	-9.7E+04	-8.9E+04	-7.7E+04	-1.0E+05	-5.0E+04
146.5	1.1E+05	1.0E+05	-1.2E+06	1.2E+06	4.1E+05	4.1E+06	-2.3E+06	1.6E+06	-5.4E+04	-7.4E+04	-5.3E+04	-7.9E+04	-5.3E+04	-6.4E+04	-4.1E+04	-6.7E+04
156.3	-1.1E+06	1.9E+06	-5.3E+05	-6.2E+05	2.1E+06	3.9E+06	-3.5E+06	1.7E+06	-4.7E+04	-6.5E+04	-5.6E+04	-8.9E+04	-7.3E+04	-1.1E+05	-9.2E+04	-1.1E+05
166.0	2.2E+05	5.2E+05	-2.7E+06	2.0E+06	1.7E+06	4.6E+06	-3.9E+06	1.7E+06	-4.8E+04	-5.0E+04	-5.4E+04	-7.5E+04	-6.3E+04	-5.5E+04	-6.7E+04	-4.9E+04
175.8	6.1E+05	4.6E+05	-2.4E+06	2.1E+06	2.3E+06	4.4E+06	-4.3E+06	2.5E+06	-4.4E+04	-4.1E+04	-3.3E+04	-5.5E+04	-4.3E+04	-5.2E+04	-3.2E+04	-4.6E+04
185.5	-2.5E+05	2.3E+06	-7.1E+05	-1.1E+06	2.5E+06	4.7E+06	-5.0E+06	2.3E+06	-4.5E+04	-5.4E+04	-5.4E+04	-6.1E+04	-5.1E+04	-5.2E+04	-5.8E+04	-4.5E+04
195.3	1.1E+06	1.4E+06	-2.5E+06	7.9E+05	2.4E+06	5.1E+06	-5.3E+06	1.9E+06	-5.0E+04	-7.0E+04	-5.0E+04	-8.6E+04	-5.0E+04	-5.7E+04	-5.0E+04	-5.8E+04
205.1	1.6E+06	2.9E+06	-2.1E+06	1.8E+06	6.9E+05	3.1E+06	-6.3E+06	1.4E+06	-7.7E+04	-6.7E+04	-6.4E+04	-6.9E+04	-7.9E+04	-7.0E+04	-6.5E+04	-5.5E+04
214.8	-1.3E+04	2.2E+04	-3.2E+06	1.4E+05	2.8E+06	5.0E+06	-5.5E+06	2.7E+06	-4.4E+04	-5.8E+04	-3.8E+04	-6.2E+04	-3.2E+04	-6.3E+04	-4.3E+04	-5.0E+04
224.6	-1.0E+05	3.6E+05	-3.0E+06	6.3E+05	2.8E+06	5.6E+06	-5.8E+06	3.0E+06	-4.3E+04	-9.9E+04	-3.1E+04	-8.1E+04	-3.6E+04	-6.3E+04	-3.6E+04	-5.6E+04

Table 16. Raw data for TOR labyrinth seal at 20,200 rpm, 0.4 PR, and medium preswirl

Freq	Re Hxx	Re Hxy	Re Hyx	Re Hyy	Im Hxx	Im Hxy	Im Hyx	Im Hyy	Re eHxx	Re eHxy	Re eHyx	Re eHyy	Im eHxx	Im eHxy	Im eHyx	Im eHyy
Hz	N/m	N/m	N/m	N/m	N/m	N/m	N/m	N/m	N/m	N/m	N/m	N/m	N/m	N/m	N/m	N/m
9.8	-9.5E+05	1.4E+06	-2.5E+06	-7.9E+05	1.4E+05	3.8E+05	5.1E+04	2.3E+05	-7.3E+04	-8.4E+04	-5.3E+04	-8.9E+04	-1.1E+05	-1.1E+05	-6.8E+04	-5.6E+04
19.5	-1.4E+06	1.9E+06	-2.6E+06	-1.1E+06	-1.7E+05	6.7E+05	-1.1E+06	4.9E+05	-9.6E+04	-1.0E+05	-1.2E+05	-9.6E+04	-1.2E+05	-8.6E+04	-1.6E+05	-5.7E+04
29.3	-1.3E+06	1.8E+06	-2.8E+06	-9.7E+05	2.2E+05	9.5E+05	-1.2E+06	6.6E+05	-4.9E+04	-1.2E+05	-6.3E+04	-1.3E+05	-9.0E+04	-1.1E+05	-4.2E+04	-6.5E+04
39.1	-2.0E+06	1.8E+06	-3.1E+06	-9.1E+05	8.7E+05	1.2E+06	-2.1E+06	4.5E+05	-2.2E+05	-5.3E+04	-3.4E+05	-7.6E+04	-1.1E+05	-6.9E+04	-1.8E+05	-4.8E+04
48.8	-1.5E+06	1.9E+06	-2.6E+06	-1.1E+06	6.7E+05	1.6E+06	-1.7E+06	6.6E+05	-4.5E+05	-3.7E+05	-1.9E+05	-1.1E+05	-6.5E+05	-3.2E+05	-1.3E+05	-1.1E+05
58.6	-1.1E+06	1.9E+06	-3.5E+06	-8.9E+05	7.9E+05	1.7E+06	-1.7E+06	9.5E+05	-1.5E+05	-1.1E+05	-8.5E+04	-8.2E+04	-1.5E+05	-7.1E+04	-2.8E+05	-9.1E+04
68.4	-1.6E+06	1.8E+06	-2.7E+06	-1.0E+06	1.1E+06	2.0E+06	-2.1E+06	5.7E+05	-1.0E+05	-5.5E+04	-7.1E+04	-7.3E+04	-5.1E+04	-5.0E+04	-6.4E+04	-6.9E+04
78.1	-1.4E+06	1.9E+06	-2.9E+06	-1.1E+06	1.5E+06	2.2E+06	-2.4E+06	1.1E+06	-9.3E+04	-7.3E+04	-1.0E+05	-7.1E+04	-1.7E+05	-6.0E+04	-1.9E+05	-7.0E+04
87.9	-1.3E+06	2.0E+06	-2.8E+06	-1.3E+06	1.3E+06	2.3E+06	-2.7E+06	1.3E+06	-5.3E+04	-5.2E+04	-3.2E+04	-8.1E+04	-6.0E+04	-6.1E+04	-9.8E+04	-6.1E+04
97.7	-1.4E+06	2.0E+06	-3.2E+06	-1.3E+06	1.3E+06	2.4E+06	-3.1E+06	1.2E+06	-1.2E+05	-9.7E+04	-1.2E+05	-7.1E+04	-1.1E+05	-1.1E+05	-8.7E+04	-5.0E+04
107.4	-1.9E+06	2.0E+06	-2.8E+06	-1.2E+06	1.6E+06	2.5E+06	-3.3E+06	1.8E+06	-5.9E+04	-6.5E+04	-6.9E+04	-7.4E+04	-5.3E+04	-5.8E+04	-6.5E+04	-6.0E+04
117.2	-1.3E+06	1.7E+06	-3.2E+06	-9.9E+05	2.0E+06	2.8E+06	-3.4E+06	1.9E+06	-6.0E+04	-4.6E+04	-6.0E+04	-5.9E+04	-4.5E+04	-5.3E+04	-6.2E+04	-4.0E+04
127.0	-1.2E+06	1.5E+06	-3.0E+06	-5.7E+05	2.3E+06	3.2E+06	-3.6E+06	1.9E+06	-5.1E+04	-4.8E+04	-6.8E+04	-8.8E+04	-5.1E+04	-7.6E+04	-5.1E+04	-5.1E+04
136.7	-1.6E+06	4.6E+05	-4.2E+06	-1.6E+06	3.3E+06	4.3E+06	-2.9E+06	2.5E+06	-5.3E+04	-5.7E+04	-5.6E+04	-9.8E+04	-9.0E+04	-6.6E+04	-1.2E+05	-6.0E+04
146.5	-1.6E+06	1.1E+06	-2.0E+06	-8.6E+05	8.9E+05	4.3E+06	-3.1E+06	1.9E+06	-3.5E+04	-5.0E+04	-4.4E+04	-6.3E+04	-5.8E+04	-7.1E+04	-4.0E+04	-5.7E+04
156.3	-3.0E+06	3.3E+06	-1.2E+06	-2.8E+06	2.6E+06	4.6E+06	-4.7E+06	2.4E+06	-6.9E+04	-7.6E+04	-3.9E+04	-8.9E+04	-4.9E+04	-6.9E+04	-1.1E+05	-9.1E+04
166.0	-1.7E+06	1.8E+06	-3.5E+06	-2.6E+05	2.0E+06	5.2E+06	-4.9E+06	2.0E+06	-6.5E+04	-5.9E+04	-4.0E+04	-7.2E+04	-7.2E+04	-6.0E+04	-7.6E+04	-5.4E+04
175.8	-1.2E+06	1.0E+06	-2.7E+06	3.5E+04	3.4E+06	4.9E+06	-5.2E+06	3.5E+06	-5.8E+04	-4.9E+04	-5.3E+04	-7.0E+04	-5.8E+04	-7.0E+04	-5.2E+04	-6.6E+04
185.5	-1.5E+06	2.7E+06	-1.2E+06	-2.9E+06	3.1E+06	6.4E+06	-6.2E+06	2.1E+06	-5.6E+04	-5.1E+04	-8.8E+04	-7.8E+04	-5.5E+04	-6.7E+04	-5.8E+04	-6.3E+04
195.3	1.5E+04	2.4E+06	-3.4E+06	-8.4E+05	3.4E+06	6.7E+06	-6.9E+06	2.4E+06	-5.6E+04	-6.7E+04	-5.3E+04	-9.2E+04	-6.0E+04	-6.0E+04	-6.8E+04	-7.7E+04
205.1	5.3E+05	3.9E+06	-2.7E+06	1.4E+05	1.7E+06	4.7E+06	-8.2E+06	1.6E+06	-6.5E+04	-6.5E+04	-5.8E+04	-7.4E+04	-4.9E+04	-5.4E+04	-6.5E+04	-7.3E+04
214.8	-8.2E+05	9.4E+05	-4.6E+06	-1.7E+06	3.0E+06	6.4E+06	-7.2E+06	3.3E+06	-2.4E+04	-6.6E+04	-3.6E+04	-6.4E+04	-4.8E+04	-5.5E+04	-3.0E+04	-5.1E+04
224.6	-1.2E+06	1.3E+06	-4.0E+06	-1.1E+06	3.2E+06	7.3E+06	-7.6E+06	3.5E+06	-2.8E+04	-6.0E+04	-2.6E+04	-8.5E+04	-3.3E+04	-8.0E+04	-4.2E+04	-5.0E+04

Table 17. Raw data for TOR labyrinth seal at 10,200 rpm, 0.5 PR, and medium preswirl

Freq	Re Hxx	Re Hxy	Re Hyx	Re Hyy	Im Hxx	Im Hxy	Im Hyx	Im Hyy	Re eHxx	Re eHxy	Re eHyx	Re eHyy	Im eHxx	Im eHxy	Im eHyx	Im eHyy
Hz	N/m	N/m	N/m	N/m	N/m	N/m	N/m	N/m	N/m	N/m	N/m	N/m	N/m	N/m	N/m	N/m
9.8	1.9E+06	4.2E+05	-1.7E+06	2.1E+06	-7.0E+04	5.7E+05	-5.5E+03	-1.7E+05	-1.5E+05	-2.7E+05	-1.4E+05	-2.5E+05	-1.5E+05	-1.3E+05	-1.5E+05	-1.1E+05
19.5	1.4E+06	1.1E+06	-1.4E+06	1.5E+06	6.0E+05	4.3E+05	-6.5E+05	-1.4E+05	-2.3E+05	-2.0E+05	-1.7E+05	-1.6E+05	-2.8E+05	-1.4E+05	-1.9E+05	-1.1E+05
29.3	1.4E+06	5.5E+05	-1.6E+06	1.7E+06	1.0E+05	4.8E+05	-2.2E+05	2.1E+05	-1.2E+05	-1.2E+05	-1.4E+05	-1.2E+05	-1.6E+05	-1.2E+05	-1.0E+05	-1.5E+05
39.1	8.0E+05	9.6E+05	-1.0E+06	1.5E+06	4.1E+05	5.6E+05	-8.3E+05	2.2E+05	-3.5E+05	-7.7E+04	-2.3E+05	-6.9E+04	-3.4E+05	-1.1E+05	-2.7E+05	-8.8E+04
48.8	1.6E+06	9.0E+05	-1.5E+06	1.5E+06	6.6E+05	5.9E+05	-8.6E+05	2.5E+05	-2.2E+05	-5.6E+04	-2.5E+05	-5.8E+04	-1.1E+05	-6.0E+04	-2.0E+05	-8.8E+04
58.6	1.6E+06	1.0E+06	-2.2E+06	1.4E+06	6.5E+05	3.8E+05	-6.1E+05	3.3E+05	-1.6E+05	-6.0E+04	-2.3E+05	-1.1E+05	-1.9E+05	-7.8E+04	-2.9E+05	-9.6E+04
68.4	1.1E+06	7.2E+05	-1.6E+06	1.1E+06	8.8E+05	3.7E+05	-3.0E+05	2.5E+05	-1.4E+05	-6.0E+04	-1.2E+05	-4.5E+04	-1.1E+05	-5.7E+04	-1.4E+05	-8.0E+04
78.1	8.6E+05	2.0E+05	-1.0E+06	5.8E+05	1.3E+06	-2.9E+04	-3.6E+05	1.3E+06	-2.6E+05	-5.9E+04	-1.9E+05	-7.9E+04	-1.5E+05	-7.0E+04	-2.5E+05	-1.1E+05
87.9	1.9E+06	7.6E+04	-8.3E+05	1.5E+06	1.6E+06	1.0E+06	-1.7E+06	1.3E+06	-6.8E+04	-5.0E+04	-9.0E+04	-4.5E+04	-1.2E+05	-8.0E+04	-8.2E+04	-6.4E+04
97.7	1.8E+06	1.4E+05	-1.3E+06	1.6E+06	1.2E+06	1.2E+06	-2.0E+06	1.0E+06	-8.5E+04	-4.4E+04	-9.2E+04	-6.0E+04	-8.7E+04	-7.0E+04	-1.1E+05	-6.5E+04
107.4	1.3E+06	2.6E+05	-1.1E+06	1.5E+06	1.3E+06	1.3E+06	-1.8E+06	1.4E+06	-1.1E+05	-5.8E+04	-8.9E+04	-6.5E+04	-8.1E+04	-5.9E+04	-8.5E+04	-6.6E+04
117.2	1.8E+06	1.2E+05	-1.5E+06	1.9E+06	1.4E+06	1.5E+06	-2.0E+06	1.4E+06	-5.9E+04	-3.3E+04	-6.8E+04	-4.6E+04	-4.4E+04	-6.1E+04	-4.8E+04	-6.2E+04
127.0	1.9E+06	-4.5E+04	-1.5E+06	2.0E+06	1.5E+06	1.9E+06	-2.1E+06	1.3E+06	-9.4E+04	-5.2E+04	-8.5E+04	-6.0E+04	-9.8E+04	-7.4E+04	-6.1E+04	-6.0E+04
136.7	1.3E+06	-9.9E+05	-2.9E+06	1.3E+06	2.1E+06	2.9E+06	-1.5E+06	2.1E+06	-4.6E+04	-4.9E+04	-5.5E+04	-5.0E+04	-1.1E+05	-6.9E+04	-1.0E+05	-1.0E+05
146.5	1.6E+06	-1.0E+05	-6.7E+05	1.8E+06	2.9E+05	2.6E+06	-1.2E+06	1.1E+06	-3.7E+04	-4.3E+04	-3.8E+04	-4.1E+04	-2.5E+04	-5.3E+04	-3.5E+04	-5.9E+04
156.3	-4.7E+05	2.3E+06	1.3E+06	-5.9E+05	2.3E+06	1.9E+06	-3.3E+06	2.5E+06	-4.4E+04	-4.4E+04	-5.1E+04	-7.7E+04	-3.4E+04	-4.4E+04	-5.8E+04	-9.9E+04
166.0	7.0E+05	5.8E+05	-1.4E+06	2.1E+06	1.3E+06	3.3E+06	-2.6E+06	1.4E+06	-7.1E+04	-4.2E+04	-6.1E+04	-3.6E+04	-9.9E+04	-5.7E+04	-4.5E+04	-6.3E+04
175.8	1.7E+06	3.4E+05	-1.3E+06	2.6E+06	2.0E+06	2.8E+06	-3.1E+06	2.1E+06	-3.8E+04	-3.8E+04	-3.7E+04	-3.9E+04	-3.2E+04	-4.6E+04	-3.5E+04	-5.3E+04
185.5	1.0E+06	2.0E+06	6.3E+04	-9.6E+05	1.5E+06	3.7E+06	-2.6E+06	1.0E+06	-7.2E+04	-3.5E+04	-7.1E+04	-5.1E+04	-4.4E+04	-4.0E+04	-6.3E+04	-5.2E+04
195.3	2.5E+06	1.1E+06	-1.7E+06	1.6E+06	2.1E+06	3.6E+06	-3.6E+06	1.7E+06	-4.4E+04	-3.9E+04	-3.7E+04	-5.4E+04	-4.7E+04	-7.4E+04	-5.1E+04	-6.5E+04
205.1	3.0E+06	2.4E+06	-1.3E+06	2.6E+06	1.8E+04	1.5E+06	-4.7E+06	9.6E+05	-6.9E+04	-5.3E+04	-7.6E+04	-4.3E+04	-8.7E+04	-4.8E+04	-5.8E+04	-5.9E+04
214.8	1.2E+06	-7.1E+05	-2.1E+06	1.1E+06	2.5E+06	3.3E+06	-3.8E+06	2.3E+06	-4.1E+04	-4.8E+04	-2.8E+04	-5.7E+04	-3.0E+04	-4.2E+04	-2.8E+04	-5.5E+04
224.6	1.4E+06	-3.1E+05	-2.0E+06	1.4E+06	2.3E+06	3.9E+06	-4.1E+06	2.5E+06	-4.0E+04	-6.5E+04	-4.8E+04	-4.8E+04	-4.0E+04	-7.2E+04	-3.1E+04	-8.0E+04

Table 18. Raw data for TOR labyrinth seal at 15,350 rpm, 0.5 PR, and medium preswirl

Freq	Re Hxx	Re Hxy	Re Hyx	Re Hyy	Im Hxx	Im Hxy	Im Hyx	Im Hyy	Re eHxx	Re eHxy	Re eHyx	Re eHyy	Im eHxx	Im eHxy	Im eHyx	Im eHyy
Hz	N/m	N/m	N/m	N/m	N/m	N/m	N/m	N/m	N/m	N/m	N/m	N/m	N/m	N/m	N/m	N/m
9.8	6.2E+05	8.9E+05	-1.8E+06	8.6E+05	-6.4E+04	3.4E+05	-2.0E+04	7.7E+04	-8.6E+04	-1.4E+05	-8.3E+04	-8.8E+04	-1.5E+05	-1.7E+05	-1.3E+05	-1.1E+05
19.5	3.9E+05	1.2E+06	-1.5E+06	6.6E+05	6.4E+05	5.4E+05	-1.1E+06	9.4E+04	-1.9E+05	-1.0E+05	-1.3E+05	-9.1E+04	-1.7E+05	-8.4E+04	-2.2E+05	-9.6E+04
29.3	3.6E+05	1.1E+06	-1.9E+06	5.7E+05	1.9E+05	6.4E+05	-7.3E+05	2.7E+05	-8.9E+04	-1.5E+05	-1.3E+05	-1.1E+05	-1.0E+05	-1.4E+05	-5.0E+04	-8.4E+04
39.1	1.6E+05	1.2E+06	-1.9E+06	5.3E+05	6.9E+05	9.1E+05	-1.9E+06	2.9E+05	-2.6E+05	-8.8E+04	-1.7E+05	-8.4E+04	-3.0E+05	-8.0E+04	-3.9E+05	-8.6E+04
48.8	4.3E+05	1.3E+06	-1.7E+06	3.7E+05	3.6E+05	1.2E+06	-1.5E+06	2.8E+05	-1.3E+05	-9.0E+04	-2.5E+05	-8.3E+04	-7.8E+04	-5.0E+04	-1.3E+05	-5.3E+04
58.6	3.8E+05	1.2E+06	-2.6E+06	6.2E+05	8.8E+05	1.3E+06	-1.5E+06	5.9E+05	-1.6E+05	-8.0E+04	-2.6E+05	-8.6E+04	-1.8E+05	-7.4E+04	-2.1E+05	-9.4E+04
68.4	2.7E+05	1.2E+06	-2.1E+06	4.9E+05	8.0E+05	1.5E+06	-1.7E+06	3.3E+05	-7.3E+04	-7.0E+04	-9.3E+04	-5.6E+04	-8.3E+04	-6.2E+04	-1.1E+05	-7.4E+04
78.1	1.3E+04	1.3E+06	-1.7E+06	7.0E+04	9.4E+05	1.6E+06	-1.4E+06	6.0E+05	-1.1E+05	-6.0E+04	-1.4E+05	-7.1E+04	-2.1E+05	-5.0E+04	-1.7E+05	-6.2E+04
87.9	1.4E+05	1.5E+06	-2.2E+06	-6.6E+04	6.9E+05	1.7E+06	-2.2E+06	5.9E+05	-7.8E+04	-7.0E+04	-7.0E+04	-3.6E+04	-1.0E+05	-4.3E+04	-6.5E+04	-8.5E+04
97.7	-1.3E+05	1.2E+06	-2.3E+06	-2.5E+05	9.0E+05	1.5E+06	-2.3E+06	7.1E+05	-8.0E+04	-3.4E+04	-5.4E+04	-4.8E+04	-7.9E+04	-4.6E+04	-7.6E+04	-6.6E+04
107.4	-5.9E+05	9.9E+05	-1.7E+06	-3.1E+05	1.4E+06	1.5E+06	-2.2E+06	1.5E+06	-7.7E+04	-5.3E+04	-7.5E+04	-4.9E+04	-8.1E+04	-7.9E+04	-6.3E+04	-7.7E+04
117.2	1.7E+04	7.0E+05	-2.0E+06	7.4E+04	1.7E+06	1.9E+06	-2.5E+06	1.6E+06	-3.4E+04	-5.0E+04	-4.4E+04	-4.7E+04	-3.2E+04	-6.1E+04	-3.6E+04	-5.6E+04
127.0	-8.8E+04	2.9E+05	-1.8E+06	-2.0E+05	2.2E+06	1.9E+06	-2.4E+06	1.9E+06	-7.9E+04	-4.0E+04	-9.5E+04	-6.2E+04	-8.8E+04	-6.9E+04	-7.3E+04	-7.1E+04
136.7	9.4E+04	-9.0E+05	-3.1E+06	9.8E+04	3.0E+06	4.1E+06	-2.6E+06	2.7E+06	-4.9E+04	-4.7E+04	-4.6E+04	-6.8E+04	-9.0E+04	-4.5E+04	-8.8E+04	-7.0E+04
146.5	3.2E+05	2.7E+05	-1.2E+06	7.6E+05	6.7E+05	4.0E+06	-2.6E+06	1.5E+06	-4.7E+04	-4.8E+04	-4.5E+04	-4.8E+04	-5.3E+04	-7.7E+04	-4.8E+04	-5.9E+04
156.3	-1.1E+06	2.1E+06	-3.5E+05	-1.3E+06	2.1E+06	3.9E+06	-3.8E+06	2.1E+06	-4.9E+04	-5.2E+04	-5.2E+04	-6.3E+04	-4.4E+04	-4.7E+04	-5.2E+04	-7.0E+04
166.0	9.1E+04	7.5E+05	-2.6E+06	1.4E+06	1.8E+06	4.6E+06	-4.1E+06	1.8E+06	-6.8E+04	-3.8E+04	-4.9E+04	-4.4E+04	-8.6E+04	-5.5E+04	-6.0E+04	-5.7E+04
175.8	6.2E+05	6.8E+05	-2.2E+06	1.6E+06	2.3E+06	4.3E+06	-4.5E+06	2.8E+06	-4.0E+04	-4.1E+04	-4.3E+04	-4.3E+04	-2.3E+04	-3.9E+04	-3.1E+04	-5.3E+04
185.5	-1.6E+05	2.6E+06	-6.7E+05	-1.9E+06	2.2E+06	5.1E+06	-4.4E+06	1.5E+06	-7.9E+04	-3.7E+04	-7.3E+04	-4.0E+04	-4.8E+04	-4.6E+04	-4.8E+04	-5.4E+04
195.3	1.2E+06	1.8E+06	-2.4E+06	4.1E+05	2.6E+06	5.2E+06	-5.4E+06	2.1E+06	-4.5E+04	-6.9E+04	-3.8E+04	-4.2E+04	-6.5E+04	-6.1E+04	-4.9E+04	-6.1E+04
205.1	1.9E+06	3.4E+06	-1.9E+06	1.4E+06	7.4E+05	3.1E+06	-6.6E+06	1.4E+06	-5.0E+04	-4.8E+04	-7.2E+04	-5.4E+04	-6.7E+04	-6.0E+04	-4.6E+04	-7.3E+04
214.8	-3.5E+04	2.3E+05	-3.0E+06	-3.0E+05	3.1E+06	5.0E+06	-5.9E+06	2.7E+06	-4.6E+04	-4.8E+04	-3.6E+04	-7.1E+04	-2.4E+04	-4.6E+04	-3.3E+04	-6.5E+04
224.6	1.2E+05	6.6E+05	-2.9E+06	6.8E+04	2.9E+06	5.5E+06	-6.2E+06	3.0E+06	-3.9E+04	-5.3E+04	-3.4E+04	-6.5E+04	-3.4E+04	-6.1E+04	-3.8E+04	-8.6E+04

Table 19. Raw data for TOR labyrinth seal at 20,200 rpm, 0.5 PR, and medium preswirl

Freq	Re Hxx	Re Hxy	Re Hyx	Re Hyy	Im Hxx	Im Hxy	Im Hyx	Im Hyy	Re eHxx	Re eHxy	Re eHyx	Re eHyy	Im eHxx	Im eHxy	Im eHyx	Im eHyy
Hz	N/m	N/m	N/m	N/m	N/m	N/m	N/m	N/m	N/m	N/m	N/m	N/m	N/m	N/m	N/m	N/m
9.8	-8.9E+05	1.6E+06	-2.4E+06	-7.7E+05	-2.8E+04	5.6E+05	-1.5E+04	-1.1E+05	-1.2E+05	-1.2E+05	-9.5E+04	-7.0E+04	-1.3E+05	-1.6E+05	-8.5E+04	-1.1E+05
19.5	-1.1E+06	1.7E+06	-2.7E+06	-9.7E+05	3.2E+05	7.4E+05	-1.1E+06	1.0E+05	-2.0E+05	-1.0E+05	-1.1E+05	-7.1E+04	-1.8E+05	-6.9E+04	-1.6E+05	-8.1E+04
29.3	-1.4E+06	2.1E+06	-2.9E+06	-1.2E+06	2.2E+05	9.8E+05	-9.3E+05	2.1E+05	-1.1E+05	-8.0E+04	-1.1E+05	-7.6E+04	-6.4E+04	-9.6E+04	-4.8E+04	-7.1E+04
39.1	-2.0E+06	2.0E+06	-3.3E+06	-1.1E+06	1.3E+06	1.3E+06	-1.6E+06	3.8E+05	-2.4E+05	-6.6E+04	-2.5E+05	-5.1E+04	-2.9E+05	-8.5E+04	-2.2E+05	-8.3E+04
48.8	-1.2E+06	1.8E+06	-2.8E+06	-1.1E+06	7.8E+05	1.5E+06	-1.9E+06	5.4E+05	-4.8E+05	-3.6E+05	-3.0E+05	-1.1E+05	-5.7E+05	-2.3E+05	-1.8E+05	-1.2E+05
58.6	-1.2E+06	2.1E+06	-3.7E+06	-9.0E+05	1.3E+06	1.6E+06	-1.6E+06	7.1E+05	-1.5E+05	-9.5E+04	-3.0E+05	-1.1E+05	-1.9E+05	-4.9E+04	-2.1E+05	-7.3E+04
68.4	-1.2E+06	1.9E+06	-3.1E+06	-1.1E+06	1.3E+06	2.0E+06	-2.0E+06	8.2E+05	-1.1E+05	-4.3E+04	-1.0E+05	-5.5E+04	-8.0E+04	-6.1E+04	-1.1E+05	-7.5E+04
78.1	-1.2E+06	2.1E+06	-2.7E+06	-1.2E+06	1.4E+06	2.1E+06	-2.5E+06	9.9E+05	-1.2E+05	-7.8E+04	-1.1E+05	-6.6E+04	-1.2E+05	-6.3E+04	-2.0E+05	-7.9E+04
87.9	-9.6E+05	2.1E+06	-3.1E+06	-1.3E+06	1.5E+06	2.5E+06	-2.7E+06	1.1E+06	-8.9E+04	-4.0E+04	-9.8E+04	-4.8E+04	-8.6E+04	-4.0E+04	-6.3E+04	-6.5E+04
97.7	-1.1E+06	2.0E+06	-3.4E+06	-1.3E+06	1.5E+06	2.6E+06	-3.1E+06	1.2E+06	-9.6E+04	-5.4E+04	-6.2E+04	-5.7E+04	-7.7E+04	-4.8E+04	-8.8E+04	-5.6E+04
107.4	-1.7E+06	2.2E+06	-3.0E+06	-1.3E+06	1.6E+06	2.6E+06	-3.0E+06	1.6E+06	-8.4E+04	-4.8E+04	-7.3E+04	-3.7E+04	-8.2E+04	-4.0E+04	-5.0E+04	-6.4E+04
117.2	-1.1E+06	2.0E+06	-3.3E+06	-1.2E+06	1.8E+06	2.9E+06	-3.3E+06	1.8E+06	-5.4E+04	-4.7E+04	-3.9E+04	-3.2E+04	-3.9E+04	-4.6E+04	-3.1E+04	-4.8E+04
127.0	-1.1E+06	1.7E+06	-3.1E+06	-9.5E+05	2.3E+06	3.1E+06	-3.4E+06	1.8E+06	-8.6E+04	-6.0E+04	-8.1E+04	-6.3E+04	-8.7E+04	-7.3E+04	-6.6E+04	-7.9E+04
136.7	-1.5E+06	4.2E+05	-4.0E+06	-1.9E+06	3.5E+06	4.4E+06	-2.6E+06	2.7E+06	-7.6E+04	-6.3E+04	-7.9E+04	-5.8E+04	-1.3E+05	-7.5E+04	-6.5E+04	-6.5E+04
146.5	-1.5E+06	1.2E+06	-1.9E+06	-9.9E+05	1.1E+06	4.4E+06	-3.0E+06	1.8E+06	-4.5E+04	-4.1E+04	-3.6E+04	-3.7E+04	-3.2E+04	-5.5E+04	-4.0E+04	-5.5E+04
156.3	-2.7E+06	3.2E+06	-1.2E+06	-3.0E+06	2.5E+06	4.6E+06	-4.8E+06	2.4E+06	-4.9E+04	-4.6E+04	-5.9E+04	-6.5E+04	-6.3E+04	-6.3E+04	-5.7E+04	-6.6E+04
166.0	-1.5E+06	1.8E+06	-3.6E+06	-3.2E+05	2.2E+06	5.5E+06	-5.0E+06	2.1E+06	-6.5E+04	-3.7E+04	-4.4E+04	-4.4E+04	-8.8E+04	-5.5E+04	-5.4E+04	-4.7E+04
175.8	-1.0E+06	1.2E+06	-2.7E+06	-4.6E+05	3.4E+06	5.0E+06	-5.5E+06	3.6E+06	-4.0E+04	-5.5E+04	-6.7E+04	-6.4E+04	-5.0E+04	-5.3E+04	-4.2E+04	-6.1E+04
185.5	-1.3E+06	3.2E+06	-1.3E+06	-3.3E+06	2.9E+06	6.8E+06	-6.0E+06	2.0E+06	-7.9E+04	-4.4E+04	-8.1E+04	-4.8E+04	-6.5E+04	-5.2E+04	-5.1E+04	-5.4E+04
195.3	1.6E+05	2.7E+06	-3.5E+06	-9.6E+05	3.4E+06	6.8E+06	-7.0E+06	2.7E+06	-3.5E+04	-6.4E+04	-3.1E+04	-4.5E+04	-5.5E+04	-5.1E+04	-4.5E+04	-6.2E+04
205.1	7.2E+05	4.2E+06	-3.0E+06	1.7E+04	1.6E+06	4.8E+06	-8.3E+06	2.0E+06	-5.3E+04	-4.2E+04	-6.1E+04	-5.5E+04	-7.4E+04	-6.7E+04	-6.1E+04	-6.6E+04
214.8	-6.7E+05	1.3E+06	-4.5E+06	-1.7E+06	3.1E+06	6.5E+06	-7.4E+06	3.4E+06	-4.4E+04	-4.6E+04	-2.9E+04	-3.9E+04	-4.4E+04	-4.6E+04	-4.1E+04	-5.4E+04
224.6	-8.8E+05	1.7E+06	-4.2E+06	-1.3E+06	3.2E+06	7.2E+06	-7.7E+06	3.7E+06	-4.3E+04	-7.5E+04	-3.9E+04	-4.0E+04	-6.1E+04	-6.3E+04	-3.8E+04	-8.6E+04

Table 20. Raw data for TOR labyrinth seal at 10,200 rpm, 0.6 PR, and medium preswirl

Freq	Re Hxx	Re Hxy	Re Hyx	Re Hyy	Im Hxx	Im Hxy	Im Hyx	Im Hyy	Re eHxx	Re eHxy	Re eHyx	Re eHyy	Im eHxx	Im eHxy	Im eHyx	Im eHyy
Hz	N/m	N/m	N/m	N/m	N/m	N/m	N/m	N/m	N/m	N/m	N/m	N/m	N/m	N/m	N/m	N/m
9.8	1.5E+06	7.6E+05	-1.4E+06	1.8E+06	3.4E+04	3.5E+05	-8.4E+04	1.0E+04	-1.1E+05	-1.9E+05	-1.4E+05	-1.3E+05	-1.5E+05	-1.2E+05	-1.5E+05	-1.2E+05
19.5	9.2E+05	1.1E+06	-1.4E+06	1.6E+06	6.3E+05	5.0E+05	-3.1E+05	-2.0E+05	-2.1E+05	-1.1E+05	-1.9E+05	-6.7E+04	-2.6E+05	-1.1E+05	-2.2E+05	-8.7E+04
29.3	1.2E+06	1.0E+06	-1.4E+06	1.6E+06	5.8E+04	4.9E+05	-3.0E+05	-2.6E+05	-1.4E+05	-1.1E+05	-8.8E+04	-9.9E+04	-1.2E+05	-2.0E+05	-8.8E+04	-1.2E+05
39.1	9.3E+05	9.7E+05	-1.2E+06	1.4E+06	1.8E+05	5.0E+05	-4.5E+05	-1.9E+04	-1.1E+05	-8.7E+04	-1.1E+05	-6.7E+04	-9.8E+04	-6.9E+04	-1.6E+05	-7.4E+04
48.8	1.2E+06	9.4E+05	-1.6E+06	1.4E+06	2.6E+05	4.9E+05	-2.5E+05	3.4E+04	-2.4E+05	-9.5E+04	-2.2E+05	-7.8E+04	-2.7E+05	-1.1E+05	-2.3E+05	-7.6E+04
58.6	1.5E+06	1.0E+06	-1.8E+06	1.4E+06	5.9E+05	5.2E+05	-9.4E+05	1.7E+05	-3.1E+05	-1.2E+05	-2.0E+05	-1.0E+05	-3.0E+05	-8.5E+04	-3.0E+05	-1.0E+05
68.4	1.1E+06	8.7E+05	-1.4E+06	9.8E+05	5.9E+05	2.2E+05	-4.0E+05	2.7E+05	-6.7E+04	-8.0E+04	-1.4E+05	-6.4E+04	-9.8E+04	-7.6E+04	-8.4E+04	-6.0E+04
78.1	4.9E+05	3.9E+05	-5.5E+05	5.5E+05	1.1E+06	1.8E+05	-2.4E+05	8.4E+05	-2.8E+05	-1.3E+05	-2.1E+05	-9.3E+04	-2.2E+05	-7.7E+04	-9.7E+04	-8.3E+04
87.9	1.4E+06	1.4E+05	-6.8E+05	1.3E+06	1.3E+06	1.2E+06	-1.4E+06	1.3E+06	-1.3E+05	-8.5E+04	-1.1E+05	-6.9E+04	-6.5E+04	-1.0E+05	-1.1E+05	-7.7E+04
97.7	1.3E+06	2.4E+05	-9.3E+05	1.2E+06	1.1E+06	1.2E+06	-1.8E+06	9.6E+05	-6.6E+04	-7.6E+04	-4.5E+04	-8.7E+04	-5.4E+04	-8.7E+04	-1.2E+05	-4.7E+04
107.4	1.1E+06	3.7E+05	-1.0E+06	1.2E+06	1.2E+06	1.3E+06	-1.8E+06	1.4E+06	-7.9E+04	-6.5E+04	-1.1E+05	-7.9E+04	-9.2E+04	-6.8E+04	-5.7E+04	-5.1E+04
117.2	1.5E+06	1.6E+05	-1.3E+06	1.5E+06	1.5E+06	1.5E+06	-2.1E+06	1.3E+06	-7.0E+04	-7.1E+04	-5.5E+04	-7.0E+04	-7.4E+04	-8.5E+04	-8.5E+04	-4.5E+04
127.0	1.6E+06	1.2E+05	-1.3E+06	1.7E+06	1.7E+06	1.8E+06	-2.0E+06	1.1E+06	-5.8E+04	-6.8E+04	-6.0E+04	-6.7E+04	-6.7E+04	-7.3E+04	-5.8E+04	-6.7E+04
136.7	9.9E+05	-7.1E+05	-2.6E+06	9.5E+05	1.9E+06	3.2E+06	-1.8E+06	2.1E+06	-8.2E+04	-8.3E+04	-6.2E+04	-8.4E+04	-9.6E+04	-1.0E+05	-1.2E+05	-7.8E+04
146.5	1.3E+06	9.8E+04	-2.9E+05	1.3E+06	2.5E+05	2.8E+06	-1.2E+06	1.1E+06	-6.3E+04	-7.5E+04	-4.9E+04	-5.8E+04	-5.9E+04	-7.8E+04	-5.6E+04	-6.2E+04
156.3	-6.9E+05	2.7E+06	1.6E+06	-1.2E+06	2.2E+06	1.7E+06	-3.3E+06	2.5E+06	-5.7E+04	-8.2E+04	-3.4E+04	-7.7E+04	-3.7E+04	-7.0E+04	-5.9E+04	-7.0E+04
166.0	7.0E+05	6.1E+05	-1.2E+06	1.9E+06	1.8E+06	3.0E+06	-3.0E+06	1.6E+06	-8.8E+04	-9.4E+04	-7.1E+04	-7.8E+04	-1.0E+05	-7.6E+04	-8.4E+04	-6.7E+04
175.8	1.3E+06	6.6E+05	-1.1E+06	2.0E+06	2.2E+06	2.7E+06	-3.4E+06	2.2E+06	-5.8E+04	-6.9E+04	-4.7E+04	-6.3E+04	-6.9E+04	-8.5E+04	-4.8E+04	-5.2E+04
185.5	1.1E+06	1.7E+06	-1.6E+05	-4.0E+05	1.8E+06	3.4E+06	-3.3E+06	1.5E+06	-4.2E+04	-7.9E+04	-6.6E+04	-7.6E+04	-6.1E+04	-6.8E+04	-6.6E+04	-6.3E+04
195.3	2.2E+06	1.2E+06	-1.5E+06	1.2E+06	2.0E+06	3.5E+06	-3.9E+06	1.7E+06	-3.6E+04	-9.6E+04	-3.2E+04	-8.1E+04	-6.1E+04	-7.6E+04	-3.7E+04	-5.0E+04
205.1	2.9E+06	2.6E+06	-1.3E+06	2.2E+06	1.2E+05	1.6E+06	-4.8E+06	1.1E+06	-5.7E+04	-6.3E+04	-5.2E+04	-6.8E+04	-4.4E+04	-7.5E+04	-3.8E+04	-5.7E+04
214.8	8.5E+05	-5.7E+05	-1.9E+06	7.9E+05	2.4E+06	3.3E+06	-4.0E+06	2.4E+06	-2.0E+04	-8.2E+04	-2.4E+04	-6.4E+04	-4.5E+04	-6.5E+04	-2.7E+04	-5.1E+04
224.6	1.1E+06	-1.7E+05	-1.8E+06	1.2E+06	2.3E+06	3.9E+06	-4.2E+06	2.6E+06	-4.1E+04	-1.0E+05	-4.5E+04	-9.6E+04	-3.9E+04	-1.1E+05	-3.7E+04	-7.2E+04

Table 21. Raw data for TOR labyrinth seal at 15,350 rpm, 0.6 PR, and medium preswirl

Freq	Re Hxx	Re Hxy	Re Hyx	Re Hyy	Im Hxx	Im Hxy	Im Hyx	Im Hyy	Re eHxx	Re eHxy	Re eHyx	Re eHyy	Im eHxx	Im eHxy	Im eHyx	Im eHyy
Hz	N/m	N/m	N/m	N/m	N/m	N/m	N/m	N/m	N/m	N/m	N/m	N/m	N/m	N/m	N/m	N/m
9.8	6.4E+04	8.2E+05	-1.5E+06	4.7E+05	-3.5E+04	5.8E+05	-2.3E+05	1.5E+05	-1.7E+05	-2.9E+05	-1.0E+05	-1.8E+05	-1.4E+05	-1.7E+05	-9.1E+04	-1.1E+05
19.5	-1.1E+05	9.6E+05	-2.1E+06	4.0E+05	3.2E+05	6.1E+05	-7.8E+05	-6.6E+04	-2.1E+05	-1.6E+05	-1.9E+05	-9.4E+04	-1.8E+05	-1.4E+05	-1.8E+05	-8.9E+04
29.3	-1.0E+05	1.0E+06	-2.0E+06	4.1E+05	1.8E+05	8.0E+05	-7.3E+05	1.6E+05	-1.1E+05	-1.1E+05	-8.6E+04	-8.0E+04	-8.3E+04	-1.4E+05	-7.2E+04	-7.8E+04
39.1	-3.2E+05	1.1E+06	-1.8E+06	2.1E+05	3.0E+05	1.0E+06	-1.2E+06	3.5E+05	-1.4E+05	-8.3E+04	-9.1E+04	-8.0E+04	-9.3E+04	-6.8E+04	-1.3E+05	-5.5E+04
48.8	6.3E+04	1.2E+06	-1.9E+06	1.6E+05	2.0E+05	1.2E+06	-8.3E+05	4.3E+05	-1.7E+05	-6.6E+04	-1.6E+05	-7.0E+04	-2.0E+05	-7.8E+04	-2.2E+05	-4.6E+04
58.6	4.7E+04	1.1E+06	-2.3E+06	4.5E+05	1.3E+06	1.4E+06	-1.5E+06	7.1E+05	-3.6E+05	-8.4E+04	-1.1E+05	-1.2E+05	-2.2E+05	-9.1E+04	-2.9E+05	-5.4E+04
68.4	1.8E+05	1.2E+06	-1.9E+06	3.8E+05	9.5E+05	1.6E+06	-1.5E+06	5.1E+05	-6.3E+04	-8.2E+04	-1.2E+05	-5.8E+04	-1.0E+05	-7.4E+04	-8.4E+04	-4.6E+04
78.1	-1.4E+05	1.4E+06	-1.9E+06	2.2E+05	5.6E+05	1.8E+06	-1.6E+06	5.1E+05	-1.9E+05	-9.1E+04	-1.4E+05	-7.6E+04	-2.0E+05	-1.1E+05	-1.3E+05	-5.4E+04
87.9	-6.5E+03	1.6E+06	-2.3E+06	-2.4E+05	6.3E+05	1.8E+06	-2.0E+06	5.6E+05	-1.1E+05	-5.9E+04	-8.4E+04	-9.1E+04	-5.6E+04	-8.5E+04	-1.1E+05	-5.3E+04
97.7	-4.9E+05	1.3E+06	-2.1E+06	-5.5E+05	1.0E+06	1.6E+06	-2.3E+06	8.1E+05	-4.3E+04	-8.2E+04	-5.8E+04	-8.3E+04	-9.7E+04	-6.8E+04	-1.0E+05	-6.4E+04
107.4	-5.6E+05	1.1E+06	-1.8E+06	-5.4E+05	1.4E+06	1.7E+06	-2.2E+06	1.5E+06	-8.2E+04	-8.1E+04	-9.2E+04	-1.1E+05	-8.6E+04	-9.8E+04	-8.3E+04	-5.3E+04
117.2	-7.3E+04	8.6E+05	-1.9E+06	-2.1E+05	1.8E+06	2.0E+06	-2.5E+06	1.6E+06	-7.3E+04	-6.5E+04	-7.1E+04	-5.8E+04	-7.3E+04	-6.4E+04	-6.9E+04	-4.7E+04
127.0	-1.3E+05	6.0E+05	-1.8E+06	-1.8E+05	2.1E+06	2.2E+06	-2.6E+06	1.6E+06	-4.9E+04	-7.0E+04	-5.3E+04	-6.6E+04	-6.9E+04	-7.4E+04	-5.9E+04	-4.8E+04
136.7	-1.5E+05	-7.8E+05	-3.0E+06	-2.8E+05	3.1E+06	4.4E+06	-2.5E+06	2.7E+06	-7.4E+04	-9.7E+04	-8.1E+04	-8.4E+04	-1.2E+05	-7.4E+04	-1.0E+05	-6.9E+04
146.5	2.5E+05	5.5E+05	-9.9E+05	3.1E+05	8.5E+05	4.3E+06	-2.6E+06	1.5E+06	-6.5E+04	-7.8E+04	-6.2E+04	-7.1E+04	-5.7E+04	-7.9E+04	-6.6E+04	-5.0E+04
156.3	-1.2E+06	2.4E+06	-5.7E+04	-1.7E+06	2.1E+06	4.2E+06	-3.8E+06	2.2E+06	-4.4E+04	-8.8E+04	-3.9E+04	-7.4E+04	-6.2E+04	-8.4E+04	-5.2E+04	-6.1E+04
166.0	2.8E+05	7.1E+05	-2.6E+06	1.4E+06	2.4E+06	4.5E+06	-4.4E+06	2.0E+06	-8.3E+04	-7.3E+04	-6.9E+04	-6.7E+04	-6.5E+04	-7.5E+04	-6.0E+04	-5.3E+04
175.8	4.8E+05	9.5E+05	-2.2E+06	1.2E+06	2.4E+06	4.5E+06	-4.5E+06	2.8E+06	-5.5E+04	-7.1E+04	-4.2E+04	-6.3E+04	-4.2E+04	-6.9E+04	-3.7E+04	-4.7E+04
185.5	9.4E+04	2.4E+06	-9.9E+05	-1.2E+06	2.4E+06	4.9E+06	-4.9E+06	1.9E+06	-4.1E+04	-6.3E+04	-5.8E+04	-6.9E+04	-4.9E+04	-6.6E+04	-6.0E+04	-4.1E+04
195.3	1.1E+06	2.1E+06	-2.3E+06	1.1E+05	2.7E+06	5.2E+06	-5.5E+06	2.0E+06	-4.7E+04	-9.2E+04	-4.3E+04	-6.5E+04	-4.9E+04	-7.3E+04	-4.2E+04	-6.0E+04
205.1	1.9E+06	3.6E+06	-2.2E+06	9.5E+05	7.2E+05	3.2E+06	-6.5E+06	1.6E+06	-7.0E+04	-7.1E+04	-6.2E+04	-7.2E+04	-7.1E+04	-7.5E+04	-6.8E+04	-6.5E+04
214.8	-2.2E+05	4.2E+05	-2.8E+06	-4.8E+05	3.1E+06	5.0E+06	-5.7E+06	2.8E+06	-1.7E+04	-8.8E+04	-3.0E+04	-6.8E+04	-4.2E+04	-6.5E+04	-2.7E+04	-4.9E+04
224.6	2.8E+04	7.7E+05	-2.7E+06	-9.2E+04	2.9E+06	5.6E+06	-6.2E+06	3.1E+06	-3.5E+04	-6.6E+04	-4.7E+04	-8.0E+04	-4.6E+04	-8.6E+04	-2.9E+04	-6.1E+04

Table 22. Raw data for TOR labyrinth seal at 20,200 rpm, 0.6 PR, and medium preswirl

Freq	Re Hxx	Re Hxy	Re Hyx	Re Hyy	Im Hxx	Im Hxy	Im Hyx	Im Hyy	Re eHxx	Re eHxy	Re eHyx	Re eHyy	Im eHxx	Im eHxy	Im eHyx	Im eHyy
Hz	N/m	N/m	N/m	N/m	N/m	N/m	N/m	N/m	N/m	N/m	N/m	N/m	N/m	N/m	N/m	N/m
9.8	-1.4E+06	2.1E+06	-2.5E+06	-9.6E+05	-1.3E+05	3.7E+05	-4.4E+04	3.1E+05	-1.4E+05	-1.3E+05	-7.0E+04	-1.3E+05	-1.2E+05	-1.5E+05	-7.2E+04	-1.1E+05
19.5	-1.6E+06	2.4E+06	-3.3E+06	-1.0E+06	2.3E+05	6.0E+05	-7.2E+05	5.7E+04	-2.3E+05	-1.5E+05	-1.5E+05	-7.6E+04	-1.9E+05	-8.1E+04	-2.0E+05	-8.6E+04
29.3	-1.7E+06	2.6E+06	-3.1E+06	-1.3E+06	3.8E+05	6.1E+05	-8.5E+05	1.2E+05	-1.0E+05	-1.3E+05	-8.1E+04	-1.1E+05	-9.4E+04	-1.4E+05	-8.3E+04	-8.7E+04
39.1	-1.9E+06	2.2E+06	-3.0E+06	-1.3E+06	8.0E+05	1.0E+06	-1.3E+06	4.5E+05	-1.8E+05	-8.1E+04	-1.1E+05	-7.3E+04	-1.5E+05	-8.4E+04	-1.6E+05	-5.9E+04
48.8	-1.4E+06	2.3E+06	-3.1E+06	-1.3E+06	4.1E+05	1.2E+06	-1.2E+06	5.3E+05	-5.7E+05	-3.4E+05	-2.7E+05	-1.0E+05	-6.4E+05	-3.0E+05	-2.7E+05	-8.2E+04
58.6	-1.2E+06	2.3E+06	-3.3E+06	-1.1E+06	8.4E+05	1.4E+06	-1.7E+06	8.9E+05	-2.6E+05	-8.7E+04	-1.8E+05	-1.4E+05	-2.1E+05	-1.0E+05	-1.9E+05	-9.8E+04
68.4	-1.3E+06	2.1E+06	-2.9E+06	-1.2E+06	1.3E+06	1.8E+06	-1.7E+06	8.1E+05	-8.9E+04	-7.8E+04	-1.5E+05	-7.4E+04	-1.1E+05	-7.7E+04	-9.8E+04	-4.1E+04
78.1	-1.5E+06	2.2E+06	-2.6E+06	-1.4E+06	1.1E+06	2.1E+06	-1.9E+06	9.6E+05	-2.0E+05	-7.9E+04	-1.3E+05	-5.8E+04	-1.9E+05	-8.6E+04	-1.1E+05	-6.1E+04
87.9	-1.2E+06	2.2E+06	-3.0E+06	-1.4E+06	1.3E+06	2.4E+06	-2.4E+06	1.2E+06	-1.1E+05	-8.5E+04	-1.1E+05	-5.7E+04	-4.3E+04	-7.4E+04	-9.3E+04	-7.2E+04
97.7	-1.2E+06	2.2E+06	-3.0E+06	-1.6E+06	1.4E+06	2.5E+06	-2.9E+06	1.3E+06	-5.0E+04	-8.5E+04	-8.0E+04	-6.9E+04	-6.3E+04	-9.4E+04	-1.2E+05	-4.5E+04
107.4	-1.7E+06	2.3E+06	-3.1E+06	-1.5E+06	1.6E+06	2.7E+06	-3.1E+06	1.7E+06	-8.6E+04	-7.4E+04	-9.5E+04	-8.4E+04	-7.9E+04	-7.6E+04	-6.2E+04	-5.5E+04
117.2	-1.3E+06	2.3E+06	-3.3E+06	-1.3E+06	1.8E+06	2.8E+06	-3.3E+06	1.7E+06	-5.7E+04	-7.5E+04	-6.2E+04	-6.6E+04	-7.1E+04	-8.0E+04	-6.3E+04	-4.7E+04
127.0	-1.4E+06	1.9E+06	-3.1E+06	-1.2E+06	2.3E+06	3.1E+06	-3.3E+06	1.7E+06	-6.8E+04	-7.7E+04	-6.4E+04	-8.6E+04	-6.8E+04	-7.1E+04	-5.8E+04	-5.8E+04
136.7	-1.9E+06	6.0E+05	-3.9E+06	-2.3E+06	3.7E+06	4.3E+06	-2.4E+06	2.5E+06	-7.1E+04	-8.8E+04	-6.2E+04	-7.9E+04	-1.2E+05	-9.5E+04	-8.8E+04	-6.1E+04
146.5	-1.4E+06	1.5E+06	-1.8E+06	-1.4E+06	1.3E+06	4.6E+06	-3.0E+06	1.9E+06	-6.4E+04	-6.9E+04	-6.6E+04	-7.8E+04	-6.9E+04	-7.7E+04	-8.3E+04	-4.7E+04
156.3	-2.8E+06	3.2E+06	-8.4E+05	-3.3E+06	2.8E+06	4.6E+06	-5.0E+06	2.4E+06	-5.2E+04	-8.3E+04	-6.3E+04	-9.6E+04	-5.5E+04	-6.9E+04	-5.9E+04	-5.6E+04
166.0	-1.2E+06	1.8E+06	-3.5E+06	-2.9E+05	2.8E+06	5.2E+06	-5.4E+06	2.4E+06	-1.0E+05	-8.6E+04	-6.8E+04	-6.5E+04	-6.8E+04	-7.6E+04	-5.1E+04	-4.6E+04
175.8	-1.1E+06	1.5E+06	-2.7E+06	-9.2E+05	3.3E+06	5.0E+06	-5.5E+06	3.5E+06	-6.1E+04	-8.0E+04	-6.8E+04	-7.7E+04	-6.0E+04	-7.5E+04	-4.3E+04	-6.4E+04
185.5	-8.9E+05	2.8E+06	-1.5E+06	-2.7E+06	3.2E+06	6.5E+06	-6.5E+06	2.5E+06	-6.0E+04	-7.8E+04	-6.2E+04	-7.4E+04	-6.4E+04	-8.2E+04	-7.5E+04	-5.6E+04
195.3	8.4E+04	2.8E+06	-3.2E+06	-1.0E+06	3.3E+06	6.7E+06	-7.1E+06	2.7E+06	-4.6E+04	-8.7E+04	-4.5E+04	-7.2E+04	-7.5E+04	-8.6E+04	-5.0E+04	-6.3E+04
205.1	1.0E+06	4.5E+06	-3.3E+06	-4.4E+05	1.3E+06	4.8E+06	-8.4E+06	2.2E+06	-6.0E+04	-8.7E+04	-6.8E+04	-6.3E+04	-6.5E+04	-8.5E+04	-3.5E+04	-6.4E+04
214.8	-1.2E+06	1.3E+06	-4.0E+06	-1.8E+06	3.5E+06	6.8E+06	-7.4E+06	3.4E+06	-4.0E+04	-7.6E+04	-3.0E+04	-6.2E+04	-5.9E+04	-9.3E+04	-2.9E+04	-5.4E+04
224.6	-1.0E+06	1.9E+06	-3.9E+06	-1.6E+06	3.4E+06	7.4E+06	-7.9E+06	3.8E+06	-3.2E+04	-1.2E+05	-5.2E+04	-9.5E+04	-5.0E+04	-8.5E+04	-3.6E+04	-9.7E+04

Table 23. Raw data for TOR labyrinth seal at 10,200 rpm, 0.4 PR, and high preswirl

Freq	Re Hxx	Re Hxy	Re Hyx	Re Hyy	Im Hxx	Im Hxy	Im Hyx	Im Hyy	Re eHxx	Re eHxy	Re eHyx	Re eHyy	Im eHxx	Im eHxy	Im eHyx	Im eHyy
Hz	N/m	N/m	N/m	N/m	N/m	N/m	N/m	N/m	N/m	N/m	N/m	N/m	N/m	N/m	N/m	N/m
9.8	1.6E+06	1.0E+06	-2.3E+06	1.8E+06	-5.1E+03	1.3E+05	-1.5E+05	7.1E+04	-9.9E+04	-1.1E+05	-4.4E+04	-1.2E+05	-1.5E+05	-8.0E+04	-1.2E+05	-6.5E+04
19.5	1.5E+06	1.3E+06	-2.4E+06	1.6E+06	6.9E+04	6.8E+05	-3.9E+05	-3.0E+05	-1.0E+05	-1.2E+05	-9.3E+04	-9.8E+04	-1.4E+05	-1.4E+05	-1.4E+05	-7.5E+04
29.3	1.5E+06	1.3E+06	-2.5E+06	1.6E+06	1.4E+05	5.4E+05	-2.6E+05	-3.6E+04	-1.6E+05	-6.3E+04	-1.3E+05	-1.1E+05	-1.3E+05	-5.9E+04	-8.8E+04	-7.4E+04
39.1	1.2E+06	1.4E+06	-2.4E+06	1.7E+06	5.3E+05	7.4E+05	-3.5E+05	1.4E+05	-1.5E+05	-4.1E+04	-1.1E+05	-7.2E+04	-1.8E+05	-1.1E+05	-6.6E+04	-8.9E+04
48.8	1.4E+06	1.7E+06	-2.4E+06	1.4E+06	-3.8E+04	8.3E+05	-3.8E+05	1.7E+05	-1.7E+05	-1.3E+05	-1.7E+05	-1.0E+05	-2.4E+05	-7.9E+04	-2.0E+05	-4.7E+04
58.6	1.5E+06	1.5E+06	-2.4E+06	1.5E+06	4.6E+05	7.6E+05	-9.2E+05	2.7E+05	-1.5E+05	-6.3E+04	-1.3E+05	-7.9E+04	-2.3E+05	-9.8E+04	-2.3E+05	-1.2E+05
68.4	1.1E+06	1.3E+06	-2.4E+06	1.1E+06	9.1E+05	7.0E+05	-8.5E+05	3.5E+05	-7.5E+04	-7.0E+04	-9.7E+04	-5.7E+04	-1.1E+05	-1.0E+05	-9.7E+04	-7.1E+04
78.1	9.7E+05	9.4E+05	-1.9E+06	1.0E+06	1.2E+06	8.1E+05	-6.2E+05	9.1E+05	-8.3E+04	-7.2E+04	-8.0E+04	-9.9E+04	-1.6E+05	-6.3E+04	-1.7E+05	-7.6E+04
87.9	1.3E+06	8.4E+05	-1.9E+06	1.3E+06	1.5E+06	1.2E+06	-1.4E+06	1.2E+06	-7.8E+04	-7.6E+04	-6.3E+04	-7.4E+04	-1.3E+05	-6.7E+04	-9.1E+04	-5.0E+04
97.7	1.5E+06	8.7E+05	-2.4E+06	1.0E+06	1.3E+06	1.2E+06	-1.8E+06	1.1E+06	-5.4E+04	-6.8E+04	-6.6E+04	-5.3E+04	-8.8E+04	-5.4E+04	-9.4E+04	-5.3E+04
107.4	1.3E+06	9.5E+05	-2.1E+06	1.4E+06	1.5E+06	1.5E+06	-1.8E+06	1.5E+06	-7.2E+04	-3.9E+04	-6.1E+04	-5.4E+04	-4.2E+04	-4.9E+04	-5.5E+04	-5.9E+04
117.2	1.6E+06	8.3E+05	-2.6E+06	1.5E+06	1.7E+06	1.5E+06	-2.1E+06	1.7E+06	-3.2E+04	-4.6E+04	-5.1E+04	-7.1E+04	-2.6E+04	-5.2E+04	-5.5E+04	-3.9E+04
127.0	1.8E+06	7.0E+05	-2.6E+06	1.7E+06	1.9E+06	1.9E+06	-2.0E+06	1.7E+06	-3.8E+04	-4.5E+04	-4.4E+04	-5.7E+04	-3.6E+04	-6.0E+04	-3.5E+04	-5.1E+04
136.7	2.8E+06	1.1E+05	-4.0E+06	2.7E+06	2.0E+06	2.4E+06	-2.2E+06	1.6E+06	-5.1E+04	-6.4E+04	-4.9E+04	-6.2E+04	-5.8E+04	-7.8E+04	-4.3E+04	-5.7E+04
146.5	2.4E+06	5.6E+05	-2.1E+06	2.5E+06	6.8E+05	3.0E+06	-1.2E+06	1.3E+06	-3.3E+04	-5.5E+04	-5.2E+04	-7.2E+04	-6.3E+04	-6.4E+04	-4.7E+04	-6.4E+04
156.3	1.4E+06	1.6E+06	-2.2E+06	5.2E+05	1.7E+06	2.7E+06	-2.5E+06	1.9E+06	-4.7E+04	-8.1E+04	-4.3E+04	-6.6E+04	-7.2E+04	-7.0E+04	-5.2E+04	-5.6E+04
166.0	-4.0E+05	2.4E+06	-1.5E+06	1.1E+06	1.3E+06	3.8E+06	-2.3E+06	1.4E+06	-1.1E+05	-1.0E+05	-8.0E+04	-9.2E+04	-1.3E+05	-9.6E+04	-8.8E+04	-7.6E+04
175.8	1.5E+06	1.6E+06	-2.5E+06	1.2E+06	2.2E+06	2.9E+06	-2.8E+06	2.3E+06	-9.7E+04	-9.6E+04	-5.2E+04	-7.8E+04	-1.0E+05	-8.8E+04	-6.8E+04	-7.0E+04
185.5	-1.8E+05	3.6E+06	-5.4E+05	-1.4E+06	2.5E+06	4.2E+06	-2.3E+06	1.4E+06	-5.6E+04	-7.3E+04	-5.9E+04	-7.5E+04	-1.2E+05	-8.9E+04	-6.4E+04	-4.6E+04
195.3	2.9E+06	1.8E+06	-2.5E+06	1.5E+06	2.6E+06	3.7E+06	-2.6E+06	2.0E+06	-5.3E+04	-6.5E+04	-4.5E+04	-8.9E+04	-5.5E+04	-8.1E+04	-3.8E+04	-7.0E+04
205.1	2.9E+06	3.4E+06	-2.6E+06	2.5E+06	3.4E+05	1.9E+06	-4.0E+06	1.3E+06	-9.2E+04	-6.7E+04	-6.0E+04	-7.9E+04	-6.5E+04	-7.2E+04	-6.3E+04	-6.5E+04
214.8	1.1E+06	6.6E+05	-3.3E+06	1.1E+06	3.1E+06	4.2E+06	-3.1E+06	3.0E+06	-2.8E+04	-5.1E+04	-2.8E+04	-7.6E+04	-2.8E+04	-6.1E+04	-4.4E+04	-5.3E+04
224.6	1.4E+06	9.3E+05	-3.3E+06	1.4E+06	2.8E+06	4.7E+06	-3.5E+06	2.9E+06	-5.7E+04	-9.1E+04	-3.3E+04	-7.2E+04	-3.2E+04	-6.5E+04	-4.1E+04	-6.6E+04

Table 24. Raw data for TOR labyrinth seal at 15,350 rpm, 0.4 PR, and high preswirl

Freq	Re Hxx	Re Hxy	Re Hyx	Re Hyy	Im Hxx	Im Hxy	Im Hyx	Im Hyy	Re eHxx	Re eHxy	Re eHyx	Re eHyy	Im eHxx	Im eHxy	Im eHyx	Im eHyy
Hz	N/m	N/m	N/m	N/m	N/m	N/m	N/m	N/m	N/m	N/m	N/m	N/m	N/m	N/m	N/m	N/m
9.8	3.5E+05	1.4E+06	-2.6E+06	6.1E+05	-6.2E+04	5.7E+05	-1.7E+05	1.4E+04	-8.6E+04	-7.1E+04	-5.1E+04	-1.0E+05	-1.1E+05	-1.3E+05	-8.0E+04	-8.7E+04
19.5	1.7E+04	1.6E+06	-2.5E+06	4.8E+05	-6.8E+04	6.1E+05	-6.7E+05	-1.5E+04	-1.1E+05	-9.4E+04	-7.6E+04	-8.8E+04	-1.2E+05	-1.4E+05	-1.4E+05	-1.2E+05
29.3	2.0E+05	1.6E+06	-2.7E+06	4.9E+05	1.3E+05	6.6E+05	-8.9E+05	1.2E+05	-1.0E+05	-1.1E+05	-1.3E+05	-1.3E+05	-1.1E+05	-1.1E+05	-7.3E+04	-6.1E+04
39.1	-9.0E+04	1.6E+06	-2.7E+06	4.4E+05	1.3E+05	1.1E+06	-9.7E+05	2.1E+05	-1.6E+05	-7.2E+04	-1.6E+05	-5.1E+04	-1.0E+05	-4.5E+04	-8.1E+04	-5.5E+04
48.8	1.2E+05	1.8E+06	-2.6E+06	3.1E+05	2.9E+05	1.1E+06	-1.4E+06	3.3E+05	-1.4E+05	-5.5E+04	-1.5E+05	-8.8E+04	-1.2E+05	-6.7E+04	-1.2E+05	-4.1E+04
58.6	-2.3E+05	1.7E+06	-3.0E+06	3.2E+05	9.0E+05	1.4E+06	-1.5E+06	4.8E+05	-1.6E+05	-5.8E+04	-1.1E+05	-7.1E+04	-1.4E+05	-7.7E+04	-1.8E+05	-7.2E+04
68.4	5.5E+04	1.7E+06	-3.0E+06	3.2E+05	9.4E+05	1.7E+06	-1.9E+06	4.7E+05	-7.2E+04	-6.9E+04	-6.5E+04	-7.8E+04	-5.9E+04	-6.6E+04	-6.6E+04	-7.1E+04
78.1	-2.4E+05	1.9E+06	-2.9E+06	9.7E+04	1.0E+06	1.9E+06	-1.6E+06	6.7E+05	-7.6E+04	-5.9E+04	-6.0E+04	-7.0E+04	-1.1E+05	-4.4E+04	-1.1E+05	-6.6E+04
87.9	9.2E+04	1.8E+06	-2.9E+06	5.4E+03	1.4E+06	1.9E+06	-2.3E+06	8.0E+05	-3.9E+04	-5.1E+04	-6.2E+04	-6.8E+04	-6.9E+04	-5.9E+04	-8.3E+04	-6.3E+04
97.7	-1.1E+05	1.9E+06	-3.2E+06	-3.1E+05	1.1E+06	1.9E+06	-2.4E+06	9.8E+05	-6.0E+04	-6.7E+04	-9.4E+04	-5.4E+04	-9.8E+04	-5.6E+04	-9.1E+04	-6.2E+04
107.4	-5.0E+05	1.6E+06	-2.9E+06	-9.1E+04	1.8E+06	1.8E+06	-2.3E+06	1.4E+06	-7.6E+04	-4.5E+04	-6.9E+04	-6.6E+04	-3.2E+04	-5.2E+04	-4.3E+04	-4.5E+04
117.2	1.1E+05	1.4E+06	-3.2E+06	-7.8E+04	1.9E+06	2.1E+06	-2.6E+06	1.7E+06	-4.9E+04	-6.2E+04	-4.3E+04	-7.2E+04	-4.7E+04	-6.3E+04	-5.3E+04	-3.7E+04
127.0	1.7E+05	1.1E+06	-3.0E+06	-1.1E+04	2.2E+06	2.5E+06	-2.7E+06	2.0E+06	-5.3E+04	-6.3E+04	-4.4E+04	-6.8E+04	-7.0E+04	-7.0E+04	-4.7E+04	-5.1E+04
136.7	1.8E+06	2.6E+05	-4.4E+06	1.5E+06	2.6E+06	3.6E+06	-3.6E+06	2.2E+06	-5.3E+04	-4.7E+04	-5.2E+04	-6.7E+04	-4.3E+04	-5.2E+04	-4.6E+04	-5.0E+04
146.5	1.1E+06	8.8E+05	-2.6E+06	1.2E+06	1.0E+06	4.3E+06	-2.6E+06	1.8E+06	-4.2E+04	-3.9E+04	-2.9E+04	-5.4E+04	-4.7E+04	-7.1E+04	-3.4E+04	-4.8E+04
156.3	2.4E+05	2.0E+06	-2.9E+06	-3.7E+05	2.2E+06	4.1E+06	-3.9E+06	2.0E+06	-4.0E+04	-5.6E+04	-4.9E+04	-6.9E+04	-5.5E+04	-6.8E+04	-4.5E+04	-5.2E+04
166.0	-1.7E+06	3.0E+06	-2.2E+06	-1.8E+05	1.7E+06	5.0E+06	-3.7E+06	1.7E+06	-5.7E+04	-5.3E+04	-3.7E+04	-5.8E+04	-5.3E+04	-5.1E+04	-4.8E+04	-4.4E+04
175.8	1.2E+05	2.4E+06	-3.5E+06	-1.9E+05	2.7E+06	4.3E+06	-4.5E+06	2.5E+06	-5.3E+04	-4.9E+04	-4.3E+04	-6.5E+04	-6.5E+04	-7.0E+04	-5.0E+04	-5.8E+04
185.5	-1.9E+06	3.9E+06	-1.7E+06	-2.7E+06	2.6E+06	5.5E+06	-4.3E+06	1.6E+06	-5.7E+04	-7.3E+04	-4.4E+04	-7.8E+04	-7.0E+04	-5.6E+04	-7.0E+04	-4.1E+04
195.3	1.6E+06	2.5E+06	-3.3E+06	1.1E+05	3.1E+06	5.3E+06	-4.5E+06	2.4E+06	-6.7E+04	-7.6E+04	-3.8E+04	-7.6E+04	-5.2E+04	-7.7E+04	-5.5E+04	-4.9E+04
205.1	1.6E+06	4.1E+06	-3.4E+06	1.2E+06	1.0E+06	3.5E+06	-5.9E+06	1.9E+06	-6.5E+04	-6.2E+04	-6.8E+04	-7.8E+04	-7.8E+04	-6.8E+04	-6.9E+04	-3.9E+04
214.8	2.4E+04	1.7E+06	-4.2E+06	-2.9E+05	3.7E+06	5.9E+06	-5.0E+06	3.4E+06	-3.8E+04	-6.7E+04	-3.2E+04	-6.7E+04	-5.6E+04	-8.5E+04	-3.4E+04	-4.1E+04
224.6	-1.4E+04	1.8E+06	-4.3E+06	-1.1E+04	3.3E+06	6.2E+06	-5.4E+06	3.5E+06	-4.0E+04	-6.8E+04	-5.1E+04	-8.0E+04	-3.6E+04	-8.0E+04	-4.8E+04	-7.0E+04

Table 25. Raw data for TOR labyrinth seal at 20,200 rpm, 0.4 PR, and high preswirl

Freq	Re Hxx	Re Hxy	Re Hyx	Re Hyy	Im Hxx	Im Hxy	Im Hyx	Im Hyy	Re eHxx	Re eHxy	Re eHyx	Re eHyy	Im eHxx	Im eHxy	Im eHyx	Im eHyy
Hz	N/m	N/m	N/m	N/m	N/m	N/m	N/m	N/m	N/m	N/m	N/m	N/m	N/m	N/m	N/m	N/m
9.8	-1.2E+06	2.2E+06	-3.6E+06	-1.1E+06	-4.9E+04	4.7E+05	-1.3E+05	1.9E+05	-1.0E+05	-1.0E+05	-4.2E+04	-7.7E+04	-1.1E+05	-1.4E+05	-1.0E+05	-8.2E+04
19.5	-1.4E+06	2.5E+06	-3.5E+06	-1.1E+06	9.8E+04	7.6E+05	-9.3E+05	3.3E+05	-1.0E+05	-8.6E+04	-7.9E+04	-2.0E+05	-1.0E+05	-1.4E+05	-1.6E+05	-8.2E+04
29.3	-1.3E+06	2.5E+06	-3.9E+06	-8.4E+05	2.8E+05	9.8E+05	-1.1E+06	5.3E+05	-7.3E+04	-1.5E+05	-9.3E+04	-1.9E+05	-9.5E+04	-7.2E+04	-9.1E+04	-8.6E+04
39.1	-1.9E+06	2.6E+06	-3.8E+06	-1.0E+06	4.9E+05	1.4E+06	-9.6E+05	5.6E+05	-1.5E+05	-5.0E+04	-1.6E+05	-8.2E+04	-1.2E+05	-5.8E+04	-7.4E+04	-5.9E+04
48.8	-9.3E+05	2.5E+06	-3.6E+06	-1.2E+06	5.8E+05	1.6E+06	-1.5E+06	6.8E+05	-5.6E+05	-3.0E+05	-1.6E+05	-1.2E+05	-4.9E+05	-3.2E+05	-2.1E+05	-1.1E+05
58.6	-1.4E+06	2.6E+06	-4.0E+06	-1.0E+06	9.9E+05	1.7E+06	-1.5E+06	9.0E+05	-2.0E+05	-5.3E+04	-1.2E+05	-9.5E+04	-1.5E+05	-7.5E+04	-2.4E+05	-5.8E+04
68.4	-1.4E+06	2.6E+06	-4.0E+06	-1.1E+06	1.3E+06	2.1E+06	-2.0E+06	8.6E+05	-7.5E+04	-4.0E+04	-7.9E+04	-6.3E+04	-4.9E+04	-6.5E+04	-5.2E+04	-6.6E+04
78.1	-1.6E+06	2.7E+06	-4.0E+06	-1.2E+06	1.4E+06	2.3E+06	-2.0E+06	1.2E+06	-1.1E+05	-5.6E+04	-8.6E+04	-9.6E+04	-9.5E+04	-6.6E+04	-1.2E+05	-5.4E+04
87.9	-1.2E+06	2.8E+06	-3.9E+06	-1.2E+06	1.6E+06	2.4E+06	-2.6E+06	1.4E+06	-5.7E+04	-5.9E+04	-3.7E+04	-6.3E+04	-6.9E+04	-5.4E+04	-8.8E+04	-4.3E+04
97.7	-1.2E+06	2.7E+06	-4.3E+06	-1.3E+06	1.6E+06	2.5E+06	-3.0E+06	1.5E+06	-2.0E+05	-1.8E+05	-1.2E+05	-9.8E+04	-1.9E+05	-1.6E+05	-1.4E+05	-1.1E+05
107.4	-1.5E+06	2.7E+06	-4.0E+06	-1.1E+06	1.9E+06	2.7E+06	-3.0E+06	1.9E+06	-6.4E+04	-4.9E+04	-5.9E+04	-6.7E+04	-4.9E+04	-5.1E+04	-4.2E+04	-5.1E+04
117.2	-1.0E+06	2.6E+06	-4.2E+06	-9.7E+05	2.2E+06	3.1E+06	-3.3E+06	2.0E+06	-3.7E+04	-3.6E+04	-2.7E+04	-6.0E+04	-4.4E+04	-6.2E+04	-3.8E+04	-4.2E+04
127.0	-1.1E+06	2.4E+06	-4.1E+06	-8.3E+05	2.4E+06	3.4E+06	-3.5E+06	2.1E+06	-4.2E+04	-3.9E+04	-5.2E+04	-6.8E+04	-4.8E+04	-6.8E+04	-4.7E+04	-4.3E+04
136.7	1.0E+05	1.7E+06	-5.7E+06	7.5E+04	2.7E+06	4.0E+06	-3.9E+06	2.2E+06	-7.0E+04	-5.4E+04	-5.5E+04	-6.8E+04	-6.3E+04	-6.1E+04	-4.5E+04	-3.9E+04
146.5	-4.6E+05	2.1E+06	-3.8E+06	-1.6E+05	1.2E+06	4.7E+06	-3.1E+06	2.0E+06	-4.9E+04	-5.6E+04	-3.6E+04	-6.0E+04	-6.1E+04	-6.7E+04	-3.4E+04	-4.0E+04
156.3	-1.3E+06	3.0E+06	-4.1E+06	-1.7E+06	2.6E+06	4.6E+06	-4.5E+06	2.3E+06	-4.5E+04	-4.9E+04	-4.1E+04	-6.5E+04	-5.3E+04	-6.9E+04	-4.3E+04	-4.3E+04
166.0	-3.4E+06	4.0E+06	-3.1E+06	-1.7E+06	2.4E+06	5.3E+06	-4.2E+06	2.1E+06	-4.9E+04	-4.7E+04	-5.0E+04	-6.6E+04	-8.2E+04	-7.2E+04	-4.8E+04	-4.4E+04
175.8	-1.4E+06	2.9E+06	-4.1E+06	-1.9E+06	3.6E+06	4.9E+06	-5.3E+06	3.1E+06	-7.0E+04	-8.0E+04	-4.7E+04	-8.4E+04	-7.7E+04	-8.4E+04	-7.7E+04	-7.9E+04
185.5	-2.9E+06	4.6E+06	-2.4E+06	-3.8E+06	3.6E+06	6.7E+06	-5.5E+06	2.1E+06	-6.8E+04	-6.5E+04	-6.3E+04	-7.3E+04	-5.5E+04	-6.6E+04	-7.6E+04	-5.7E+04
195.3	5.1E+05	3.4E+06	-4.1E+06	-9.5E+05	3.9E+06	6.7E+06	-5.7E+06	2.9E+06	-7.4E+04	-7.8E+04	-6.2E+04	-9.4E+04	-4.9E+04	-7.3E+04	-6.3E+04	-8.6E+04
205.1	9.0E+05	5.2E+06	-4.4E+06	-9.8E+04	1.8E+06	4.9E+06	-7.5E+06	2.2E+06	-1.1E+05	-1.0E+05	-6.4E+04	-9.4E+04	-8.2E+04	-9.5E+04	-6.9E+04	-8.2E+04
214.8	-1.0E+06	2.6E+06	-5.4E+06	-1.6E+06	3.5E+06	7.1E+06	-6.2E+06	4.2E+06	-3.9E+04	-6.2E+04	-4.3E+04	-1.0E+05	-4.3E+04	-9.4E+04	-5.1E+04	-4.5E+04
224.6	-1.1E+06	2.9E+06	-5.2E+06	-1.4E+06	3.5E+06	7.7E+06	-7.1E+06	3.9E+06	-3.6E+04	-5.0E+04	-4.2E+04	-9.7E+04	-2.2E+04	-9.2E+04	-4.0E+04	-7.4E+04

Table 26. Raw data for TOR labyrinth seal at 10,200 rpm, 0.5 PR, and high preswirl

Freq	Re Hxx	Re Hxy	Re Hyx	Re Hyy	Im Hxx	Im Hxy	Im Hyx	Im Hyy	Re eHxx	Re eHxy	Re eHyx	Re eHyy	Im eHxx	Im eHxy	Im eHyx	Im eHyy
Hz	N/m	N/m	N/m	N/m	N/m	N/m	N/m	N/m	N/m	N/m	N/m	N/m	N/m	N/m	N/m	N/m
9.8	1.4E+06	1.4E+06	-2.1E+06	1.4E+06	6.2E+04	3.2E+05	-1.7E+05	-1.1E+05	-9.7E+04	-7.9E+04	-7.6E+04	-1.0E+05	-9.1E+04	-8.5E+04	-6.9E+04	-7.8E+04
19.5	1.4E+06	1.4E+06	-2.0E+06	1.2E+06	5.8E+05	4.4E+05	-6.1E+05	-9.0E+04	-1.8E+05	-1.2E+05	-1.4E+05	-6.2E+04	-2.3E+05	-8.0E+04	-1.8E+05	-6.1E+04
29.3	1.4E+06	1.4E+06	-2.4E+06	1.3E+06	7.9E+04	7.7E+05	-3.7E+05	-2.5E+05	-1.0E+05	-7.7E+04	-9.8E+04	-5.6E+04	-1.3E+05	-1.1E+05	-6.9E+04	-7.7E+04
39.1	1.3E+06	1.5E+06	-2.4E+06	1.4E+06	3.1E+05	6.7E+05	-6.4E+05	1.6E+05	-1.5E+05	-6.1E+04	-1.6E+05	-5.8E+04	-1.2E+05	-5.5E+04	-1.7E+05	-6.0E+04
48.8	9.4E+05	1.6E+06	-2.1E+06	1.3E+06	3.9E+05	7.6E+05	-8.8E+05	1.7E+05	-2.0E+05	-6.5E+04	-2.6E+05	-4.3E+04	-1.2E+05	-5.2E+04	-2.3E+05	-9.7E+04
58.6	1.2E+06	1.6E+06	-2.9E+06	1.3E+06	5.2E+05	8.1E+05	-6.0E+05	1.5E+05	-1.7E+05	-7.3E+04	-2.0E+05	-9.7E+04	-1.8E+05	-7.2E+04	-2.2E+05	-7.4E+04
68.4	9.4E+05	1.4E+06	-2.5E+06	1.0E+06	9.8E+05	5.8E+05	-7.4E+05	3.3E+05	-9.5E+04	-4.7E+04	-1.1E+05	-6.4E+04	-8.8E+04	-6.3E+04	-1.0E+05	-7.0E+04
78.1	8.1E+05	1.1E+06	-2.0E+06	7.3E+05	1.3E+06	6.2E+05	-6.6E+05	8.1E+05	-1.7E+05	-6.4E+04	-1.5E+05	-7.8E+04	-1.2E+05	-9.2E+04	-9.7E+04	-6.5E+04
87.9	1.4E+06	8.0E+05	-1.8E+06	9.8E+05	1.4E+06	1.1E+06	-1.4E+06	1.2E+06	-1.0E+05	-6.0E+04	-1.3E+05	-5.5E+04	-1.3E+05	-5.7E+04	-1.1E+05	-1.2E+05
97.7	1.6E+06	9.0E+05	-2.2E+06	9.5E+05	1.6E+06	1.3E+06	-1.9E+06	1.1E+06	-7.2E+04	-4.8E+04	-8.6E+04	-6.0E+04	-7.6E+04	-6.4E+04	-9.6E+04	-8.0E+04
107.4	1.3E+06	1.0E+06	-1.8E+06	1.2E+06	1.5E+06	1.3E+06	-1.7E+06	1.4E+06	-7.3E+04	-4.1E+04	-6.1E+04	-4.3E+04	-7.3E+04	-4.8E+04	-5.0E+04	-5.2E+04
117.2	1.7E+06	8.5E+05	-2.3E+06	1.3E+06	1.7E+06	1.5E+06	-2.1E+06	1.5E+06	-4.9E+04	-4.1E+04	-7.7E+04	-4.2E+04	-3.3E+04	-3.3E+04	-3.8E+04	-5.5E+04
127.0	1.8E+06	7.6E+05	-2.4E+06	1.5E+06	1.8E+06	1.9E+06	-2.1E+06	1.5E+06	-7.2E+04	-3.0E+04	-7.4E+04	-4.2E+04	-7.3E+04	-4.1E+04	-6.3E+04	-5.8E+04
136.7	2.7E+06	8.1E+04	-3.8E+06	2.4E+06	1.8E+06	2.4E+06	-2.2E+06	1.5E+06	-5.2E+04	-3.8E+04	-5.5E+04	-4.9E+04	-5.0E+04	-4.8E+04	-3.1E+04	-5.7E+04
146.5	2.1E+06	5.2E+05	-1.9E+06	2.3E+06	4.9E+05	3.1E+06	-1.4E+06	1.2E+06	-4.6E+04	-3.5E+04	-4.5E+04	-4.3E+04	-2.9E+04	-3.9E+04	-4.2E+04	-5.3E+04
156.3	1.4E+06	1.4E+06	-2.2E+06	6.1E+05	1.7E+06	2.7E+06	-2.6E+06	1.7E+06	-4.7E+04	-3.6E+04	-6.5E+04	-6.5E+04	-3.4E+04	-4.4E+04	-6.0E+04	-7.3E+04
166.0	-5.3E+05	2.4E+06	-1.4E+06	9.6E+05	1.3E+06	3.7E+06	-2.4E+06	1.3E+06	-8.6E+04	-7.9E+04	-8.9E+04	-6.9E+04	-1.2E+05	-6.2E+04	-9.3E+04	-8.3E+04
175.8	1.2E+06	1.6E+06	-2.2E+06	1.1E+06	2.3E+06	2.7E+06	-3.3E+06	2.3E+06	-9.9E+04	-7.8E+04	-1.1E+05	-8.8E+04	-7.7E+04	-8.5E+04	-1.0E+05	-1.2E+05
185.5	-5.3E+05	3.7E+06	-3.0E+05	-1.9E+06	2.4E+06	4.4E+06	-2.2E+06	1.1E+06	-1.1E+05	-5.1E+04	-8.9E+04	-4.3E+04	-1.6E+05	-8.5E+04	-6.2E+04	-5.5E+04
195.3	2.7E+06	1.9E+06	-2.4E+06	1.2E+06	2.3E+06	3.7E+06	-2.7E+06	2.2E+06	-5.7E+04	-5.5E+04	-4.5E+04	-5.8E+04	-6.8E+04	-4.5E+04	-6.6E+04	-8.3E+04
205.1	2.6E+06	3.3E+06	-2.3E+06	2.4E+06	2.3E+05	2.0E+06	-4.1E+06	1.3E+06	-6.7E+04	-5.3E+04	-6.8E+04	-6.2E+04	-8.8E+04	-5.6E+04	-5.0E+04	-5.7E+04
214.8	1.1E+06	9.5E+05	-3.1E+06	8.3E+05	2.9E+06	4.2E+06	-3.3E+06	2.8E+06	-4.1E+04	-4.0E+04	-4.6E+04	-4.3E+04	-4.0E+04	-5.3E+04	-4.1E+04	-5.7E+04
224.6	1.2E+06	1.2E+06	-3.2E+06	1.1E+06	2.5E+06	4.6E+06	-3.6E+06	2.8E+06	-3.9E+04	-5.5E+04	-4.6E+04	-5.9E+04	-5.1E+04	-6.2E+04	-4.7E+04	-5.1E+04

Table 27. Raw data for TOR labyrinth seal at 15,350 rpm, 0.5 PR, and high preswirl

Freq	Re Hxx	Re Hxy	Re Hyx	Re Hyy	Im Hxx	Im Hxy	Im Hyx	Im Hyy	Re eHxx	Re eHxy	Re eHyx	Re eHyy	Im eHxx	Im eHxy	Im eHyx	Im eHyy
Hz	N/m	N/m	N/m	N/m	N/m	N/m	N/m	N/m	N/m	N/m	N/m	N/m	N/m	N/m	N/m	N/m
9.8	4.9E+05	1.4E+06	-2.6E+06	3.9E+05	-1.0E+05	3.9E+05	-8.6E+04	-3.0E+03	-7.6E+04	-3.6E+04	-7.5E+04	-5.1E+04	-8.8E+04	-4.6E+04	-8.0E+04	-5.3E+04
19.5	4.4E+05	1.7E+06	-2.3E+06	2.5E+05	3.9E+05	6.5E+05	-9.2E+05	1.6E+05	-1.8E+05	-6.5E+04	-1.4E+05	-4.6E+04	-1.6E+05	-8.3E+04	-1.7E+05	-7.1E+04
29.3	2.1E+05	1.5E+06	-2.6E+06	2.8E+05	7.3E+04	9.6E+05	-9.3E+05	9.5E+04	-1.3E+05	-8.5E+04	-1.0E+05	-8.0E+04	-1.0E+05	-9.7E+04	-5.3E+04	-9.3E+04
39.1	1.1E+04	1.7E+06	-3.0E+06	2.4E+05	7.7E+04	1.1E+06	-1.2E+06	3.5E+05	-1.5E+05	-4.6E+04	-1.8E+05	-4.5E+04	-1.7E+05	-4.6E+04	-1.4E+05	-6.3E+04
48.8	1.6E+05	1.7E+06	-2.6E+06	1.3E+05	4.1E+05	1.4E+06	-1.5E+06	5.1E+05	-1.5E+05	-3.8E+04	-2.1E+05	-5.5E+04	-9.3E+04	-4.7E+04	-1.5E+05	-6.7E+04
58.6	1.3E+05	1.7E+06	-3.4E+06	3.1E+05	1.1E+06	1.6E+06	-1.0E+06	6.2E+05	-2.0E+05	-5.3E+04	-1.8E+05	-5.2E+04	-1.2E+05	-6.3E+04	-2.0E+05	-5.3E+04
68.4	2.0E+05	1.7E+06	-2.9E+06	3.0E+05	9.8E+05	1.8E+06	-1.8E+06	6.8E+05	-7.1E+04	-4.1E+04	-9.6E+04	-5.1E+04	-8.0E+04	-6.5E+04	-1.1E+05	-5.5E+04
78.1	-1.9E+05	1.9E+06	-2.8E+06	2.3E+04	1.0E+06	1.9E+06	-1.7E+06	6.9E+05	-7.3E+04	-4.5E+04	-1.2E+05	-7.0E+04	-1.5E+05	-7.1E+04	-1.3E+05	-7.0E+04
87.9	1.0E+05	2.0E+06	-2.8E+06	1.0E+04	1.1E+06	2.1E+06	-2.2E+06	8.0E+05	-8.0E+04	-4.9E+04	-8.6E+04	-5.3E+04	-8.9E+04	-4.7E+04	-7.8E+04	-5.1E+04
97.7	-6.3E+04	2.0E+06	-3.1E+06	-2.1E+05	1.2E+06	2.1E+06	-2.5E+06	8.0E+05	-6.3E+04	-4.9E+04	-5.7E+04	-3.8E+04	-6.2E+04	-4.4E+04	-7.7E+04	-6.4E+04
107.4	-4.0E+05	1.9E+06	-2.7E+06	-1.7E+05	1.6E+06	2.0E+06	-2.4E+06	1.3E+06	-8.3E+04	-5.5E+04	-7.4E+04	-3.8E+04	-6.1E+04	-3.4E+04	-5.2E+04	-5.8E+04
117.2	1.9E+03	1.8E+06	-3.1E+06	-2.3E+05	1.8E+06	2.2E+06	-2.6E+06	1.6E+06	-3.9E+04	-3.7E+04	-5.5E+04	-4.0E+04	-4.3E+04	-3.8E+04	-4.9E+04	-4.4E+04
127.0	-5.6E+03	1.1E+06	-2.7E+06	-2.0E+05	2.3E+06	2.4E+06	-2.6E+06	2.1E+06	-8.9E+04	-5.6E+04	-8.1E+04	-4.8E+04	-9.2E+04	-6.1E+04	-7.5E+04	-5.0E+04
136.7	1.5E+06	4.6E+05	-4.2E+06	1.4E+06	2.5E+06	3.7E+06	-3.4E+06	2.1E+06	-4.8E+04	-4.4E+04	-4.6E+04	-4.1E+04	-5.1E+04	-5.8E+04	-4.9E+04	-7.4E+04
146.5	8.2E+05	1.0E+06	-2.4E+06	1.2E+06	8.9E+05	4.2E+06	-2.6E+06	1.7E+06	-6.5E+04	-3.1E+04	-3.9E+04	-3.6E+04	-2.0E+04	-4.4E+04	-3.7E+04	-5.4E+04
156.3	3.6E+05	2.1E+06	-2.8E+06	-3.7E+05	2.2E+06	4.2E+06	-4.0E+06	2.1E+06	-5.5E+04	-4.7E+04	-3.7E+04	-4.7E+04	-5.4E+04	-6.1E+04	-6.1E+04	-7.5E+04
166.0	-1.7E+06	3.2E+06	-2.0E+06	-1.6E+05	1.9E+06	5.0E+06	-3.8E+06	1.8E+06	-4.4E+04	-3.6E+04	-4.1E+04	-4.1E+04	-7.5E+04	-3.6E+04	-4.4E+04	-4.5E+04
175.8	3.2E+05	2.6E+06	-3.1E+06	-1.5E+05	2.7E+06	4.2E+06	-4.5E+06	2.6E+06	-4.0E+04	-4.0E+04	-5.7E+04	-5.6E+04	-2.7E+04	-5.0E+04	-4.4E+04	-7.1E+04
185.5	-2.1E+06	4.3E+06	-1.5E+06	-3.1E+06	2.5E+06	5.7E+06	-3.9E+06	1.4E+06	-9.2E+04	-4.3E+04	-7.2E+04	-4.1E+04	-7.0E+04	-5.3E+04	-5.5E+04	-6.2E+04
195.3	1.6E+06	2.8E+06	-3.0E+06	1.6E+05	3.1E+06	5.4E+06	-4.5E+06	2.5E+06	-3.9E+04	-7.1E+04	-3.7E+04	-5.5E+04	-5.8E+04	-6.0E+04	-5.7E+04	-7.1E+04
205.1	2.1E+06	4.5E+06	-3.3E+06	1.0E+06	1.0E+06	3.5E+06	-6.2E+06	1.7E+06	-4.8E+04	-5.1E+04	-5.7E+04	-5.8E+04	-8.3E+04	-4.1E+04	-9.6E+04	-7.0E+04
214.8	-1.7E+05	1.8E+06	-3.9E+06	-2.7E+05	3.1E+06	5.6E+06	-4.9E+06	3.4E+06	-4.5E+04	-6.9E+04	-4.1E+04	-5.0E+04	-5.8E+04	-7.0E+04	-3.6E+04	-7.7E+04
224.6	-1.1E+04	2.0E+06	-4.0E+06	-1.2E+05	3.1E+06	6.1E+06	-5.5E+06	3.3E+06	-4.3E+04	-7.8E+04	-3.8E+04	-5.5E+04	-4.8E+04	-5.8E+04	-4.8E+04	-7.5E+04

Table 28. Raw data for TOR labyrinth seal at 20,200 rpm, 0.5 PR, and high preswirl

Freq	Re Hxx	Re Hxy	Re Hyx	Re Hyy	Im Hxx	Im Hxy	Im Hyx	Im Hyy	Re eHxx	Re eHxy	Re eHyx	Re eHyy	Im eHxx	Im eHxy	Im eHyx	Im eHyy
Hz	N/m	N/m	N/m	N/m	N/m	N/m	N/m	N/m	N/m	N/m	N/m	N/m	N/m	N/m	N/m	N/m
9.8	-1.1E+06	2.7E+06	-3.8E+06	-1.2E+06	-6.5E+04	4.4E+05	-8.5E+04	-1.2E+04	-7.1E+04	-8.1E+04	-1.1E+05	-9.6E+04	-7.0E+04	-8.3E+04	-7.2E+04	-7.6E+04
19.5	-1.2E+06	2.8E+06	-3.6E+06	-1.3E+06	3.9E+05	8.7E+05	-8.2E+05	1.3E+05	-1.7E+05	-9.5E+04	-1.3E+05	-1.1E+05	-1.6E+05	-1.0E+05	-1.6E+05	-1.2E+05
29.3	-1.4E+06	3.0E+06	-4.0E+06	-1.4E+06	5.6E+04	1.1E+06	-1.0E+06	1.1E+05	-1.3E+05	-4.4E+04	-1.2E+05	-9.3E+04	-6.7E+04	-5.9E+04	-7.9E+04	-9.0E+04
39.1	-1.9E+06	2.9E+06	-3.9E+06	-1.2E+06	5.3E+05	1.1E+06	-9.1E+05	4.3E+05	-1.5E+05	-7.2E+04	-1.8E+05	-4.6E+04	-1.6E+05	-5.3E+04	-1.9E+05	-6.2E+04
48.8	-1.7E+06	3.0E+06	-3.8E+06	-1.4E+06	8.3E+05	1.4E+06	-1.5E+06	8.1E+05	-6.4E+05	-2.6E+05	-2.6E+05	-8.6E+04	-4.2E+05	-3.2E+05	-2.4E+05	-1.2E+05
58.6	-1.6E+06	2.8E+06	-4.6E+06	-1.2E+06	1.1E+06	1.6E+06	-1.1E+06	9.2E+05	-1.7E+05	-6.5E+04	-2.2E+05	-7.9E+04	-1.5E+05	-5.6E+04	-1.4E+05	-7.3E+04
68.4	-1.5E+06	2.8E+06	-4.2E+06	-1.2E+06	1.3E+06	1.8E+06	-1.7E+06	8.9E+05	-7.4E+04	-5.4E+04	-9.8E+04	-5.6E+04	-7.3E+04	-5.8E+04	-1.1E+05	-6.4E+04
78.1	-1.6E+06	2.7E+06	-4.0E+06	-1.4E+06	1.5E+06	2.1E+06	-2.0E+06	1.2E+06	-1.1E+05	-9.0E+04	-9.6E+04	-4.8E+04	-1.4E+05	-5.2E+04	-1.2E+05	-5.3E+04
87.9	-1.4E+06	2.7E+06	-3.8E+06	-1.4E+06	1.7E+06	2.3E+06	-2.3E+06	1.4E+06	-9.3E+04	-4.3E+04	-1.1E+05	-3.9E+04	-1.3E+05	-5.4E+04	-9.0E+04	-6.1E+04
97.7	-1.2E+06	2.8E+06	-4.2E+06	-1.4E+06	1.8E+06	2.5E+06	-2.9E+06	1.5E+06	-1.4E+05	-1.3E+05	-1.0E+05	-4.6E+04	-1.9E+05	-1.3E+05	-1.1E+05	-8.8E+04
107.4	-1.6E+06	2.7E+06	-3.7E+06	-1.3E+06	2.2E+06	2.7E+06	-2.7E+06	1.9E+06	-9.6E+04	-3.5E+04	-6.8E+04	-4.8E+04	-6.2E+04	-6.0E+04	-6.0E+04	-6.3E+04
117.2	-1.1E+06	2.7E+06	-4.0E+06	-1.1E+06	2.4E+06	3.0E+06	-3.3E+06	2.1E+06	-3.8E+04	-3.4E+04	-4.7E+04	-3.9E+04	-3.4E+04	-4.4E+04	-4.8E+04	-5.6E+04
127.0	-1.0E+06	2.6E+06	-4.0E+06	-9.5E+05	2.4E+06	3.4E+06	-3.3E+06	2.1E+06	-9.7E+04	-7.6E+04	-8.1E+04	-4.0E+04	-7.2E+04	-4.1E+04	-7.0E+04	-6.2E+04
136.7	1.0E+05	1.9E+06	-5.4E+06	-9.3E+04	2.6E+06	4.0E+06	-3.8E+06	2.2E+06	-6.0E+04	-4.8E+04	-5.3E+04	-5.3E+04	-5.8E+04	-4.9E+04	-3.9E+04	-5.9E+04
146.5	-6.3E+05	2.1E+06	-3.5E+06	-2.4E+05	1.2E+06	4.6E+06	-3.1E+06	2.0E+06	-5.3E+04	-4.3E+04	-5.0E+04	-5.0E+04	-3.2E+04	-4.6E+04	-5.5E+04	-6.4E+04
156.3	-1.4E+06	3.1E+06	-3.8E+06	-1.8E+06	2.6E+06	4.7E+06	-4.6E+06	2.5E+06	-4.0E+04	-3.8E+04	-3.2E+04	-4.4E+04	-4.3E+04	-4.2E+04	-4.6E+04	-5.2E+04
166.0	-3.4E+06	4.3E+06	-2.9E+06	-1.9E+06	2.3E+06	5.3E+06	-4.4E+06	2.1E+06	-6.4E+04	-5.2E+04	-5.0E+04	-3.9E+04	-8.8E+04	-4.3E+04	-6.0E+04	-6.4E+04
175.8	-1.8E+06	2.8E+06	-3.2E+06	-2.0E+06	3.9E+06	5.0E+06	-5.5E+06	3.1E+06	-9.3E+04	-7.4E+04	-6.6E+04	-7.1E+04	-1.2E+05	-1.2E+05	-5.4E+04	-7.4E+04
185.5	-3.1E+06	5.1E+06	-2.1E+06	-4.3E+06	3.3E+06	6.8E+06	-5.1E+06	1.9E+06	-1.3E+05	-5.5E+04	-7.6E+04	-5.4E+04	-9.2E+04	-7.9E+04	-9.1E+04	-7.5E+04
195.3	4.8E+05	3.5E+06	-4.0E+06	-1.2E+06	3.8E+06	6.6E+06	-5.9E+06	3.0E+06	-5.2E+04	-5.7E+04	-4.6E+04	-5.0E+04	-4.0E+04	-6.9E+04	-5.3E+04	-6.9E+04
205.1	1.1E+06	5.4E+06	-4.4E+06	-3.1E+05	1.6E+06	4.8E+06	-7.5E+06	2.4E+06	-8.7E+04	-6.0E+04	-6.6E+04	-6.5E+04	-9.8E+04	-9.1E+04	-6.8E+04	-7.7E+04
214.8	-1.3E+06	2.5E+06	-4.9E+06	-1.7E+06	3.7E+06	7.1E+06	-6.3E+06	4.1E+06	-4.5E+04	-5.5E+04	-3.8E+04	-4.5E+04	-4.8E+04	-4.9E+04	-3.6E+04	-6.9E+04
224.6	-9.7E+05	3.1E+06	-5.1E+06	-1.4E+06	3.6E+06	7.8E+06	-7.1E+06	4.0E+06	-5.4E+04	-5.7E+04	-3.9E+04	-7.2E+04	-4.3E+04	-8.6E+04	-4.1E+04	-6.6E+04

Table 29. Raw data for TOR labyrinth seal at 10,200 rpm, 0.6 PR, and high preswirl

Freq	Re Hxx	Re Hxy	Re Hyx	Re Hyy	Im Hxx	Im Hxy	Im Hyx	Im Hyy	Re eHxx	Re eHxy	Re eHyx	Re eHyy	Im eHxx	Im eHxy	Im eHyx	Im eHyy
Hz	N/m	N/m	N/m	N/m	N/m	N/m	N/m	N/m	N/m	N/m	N/m	N/m	N/m	N/m	N/m	N/m
9.8	1.1E+06	1.1E+06	-1.9E+06	1.3E+06	-7.5E+04	5.3E+05	-1.1E+05	-1.9E+05	-1.1E+05	-1.3E+05	-9.2E+04	-9.0E+04	-1.4E+05	-1.1E+05	-8.0E+04	-5.9E+04
19.5	1.3E+06	1.5E+06	-2.4E+06	1.2E+06	3.3E+05	5.5E+05	-2.6E+05	-9.4E+04	-1.4E+05	-1.3E+05	-1.7E+05	-7.9E+04	-1.2E+05	-1.2E+05	-1.4E+05	-1.1E+05
29.3	1.1E+06	1.7E+06	-2.1E+06	1.0E+06	2.2E+05	8.1E+05	-4.9E+05	-2.1E+05	-1.2E+05	-1.5E+05	-1.4E+05	-1.7E+05	-5.4E+04	-1.1E+05	-9.3E+04	-8.0E+04
39.1	1.0E+06	1.4E+06	-2.1E+06	1.1E+06	2.5E+05	7.4E+05	-6.4E+05	1.3E+05	-9.9E+04	-8.6E+04	-1.4E+05	-9.2E+04	-1.1E+05	-1.6E+05	-1.5E+05	-7.5E+04
48.8	1.1E+06	1.5E+06	-2.1E+06	1.1E+06	8.5E+04	7.2E+05	-4.0E+05	1.8E+05	-2.1E+05	-6.6E+04	-1.7E+05	-7.7E+04	-2.2E+05	-1.0E+05	-1.8E+05	-1.0E+05
58.6	1.2E+06	1.4E+06	-2.0E+06	1.1E+06	1.0E+06	8.3E+05	-1.2E+06	3.8E+05	-3.1E+05	-9.9E+04	-2.0E+05	-1.1E+05	-2.6E+05	-1.3E+05	-2.8E+05	-6.3E+04
68.4	1.0E+06	1.3E+06	-2.0E+06	9.8E+05	9.4E+05	6.1E+05	-8.7E+05	5.3E+05	-1.1E+05	-1.0E+05	-1.2E+05	-8.7E+04	-9.8E+04	-1.1E+05	-9.1E+04	-6.6E+04
78.1	5.4E+05	1.2E+06	-1.5E+06	8.5E+05	8.8E+05	8.8E+05	-7.8E+05	7.6E+05	-1.8E+05	-6.8E+04	-1.2E+05	-7.7E+04	-2.8E+05	-1.2E+05	-1.6E+05	-6.1E+04
87.9	1.2E+06	8.4E+05	-1.6E+06	8.7E+05	1.4E+06	1.3E+06	-1.5E+06	1.1E+06	-1.1E+05	-8.0E+04	-9.8E+04	-6.8E+04	-8.3E+04	-9.6E+04	-1.2E+05	-6.2E+04
97.7	1.0E+06	1.0E+06	-1.9E+06	7.8E+05	1.4E+06	1.4E+06	-1.8E+06	9.0E+05	-4.3E+04	-6.6E+04	-6.7E+04	-7.1E+04	-6.8E+04	-6.2E+04	-1.1E+05	-6.9E+04
107.4	1.0E+06	1.1E+06	-1.8E+06	1.0E+06	1.3E+06	1.6E+06	-1.8E+06	1.3E+06	-8.0E+04	-6.4E+04	-1.2E+05	-6.2E+04	-9.0E+04	-9.6E+04	-6.5E+04	-5.6E+04
117.2	1.3E+06	1.0E+06	-2.1E+06	1.0E+06	1.6E+06	1.6E+06	-2.1E+06	1.5E+06	-4.7E+04	-7.5E+04	-6.0E+04	-6.5E+04	-5.6E+04	-6.8E+04	-7.0E+04	-5.1E+04
127.0	1.5E+06	9.4E+05	-2.1E+06	1.2E+06	1.8E+06	1.9E+06	-2.1E+06	1.4E+06	-6.3E+04	-8.1E+04	-6.6E+04	-5.6E+04	-6.3E+04	-6.6E+04	-6.5E+04	-5.1E+04
136.7	2.4E+06	2.3E+05	-3.5E+06	2.0E+06	1.9E+06	2.5E+06	-2.2E+06	1.2E+06	-6.1E+04	-5.9E+04	-5.6E+04	-5.8E+04	-5.7E+04	-8.2E+04	-3.2E+04	-4.6E+04
146.5	1.5E+06	5.5E+05	-1.6E+06	1.9E+06	2.4E+05	3.1E+06	-1.3E+06	1.1E+06	-5.9E+04	-6.0E+04	-7.1E+04	-7.6E+04	-5.9E+04	-7.5E+04	-6.2E+04	-5.6E+04
156.3	1.1E+06	1.7E+06	-1.8E+06	2.4E+04	1.7E+06	2.8E+06	-2.7E+06	1.7E+06	-5.9E+04	-8.0E+04	-3.7E+04	-9.0E+04	-5.6E+04	-8.3E+04	-6.6E+04	-4.6E+04
166.0	-4.1E+05	2.4E+06	-1.3E+06	7.9E+05	1.8E+06	3.4E+06	-2.7E+06	1.4E+06	-1.3E+05	-1.0E+05	-1.2E+05	-9.7E+04	-1.0E+05	-1.1E+05	-1.0E+05	-8.7E+04
175.8	1.0E+06	1.7E+06	-1.7E+06	6.3E+05	2.2E+06	2.9E+06	-3.1E+06	2.2E+06	-7.4E+04	-1.0E+05	-1.1E+05	-1.1E+05	-1.1E+05	-1.1E+05	-8.2E+04	-1.1E+05
185.5	-3.3E+05	3.5E+06	-5.9E+05	-1.5E+06	2.1E+06	3.9E+06	-2.6E+06	1.4E+06	-9.5E+04	-1.2E+05	-6.6E+04	-8.4E+04	-9.0E+04	-1.0E+05	-8.2E+04	-5.8E+04
195.3	2.4E+06	1.9E+06	-2.2E+06	1.1E+06	2.4E+06	3.7E+06	-2.7E+06	2.2E+06	-5.9E+04	-7.3E+04	-4.5E+04	-7.9E+04	-4.1E+04	-1.1E+05	-6.5E+04	-6.3E+04
205.1	2.9E+06	3.5E+06	-2.3E+06	1.9E+06	3.8E+05	2.1E+06	-4.2E+06	1.3E+06	-6.6E+04	-7.7E+04	-7.6E+04	-6.5E+04	-7.7E+04	-9.4E+04	-5.8E+04	-5.5E+04
214.8	8.0E+05	9.3E+05	-2.8E+06	7.2E+05	2.5E+06	4.2E+06	-3.1E+06	2.9E+06	-3.0E+04	-6.7E+04	-3.4E+04	-7.1E+04	-4.0E+04	-7.4E+04	-3.5E+04	-6.7E+04
224.6	9.4E+05	1.2E+06	-2.8E+06	9.7E+05	2.6E+06	4.6E+06	-3.6E+06	2.8E+06	-5.7E+04	-9.8E+04	-5.1E+04	-1.0E+05	-5.1E+04	-8.5E+04	-3.4E+04	-8.1E+04

Table 30. Raw data for TOR labyrinth seal at 15,350 rpm, 0.6 PR, and high preswirl

Freq	Re Hxx	Re Hxy	Re Hyx	Re Hyy	Im Hxx	Im Hxy	Im Hyx	Im Hyy	Re eHxx	Re eHxy	Re eHyx	Re eHyy	Im eHxx	Im eHxy	Im eHyx	Im eHyy
Hz	N/m	N/m	N/m	N/m	N/m	N/m	N/m	N/m	N/m	N/m	N/m	N/m	N/m	N/m	N/m	N/m
9.8	-5.9E+04	1.6E+06	-2.3E+06	-5.6E+04	-1.2E+05	5.6E+05	-2.4E+05	-7.0E+04	-8.1E+04	-1.1E+05	-5.3E+04	-7.7E+04	-7.3E+04	-7.4E+04	-3.9E+04	-4.8E+04
19.5	7.1E+04	1.7E+06	-2.8E+06	5.1E+04	1.8E+05	7.1E+05	-6.0E+05	1.0E+05	-1.6E+05	-1.1E+05	-1.9E+05	-1.2E+05	-1.1E+05	-1.2E+05	-1.6E+05	-9.0E+04
29.3	-1.5E+05	1.9E+06	-2.6E+06	4.3E+04	-3.8E+04	8.2E+05	-8.9E+05	1.9E+05	-1.2E+05	-1.1E+05	-1.1E+05	-6.7E+04	-9.5E+04	-1.1E+05	-9.4E+04	-9.6E+04
39.1	-1.2E+05	1.8E+06	-2.8E+06	-1.9E+05	1.8E+05	1.0E+06	-1.2E+06	5.3E+05	-1.0E+05	-9.9E+04	-6.5E+04	-8.6E+04	-1.2E+05	-7.8E+04	-1.1E+05	-7.2E+04
48.8	-2.0E+05	1.8E+06	-2.8E+06	-1.5E+05	-2.7E+03	1.2E+06	-1.0E+06	6.3E+05	-1.8E+05	-8.0E+04	-1.4E+05	-7.1E+04	-1.8E+05	-8.1E+04	-1.7E+05	-6.4E+04
58.6	-2.1E+05	1.6E+06	-2.9E+06	9.1E+04	1.3E+06	1.6E+06	-1.2E+06	8.8E+05	-2.3E+05	-8.1E+04	-1.9E+05	-6.5E+04	-3.3E+05	-1.0E+05	-2.1E+05	-6.1E+04
68.4	-1.8E+05	1.8E+06	-2.7E+06	4.1E+04	1.1E+06	1.7E+06	-1.6E+06	8.7E+05	-9.2E+04	-7.9E+04	-1.3E+05	-7.2E+04	-9.9E+04	-7.3E+04	-9.9E+04	-5.9E+04
78.1	-7.0E+05	2.0E+06	-2.7E+06	7.6E+04	1.0E+06	2.0E+06	-1.6E+06	8.8E+05	-1.6E+05	-9.5E+04	-9.7E+04	-5.6E+04	-2.0E+05	-8.4E+04	-8.1E+04	-6.3E+04
87.9	-2.2E+05	2.1E+06	-2.6E+06	-1.3E+05	1.2E+06	2.2E+06	-2.0E+06	1.0E+06	-1.3E+05	-7.5E+04	-1.0E+05	-6.7E+04	-7.6E+04	-8.0E+04	-1.1E+05	-5.4E+04
97.7	-4.4E+05	1.9E+06	-2.9E+06	-3.1E+05	1.4E+06	2.0E+06	-2.3E+06	1.0E+06	-4.2E+04	-7.3E+04	-5.9E+04	-8.1E+04	-5.1E+04	-9.0E+04	-1.0E+05	-3.8E+04
107.4	-5.1E+05	2.0E+06	-2.6E+06	-2.9E+05	1.8E+06	2.2E+06	-2.2E+06	1.5E+06	-9.2E+04	-6.4E+04	-8.6E+04	-6.5E+04	-8.7E+04	-6.5E+04	-8.2E+04	-6.3E+04
117.2	-1.1E+05	1.9E+06	-2.9E+06	-2.4E+05	2.2E+06	2.2E+06	-2.7E+06	1.6E+06	-4.2E+04	-6.2E+04	-5.2E+04	-7.1E+04	-5.1E+04	-6.5E+04	-6.8E+04	-6.0E+04
127.0	-1.4E+05	1.5E+06	-2.6E+06	-2.7E+05	2.5E+06	2.5E+06	-2.5E+06	1.9E+06	-6.5E+04	-7.7E+04	-7.0E+04	-7.0E+04	-6.9E+04	-6.1E+04	-6.4E+04	-6.7E+04
136.7	1.4E+06	6.8E+05	-3.9E+06	1.1E+06	2.6E+06	3.8E+06	-3.2E+06	1.9E+06	-5.3E+04	-8.5E+04	-4.2E+04	-6.1E+04	-6.5E+04	-7.6E+04	-5.3E+04	-5.2E+04
146.5	6.5E+05	1.3E+06	-2.0E+06	9.0E+05	1.0E+06	4.4E+06	-2.5E+06	1.6E+06	-6.7E+04	-8.8E+04	-5.3E+04	-6.3E+04	-5.0E+04	-6.7E+04	-5.8E+04	-5.5E+04
156.3	2.6E+05	2.5E+06	-2.6E+06	-6.3E+05	2.3E+06	4.2E+06	-4.0E+06	2.0E+06	-5.2E+04	-6.9E+04	-2.4E+04	-6.6E+04	-5.1E+04	-8.3E+04	-5.5E+04	-5.6E+04
166.0	-1.4E+06	3.3E+06	-2.0E+06	-2.1E+05	2.3E+06	4.7E+06	-3.9E+06	1.9E+06	-8.1E+04	-7.1E+04	-6.1E+04	-6.3E+04	-5.2E+04	-6.8E+04	-4.9E+04	-4.5E+04
175.8	-8.6E+04	2.5E+06	-2.5E+06	-2.7E+05	2.9E+06	4.2E+06	-4.5E+06	2.6E+06	-5.6E+04	-7.1E+04	-6.5E+04	-8.1E+04	-5.8E+04	-7.8E+04	-4.2E+04	-5.7E+04
185.5	-1.1E+06	4.3E+06	-1.2E+06	-2.5E+06	2.7E+06	5.3E+06	-4.1E+06	1.8E+06	-8.1E+04	-8.1E+04	-7.4E+04	-8.4E+04	-7.9E+04	-1.1E+05	-7.5E+04	-5.2E+04
195.3	1.6E+06	2.8E+06	-2.8E+06	-1.5E+05	3.0E+06	5.1E+06	-4.5E+06	2.5E+06	-3.3E+04	-8.6E+04	-6.5E+04	-8.3E+04	-6.9E+04	-8.0E+04	-4.7E+04	-6.0E+04
205.1	2.1E+06	4.6E+06	-3.1E+06	6.0E+05	9.3E+05	3.5E+06	-6.2E+06	1.8E+06	-7.7E+04	-7.6E+04	-5.4E+04	-8.3E+04	-6.7E+04	-9.6E+04	-5.6E+04	-5.1E+04
214.8	-2.0E+05	1.8E+06	-3.7E+06	-5.9E+05	3.0E+06	5.6E+06	-4.9E+06	3.5E+06	-2.0E+04	-9.1E+04	-4.0E+04	-8.1E+04	-5.1E+04	-9.9E+04	-3.4E+04	-7.3E+04
224.6	-3.9E+04	2.1E+06	-3.6E+06	-3.1E+05	3.1E+06	6.1E+06	-5.5E+06	3.5E+06	-6.7E+04	-1.1E+05	-5.6E+04	-1.4E+05	-3.8E+04	-1.5E+05	-5.1E+04	-7.8E+04

Table 31. Raw data for TOR labyrinth seal at 20,200 rpm, 0.6 PR, and high preswirl

Freq	Re Hxx	Re Hxy	Re Hyx	Re Hyy	Im Hxx	Im Hxy	Im Hyx	Im Hyy	Re eHxx	Re eHxy	Re eHyx	Re eHyy	Im eHxx	Im eHxy	Im eHyx	Im eHyy
Hz	N/m	N/m	N/m	N/m	N/m	N/m	N/m	N/m	N/m	N/m	N/m	N/m	N/m	N/m	N/m	N/m
9.8	-1.2E+06	2.8E+06	-3.6E+06	-1.4E+06	-4.2E+04	3.6E+05	-1.8E+05	-3.6E+04	-6.6E+04	-9.8E+04	-6.9E+04	-7.1E+04	-7.2E+04	-8.4E+04	-5.0E+04	-6.0E+04
19.5	-1.2E+06	2.8E+06	-4.0E+06	-1.3E+06	1.9E+05	6.8E+05	-6.1E+05	3.6E+04	-1.6E+05	-1.1E+05	-1.6E+05	-1.2E+05	-1.1E+05	-9.5E+04	-1.4E+05	-6.2E+04
29.3	-1.4E+06	3.0E+06	-3.8E+06	-1.7E+06	1.2E+05	9.6E+05	-9.4E+05	5.2E+04	-1.2E+05	-7.6E+04	-8.2E+04	-1.1E+05	-9.1E+04	-1.6E+05	-8.1E+04	-9.8E+04
39.1	-1.9E+06	3.0E+06	-3.9E+06	-1.7E+06	2.5E+05	1.1E+06	-8.4E+05	4.1E+05	-1.2E+05	-1.1E+05	-1.1E+05	-9.0E+04	-1.1E+05	-8.2E+04	-1.5E+05	-4.5E+04
48.8	-1.1E+06	3.0E+06	-3.9E+06	-1.7E+06	4.5E+05	1.1E+06	-1.0E+06	7.0E+05	-5.0E+05	-3.6E+05	-2.6E+05	-1.2E+05	-5.9E+05	-3.0E+05	-2.6E+05	-1.0E+05
58.6	-1.7E+06	2.8E+06	-3.6E+06	-1.6E+06	1.1E+06	1.5E+06	-1.5E+06	1.2E+06	-3.0E+05	-7.1E+04	-1.6E+05	-8.7E+04	-2.2E+05	-7.6E+04	-2.1E+05	-5.9E+04
68.4	-1.3E+06	2.7E+06	-3.8E+06	-1.5E+06	1.1E+06	1.7E+06	-1.8E+06	1.2E+06	-8.8E+04	-9.2E+04	-1.2E+05	-6.7E+04	-1.0E+05	-8.5E+04	-9.9E+04	-8.8E+04
78.1	-1.7E+06	2.8E+06	-3.8E+06	-1.5E+06	1.1E+06	2.1E+06	-1.8E+06	1.4E+06	-1.5E+05	-7.5E+04	-9.9E+04	-9.4E+04	-1.8E+05	-7.7E+04	-1.1E+05	-5.6E+04
87.9	-1.5E+06	2.8E+06	-3.7E+06	-1.7E+06	1.7E+06	2.3E+06	-2.3E+06	1.7E+06	-1.0E+05	-7.5E+04	-8.3E+04	-6.2E+04	-7.7E+04	-9.3E+04	-1.1E+05	-6.4E+04
97.7	-1.3E+06	2.6E+06	-3.8E+06	-1.5E+06	1.7E+06	2.7E+06	-2.9E+06	1.8E+06	-1.3E+05	-1.5E+05	-5.2E+04	-1.1E+05	-1.2E+05	-1.3E+05	-1.3E+05	-7.6E+04
107.4	-1.6E+06	2.8E+06	-3.6E+06	-1.3E+06	1.9E+06	2.8E+06	-2.8E+06	2.1E+06	-7.2E+04	-7.2E+04	-1.0E+05	-7.9E+04	-7.6E+04	-7.5E+04	-6.8E+04	-4.9E+04
117.2	-1.1E+06	2.8E+06	-3.9E+06	-1.2E+06	2.1E+06	3.0E+06	-3.3E+06	2.1E+06	-5.6E+04	-7.5E+04	-6.2E+04	-7.0E+04	-6.7E+04	-8.3E+04	-7.7E+04	-5.9E+04
127.0	-1.3E+06	2.7E+06	-3.7E+06	-1.1E+06	2.3E+06	3.4E+06	-3.3E+06	2.1E+06	-6.6E+04	-7.0E+04	-7.0E+04	-5.9E+04	-7.6E+04	-8.5E+04	-4.6E+04	-4.6E+04
136.7	-2.8E+05	1.9E+06	-4.9E+06	-3.8E+05	2.6E+06	4.2E+06	-3.8E+06	2.0E+06	-5.8E+04	-6.4E+04	-8.0E+04	-8.7E+04	-6.0E+04	-8.2E+04	-4.6E+04	-4.3E+04
146.5	-1.1E+06	2.2E+06	-3.2E+06	-4.9E+05	9.7E+05	4.9E+06	-3.1E+06	1.9E+06	-6.3E+04	-7.0E+04	-6.1E+04	-6.6E+04	-6.1E+04	-7.4E+04	-6.5E+04	-5.1E+04
156.3	-1.6E+06	3.3E+06	-3.6E+06	-2.1E+06	2.4E+06	4.8E+06	-4.7E+06	2.4E+06	-4.4E+04	-7.4E+04	-3.4E+04	-6.6E+04	-6.6E+04	-8.1E+04	-4.5E+04	-5.1E+04
166.0	-3.3E+06	4.2E+06	-2.9E+06	-1.7E+06	2.6E+06	5.4E+06	-4.8E+06	2.2E+06	-8.0E+04	-8.7E+04	-7.1E+04	-6.3E+04	-7.9E+04	-7.2E+04	-6.4E+04	-6.3E+04
175.8	-2.2E+06	3.0E+06	-3.2E+06	-2.0E+06	3.6E+06	5.3E+06	-5.4E+06	3.0E+06	-1.1E+05	-1.2E+05	-5.5E+04	-8.2E+04	-1.4E+05	-1.5E+05	-4.9E+04	-6.1E+04
185.5	-3.2E+06	5.6E+06	-2.0E+06	-3.7E+06	3.6E+06	6.5E+06	-5.6E+06	2.4E+06	-8.2E+04	-1.4E+05	-7.4E+04	-1.1E+05	-1.1E+05	-1.1E+05	-1.1E+05	-8.1E+04
195.3	-5.9E+04	3.6E+06	-3.7E+06	-1.2E+06	3.8E+06	6.7E+06	-5.8E+06	3.1E+06	-5.6E+04	-1.1E+05	-5.8E+04	-8.1E+04	-7.7E+04	-9.7E+04	-5.3E+04	-7.6E+04
205.1	7.1E+05	5.5E+06	-4.3E+06	-5.3E+05	1.6E+06	5.1E+06	-7.6E+06	2.5E+06	-5.8E+04	-8.0E+04	-7.5E+04	-6.7E+04	-9.9E+04	-8.2E+04	-4.0E+04	-5.3E+04
214.8	-1.5E+06	2.8E+06	-4.7E+06	-1.8E+06	3.6E+06	7.3E+06	-6.4E+06	4.1E+06	-3.3E+04	-8.0E+04	-2.4E+04	-1.1E+05	-3.5E+04	-9.3E+04	-5.4E+04	-5.3E+04
224.6	-1.1E+06	3.4E+06	-4.8E+06	-1.5E+06	3.8E+06	7.8E+06	-7.2E+06	4.1E+06	-4.9E+04	-9.8E+04	-6.4E+04	-9.4E+04	-4.8E+04	-9.3E+04	-3.5E+04	-6.2E+04